CAPITAL UNIVERSITY OF SCIENCE AND
TECHNOLOGY, ISLAMABAD

Synthesis and Characterization of Sodium Alginate Based Antimicrobial Hydrogels

by

Kamran Khan

A thesis submitted in partial fulfillment for the
degree of Master of Science

in the

Faculty of Health and Life Sciences
Department of Bioinformatics and Biosciences

2026

CERTIFICATE OF APPROVAL

Synthesis and Characterization of Sodium Alginate Based Antimicrobial Hydrogels

by

Kamran Khan

(MBS241012)

THESIS EXAMINING COMMITTEE

S. No.	Examiner	Name	Organization
(a)	External Examiner	Dr. Sayed Afzal Shah	NUMS, Rawalpindi
(b)	Internal Examiner	Dr. M. Asad Anwar	CUST, Islamabad

Dr. Sohail Ahmad Jan
Thesis Supervisor
March, 2026

Dr. Syeda Marriam Bakhtiar
Head
Dept. of Bioinfo & Biosciences
March, 2026

Dr. Sahar Fazal
Dean
Faculty of Health & Life Sciences
March, 2026

Author's Declaration

I, **Kamran Khan** hereby state that my MS thesis titled "**Synthesis and Characterization of Sodium Alginate Based Antimicrobial Hydrogels**" is my own work and has not been submitted previously by me for taking any degree from Capital University of Science and Technology, Islamabad or anywhere else in the country/abroad.

At any time if my statement is found to be incorrect even after my graduation, the University has the right to withdraw my MS Degree.

(Kamran Khan)

Registration No: MBS241012

Plagiarism Undertaking

I solemnly declare that research work presented in this thesis titled "**Synthesis and Characterization of Sodium Alginate Based Antimicrobial Hydrogels**" is solely my research work with no significant contribution from any other person. Small contribution/help wherever taken has been duly acknowledged and that complete thesis has been written by me.

I understand the zero tolerance policy of the HEC and Capital University of Science and Technology towards plagiarism. Therefore, I as an author of the above titled thesis declare that no portion of my thesis has been plagiarized and any material used as reference is properly referred/cited.

I undertake that if I am found guilty of any formal plagiarism in the above titled thesis even after award of MS Degree, the University reserves the right to withdraw/revoke my MS degree and that HEC and the University have the right to publish my name on the HEC/University website on which names of students are placed who submitted plagiarized work.

(Kamran Khan)

Registration No: MBS241012

Acknowledgement

In the name of **Allah**, the most gracious and the most merciful; and prayers and peace be upon **Muhammad**, His servant and messenger. First and foremost, I would like to acknowledge my limitless thanks to **Allah Almighty** and to his last **Prophet Muhammad (S.A.W)**. Without their guidance, this work would never have been completed. I owe deep gratitude to our University, **Capital University of Science & Technology (CUST)**, for giving me the opportunity to complete this work. Special thanks to **Dean Dr. Sahar Fazal** for his encouragement throughout the entire process.

I would like to acknowledge and am very grateful to my **Supervisor Dr. Sohail Ahmad Jan**, who has been generous during all phases of the research and for all the valuable lessons that I learned during this period; I thank him from the bottom of my heart.

Finally, I want to express my heartfelt gratitude to **Dr. Asad Anwar**, my **family**, especially **my parents**, who have provided me with generous support throughout my life and especially in conducting my research. Because of their unconditional love, support, and prayers, I have completed this thesis.

(Kamran Khan)

Abstract

A common broad-spectrum oxazolidinone antibiotic for the treatment of bacterial infections, linezolid (LNZ) has limited topical applicability due to its poor solubility, low bioavailability, and inadequate tissue penetration. This study used the solution casting approach to systematically develop sodium alginate-based hydrogels that would distribute LNZ in a regulated and sustained manner. K2 was determined to be the best hydrogel formulation out of the six that were made (K1–K6) because of its balanced swelling behavior and greater structural stability. Following selection, LNZ (K2-LNZ) was added to the formulation. Scanning electron microscopy (SEM) and Fourier transform infrared (FTIR) spectroscopy were used for thorough characterization, which verified the development of a homogeneous polymeric network, effective drug encapsulation, and potent polymer–drug interactions. Degradation investigation over seven days revealed regulated hydrolytic breakdown and excellent structural integrity, whereas swelling studies showed equilibrium attainment within 24 hours. The Korsmeyer–Peppas kinetic model was followed by the in vitro drug release from K2-LNZ, which showed a sustained release profile controlled by non-Fickian diffusion. Antimicrobial study revealed strong inhibitory efficacy against Gram-negative *Escherichia coli* and Gram-positive *Staphylococcus aureus*. Additionally, the manufactured hydrogel system demonstrated mechanical resilience, biodegradability, and pH-responsive swelling. All things considered, these results point to the K2-LNZ hydrogel as a viable platform for wound care, targeted drug administration, and possible translational uses in tissue engineering and long-term antibiotic therapy.

Keywords: Hydrogel, Sodium Alginate, PVP, $CaCl_2$, Linezolid, Drug delivery.

Contents

List of Figures

List of Tables

Abbreviations

AgNPs	Silver nanoparticles
CS	Chitosan
$CaCl_2$	Calcium Chloride
E. coli	*Escherichia coli*
FE-SEM	Field emission scanning electron microscope
FTIR	Fourier transforms infrared spectroscopy
K2-LNZ	Optimized Linezolid-Loaded Hydrogel Formulation
LNZ	Linezolid
MIC	Minimum Inhibitory Concentration
MMPs	Matrix metalloproteinases
PAM	Polyacrylamide
PBS	Phosphate buffer saline
PEG	polyethylene glycol
PH	Potential of Hydrogen
PHEMA	poly-2-hydroxyethylmethacrylate
PVA	Poly (vinyl alcohol)
PVA	Poly vinyl alcohol
PVP	Poly (N-vinylpyrolidone)
S. aureus	*Staphylococcus aureus*
SA	Sodium Alginate
TGA	Thermogravimetric analysis
UV–Vis	Ultraviolet–Visible Spectroscopy
XRD	X-ray diffraction
ZOI	Zone of inhibition

Chapter 1

Introduction

Destruction to healthy skin or tissue is referred to as a wound [1]. Wounds are referred to as cuts, bruises, incisions, and injuries based on different damage variables. It is primarily brought on by internal factors like problems with the local blood supply and external harm factors including surgery, outside force, heat, electricity, chemicals, and low temperature. There are two types of wounds: acute and chronic. Depending on the size and depth of the incision, acute wounds can recover in 60 to 90 days [2]. Chronic wounds are those that heal far more slowly, don't go through all the stages of the typical wound healing process, and typically stop at the inflammatory stage[3].In addition to creating a significant financial burden for both patients and the public healthcare system, these wounds present numerous difficulties for patients, including extreme emotional and physical stress. According to research, between 1% and 2% of people worldwide experience chronic, non-healing wounds at some point in their lives in developed countries. Conventional wound dressings lack antibacterial qualities and are dry, making it unable to provide an environment of moisture for wound healing [4]. These days, films, foams, plaster patches, even hydrogels are employed as wound dressings. Hydrogels are receiving a lot of interest these days because of their ability to store water and provide a moist wound environment. These days, materials such as foams, bandages, scars, and hydrogels are employed as wound dressings. Hydrogels are receiving a lot of study these days because of their ability to store water and

provide a moist wound environment. Because of its distinct chemical and antibacterial properties, chitosan is a biopolymer molecule that has recently attracted a lot of interest in the pharmaceutical industry. However, because of its low mechanical qualities, chitosan is combined with other biopolymers has to benefit from its desirable biocompatibility while also having the hydrogels' better mechanical and physical qualities. Because cellulose is readily available, biodegradable, and non-toxicit is a very common natural polymer that has garnered a lot of attention up to this point [5, 6].

Because cellulose has a wide surface area, is non-toxic, has good mechanical qualities, is biodegradable, and has a low density [7], it is typically combined with other polymers. The reinforcement of chitosan using cellulose-based substances in wound dressings is still of significant interest, despite the vast number of studies focused on the production of hydrogels from cellulose-based in diverse applications. Additionally, wound healing will be improved by the encapsulating of therapeutic substances in hydrogels, such as growth factors and cells, antioxidants, and antibiotics.

Hydrogels are three-dimensional networks of hydrophilic polymers that are crosslinked and have a high water absorption capacity (up to 99%) [6, 8, 9]. Hydrophilic compounds units (-OH, -CONH-, -CONH2, as well as -SO3H) found in the gels' polymeric constituents give hydrogels their capacity to swell [10].

Physical or crosslinking by chemical is used to create hydrogels from both natural and synthetic polymers. Hydrogels' high water content allows them to be used widely in the pharmaceutical and biomedical industries because they are compatible with the majority of biological tissues. In recent years, researchers have concentrated on finding materials that are both biocompatible and non-toxic for living things [11]. Hydrogels have been employed in systems for drug delivery [12], wound dressings [9, 13], gene transfection [14, 15], scaffolds for tissue engineering [16, 17], and biosensors [18].This brief overview focuses on hydrogels, which are systems of polymers that have been significantly inflated with water. Hydrophilic gels, also known as hydrogels, are frameworks of chain polymers that can be found as dispersion gels in which water serves as the dispersion medium [19]. Over time,

researchers have described hydrogels in a variety of ways. The most common of them is hydrogel, which is a water-swollen, cross-linked polymeric network formed by the simple response from one or more monomers. Another description is a polymeric substance that can swell and hold a substantial amount of water inside its physical makeup but cannot disintegrate in water.

Hydrogels have garnered substantial attention across the last fifty years, due to their remarkable promise in a broad range of applications. Because of their high water content, they also have a degree about flexibility that is quite close to that of natural tissue. Cross-links among network chains provide hydrogels their resistance to dissolution, while hydrophilic functional groups affixed to the polymeric backbone give them the capacity to absorb water. Numerous substances, both manmade and naturally occurring, meet the criteria for hydrogels [20–22].

Natural hydrogels have been steadily supplanted over the past 20 years by synthetic hydrogels, which have a long service life, a high water absorption capacity, and high gel strength. Fortunately, synthetic polymers typically contain distinct structures that can be altered to provide customized functionality and degradability. It is possible to create hydrogels using only synthetic materials. Additionally, it remains steady even when there are significant temperature swings [23].

There are several "classical" chemical methods for creating hydrogels. These include one-step processes such as parallel cross-linking of dual-purpose monomers and polymerization, as well as multi-step processes involving the synthesis of polymer molecules with reactive functional groups and their subsequent cross-linked formation, possibly also by reacting polymerization with appropriate cross-linking agents. Polymer engineers are able to create networks of polymers with specific features like decomposition, mechanical strength, and biochemical and biological reaction to stimuli, as well as microscopic control over structure like cross-linking density [24].

As previously stated, hydrogels are three-dimensional linked together hydrophilic polymer networks that may reversibly swell or de-swell in water while holding a significant amount of liquid in their swelled form. Hydrogels can be made to react

to changes in the external environment by expanding or contracting. A wide range of chemical and physical stimuli, such as temperatures, electric or magnetic fields, light, stress, and sound, as well as pH, solvent structure, strength of ion, and molecular species, can cause them to exhibit dramatic volume transitions.The event is known as volume collapsing or phase transition because the degree of expanding or de-swelling in reaction to changes in the hydrogel's external environment may be so extreme. For the past forty years, synthetic hydrogels that have been the subject of much research, and this sector is still quite active today [25].

Hydrogels are by definition networks of polymers with hydrophilic characteristics. Although hydrophilic monomers are typically utilized to prepare hydrogels, hydrophobic monomers are occasionally employed to control the characteristics for certain uses. Generally speaking, synthetic or natural polymers can be used to create hydrogels. Compared to natural polymers, synthetic polymers are chemically stronger and hydrophobic [26]. Although their mechanical strength slows down the rate of deterioration, it also contributes to their durability. Optimal design should balance these two opposing characteristics .If natural polymers have appropriate functional categories or have been functionalized with radically polymerizable groups, it can be used to construct hydrogels based on these polymers [27].To put it simply, a hydrogel is just a network of hydrophilic polymers that have been cross-linked in some way to create an elastic structure. Therefore, a hydrogel can be made using any method that can be used to make a cross-linked polymer. Hydrogels are frequently created by copolymerization, cross-linking and free-radical polymerizations, which involve the reaction of aqueous monomers with multifunctional cross-linkers. Hydrogels are created by cross-linking water-soluble linear polymers, both synthetic and natural:

i. Using a chemical reaction to join polymer chains.

ii. Creating main-chain free radicals with ionising radiation, which can recombine to form cross-link junctions?

iii. Physical interactions such crystallite formation, electrostatics, and entanglements.

Gels can be created using any of the several polymerization methods, such as large quantities, solution, and suspension polymerization. Generally speaking, the monomer, starter, and cross-linker are the three essential components of the hydrogel synthesis. Diluents, that include water-based or other aqueous solutions, can be used to regulate the heat of polymerization and the final characteristics of hydrogels.

After that, the hydrogel mass must be cleaned to get rid of any remaining contaminants from the preparation procedure. These consist of initiators, cross-linkers, non-reacted monomer, and undesirable byproducts from reactions. Inverse - suspension polymerization and dilute solution polymerizationhave been investigated for the creation of a hydrogel that use acrylamide, which is an acrylic acid, and its salts. Highly concentrated solution polymerization of acrylic monomers, which are primarily patented, has been the subject of fewer investigations [28, 29].

Chen used potassium per sulphur as a thermal initiator in concentrated (43.6 weight percent) solution polymerization to create acrylic acid-sodium acrylate superabsorbent.Hydrogels is often made from polar monomers. They can be classified as natural polymers hydrogels, which are synthetic polymer hydrogels, or mixtures of the two classes based on their starting ingredients.

Alginate, an innately occurring electrostatic polysaccharide derived from brown algae fauna, is a linear copolymer made up of two uranic sugars, notably guluronic acid and mannuronic acid salts. Along the chain, linkage 1→4-Dmannuronic acid (M) and L-guluronic acid (G) combine in a block pattern, comprising three types of blocks: homopolymer M-M blocks, G-G blocks, and heteropolymer blocks with irregular M-G structures. The arrangement of the blocks establishes the physical and chemical characteristics of the alginate molecule [30].

Alginate hasadvantageous features due to its polyelectrolyte and biopolymer structure. The capacity of alginates to gel easily in the presence extremely magnetized or polyvalent cationsparticularly bivalent cations like Ca^{2+} is their most significant property. In addition, alginate is big, biocompatible, bioadhesive, biodegradable, non-toxic, largely nonimmunogenic, sufficiently transparent, reasonably stable,

and simple to use. It is also comparatively highly soluble in water. Alginate is often used in many fields of the biological and engineering sciences because of all of these characteristics. However, due to environmental factors, alginate's stability is limited [31].

Prior work has demonstrated that the functional properties of alginate gels, such as porosity, expanding behaviour, stability, decomposition, gel strength, gel immune response characteristics, and biocompatibility, as well as formation kinetics and gel cation type, are influenced by the chemical composition and molecular size of alginate. Enhancements of alginic acid instruments such as derivatives using various chemical and biological methods have become more popular in recent years [30].

Alginates are used in drug delivery, the dressing for the wound and other pharmaceutical applications. They are created to create hydrogels by combining them with other polymers. Alginate hydrogel has been developed as an antibacterial wound dressing medium using a variety of polymers, including alginate/ZnO hydrogel, alginate/gelatin/Poly Vinyl Alcohol (PVA) hydrogel, alginate/chitosan with vitamin E hydrogel, alginate/PVA/PVP, etc. Its capacity to take in and eliminate the active ingredients that can aid in the healing of wounds, along with its physical, chemical, biological, and antibacterial qualities, are the foundation of this development .

Alginates can be ionically or covalently crosslinked. Treenatthi investigated the various impacts of Ca^{2+}, Zn^{2+}, and Cu^{2+} ions on the development of hydroxyethylacrylchitosan alginate hydrogel, which is employed as an analgesic delivery medium[32]. Wu employed Ca^{2+} as a lysozyme carrier medium while combining alginate and chitosan[33]. Leveraging electrostatic interactions with silver nanoparticles (AgNP), Zia created an antibacterial burn treatment from alginate and carrageenan. Grafting alginate with PEG as the dressing of wounds material using Sr^{2+} was reported by GP & MR [34]. One kind of cation cross linking compound, that includes Ca^{2+}, Cu^{2+}, Zn^{2+}, and Sr^{2+}, was used in the earlier investigation. One kind of cation linker, such as Ca^{2+}, Cu^{2+}, Zn^{2+}, and Sr^{2+}, was used in the earlier investigation. A recent study has not yet examined the

combination of two or more cations. When added to alginate hydrogel, Sr^{2+} exhibits greater mechanical performance and greater chemical stability than Ca^{2+} and Sr^{2+}, which are both less hazardous than Ba^{2+}. The combined effect of Ca and Sr is anticipated to produce hydrogels with greater stability and stronger mechanical characteristics since Ca^{2+} has fewer interaction sites in alginate than Ba^{2+} and more sites for physical adsorption. Poly (N-vinyl-2-pyrrolidone) (PVP) is a linear, nontoxic, water-soluble polymer that is biocompatible. PVP-based hydrogel exhibits high the hydrophilicity and chemically stable behaviour. Thus, it raises the water affinity of polymers [35].

PVP is used to create a variety of hydrogels that are used in the pharmaceutical sector, including scaffolds for tissue engineering, wound dressings, and drug delivery system [33]. PVP and polymer made from nature have been combined in a number of experiments to enhance the hydrogel's capacity to absorb water. To enhance hydrogel surface shape and water absorption capacity, Wang & Wang combined anionic monomers Na-alginate and Na-acrylate with non-ionic polymers poly (N-vinyl-2-pyrrolidone)[36]. In the meantime, Sadeghi's study increased the capacity of superabsorbent hydrogels by copolymerising acrylic acid anionic monomer with Nvinyl-2-pyrrolidone [37].

In order to improve the hydrogel's capacity as a way to deliver drugs medium, two cations were combined to create crosslinked alginate hydrogels. Alginate and Poly (N-vinyl-2-pyrrolidone) can improve hydrogel's affinity for water [38]. This study examined the hydrogel using Ca^{2+} and Sr^{2+} as a crosslinker, the impact of the alginate/PVP ratio and different Ca^{2+}/Sr^{2+} ratios on the hydrogel's water absorption capacity, the gel portion, and the hydrogel's potential as a drug delivery medium.

Sodium alginate is an inexpensive, bio adhesive poly-anionic copolymer, linear [39], sensitive to pH [40], easily soluble in water [41], non-toxic, disintegrating [40], highly hydrophilic, breathable, harmless, perishable, and non-immunogenic. Na-Alg possesses the following properties chelating, inexpensive transparency, convenience of gel formation, adhesion, strengthening, and film-making.It possesses the qualities of a gelling negotiator, high water density, and stabilizing nature.

Hydrogels containing sodium alginate have the characteristic of much delayed medication discharge delivery in an environment of a gastrointestinal environment. Na-Alg has a steady temperature. This polymer's application in industries is restricted due to a number of problems. Although sodium alginate is utilized in many medications, it frequently causes gastrointestinal adverse effects, including nausea, diarrhea, and bloating. Its acidic nature makes it unsuitable for nutritious foods because it is generated from alginic acid. Low toughness and cell adhesion, low drug loading, hydrophilic properties, microbial breakdown, and rapid release are some of its characteristics. Sodium alginate is being mixed with various natural as well as synthetic polymers to improve its qualities in order to address these issues. It has been claimed that Na-Alg can combine with a variety of natural and synthetic polymers to boost its adhesion and mechanical strength.

To provide them mechanical strength, it is combined with several less expensive materials. It can be used to create blends, hydrogels, micelles, nano- carriers, nano-gels, nano-composites, tiny particles, tubes, cationic systems, and aerogels, etc. All of these materials showcase its exceptional qualities when applied to drug delivery, gene transfer, tissues and bones engineering, and food technology. Blends and composites of this polymer show promise for treating wastewater; hydrogels, material composites, and blends are being developed to eliminate various contaminants, particularly organic and inorganic Hydrogels. Adding various antibacterial agents makes the Na-Alg coating even more outstanding. The many types of sodium alginate-based composites show great utility in managing diabetes and other forms of cancer. This polymer has numerous uses in stem cell therapies, chemotherapy, and medication delivery. This polysaccharide aids in food packing and gelling. This polymer combines with other elements to create composites that eliminate organic contaminants and seize both organic and metallic pigments from aqueous solutions.

An essential method for creating novel polymeric materials with desired features is polymers blending. Numerous studies have been published in the Literature from previous decades on polymer miscibility and intermolecular interactions. In order to uncover further uses for the resulting blend materials for pharmaceutical

and biomedical devices, it is crucial to select polymers that have the capacity to generate hydrogen bonds when two polymers are combined and to investigate the features of the blend. Synthetic polymers' success as biomaterials depends on their broad range of mechanical properties, transformation methods that make it simple to generate a variety of various shapes, and low production costs. As a result, synthetic and natural polymer blends have been used to create biologically significant compounds such poly (N-vinyl-2pyrrolidone)-kappa-carrageenan (PVP=KC), poly(N-vinyl2-pyrrolidone)-iota-carrageenan (PVP=IC), poly(ethylene oxide) hydroxypropyl methylcellulose (PEO=HPMC), and poly (vinyl alcohol) - chitosan (PVA=C) [42].

Alginates are a polysaccharide that occurs naturally derived from coastal brown algae that is made up of a linear chain of 1, 4- linked a-L-gulonic acid and b-D-mannonic acid [7]. Calcium Alginate (NaAlg), an electronic compound with a stiff molecular chain [8] and a strong ability to form films, has been widely used and thoroughly investigated as a drug carrier in biomedical applications .PVP is a water-soluble polymer, and its carbonyl groups should interact with sodium alginate's hydroxyl groups to produce hydrogen bonds. Therefore, PVP was utilized as an appropriate candidate blend with sodium alginate. The morphological traits and surface characteristics of PVP and Na-Alg blends made using the solution casting approach were described in a prior research. In this study, we use infrared spectroscopy with the Fourier transform (FT) to report on the mechanical, spectroscopic, and thermal characteristics of these blend films [42].

Polyvinylpyrrolidone (PVP) is a versatile, non-toxic, and non-ionic polymer that excels as a stabilizer for nanoparticles (NPs) due to its unique hydrophobic and hydrophilic components, which prevent aggregation via steric hindrance, ensuring uniform dispersion. PVP-based hydrogels, such as PVP-Na-Alg hydrogels are synthesized through a sequential method, enabling controlled release of active agents, making them ideal for drug delivery, tissue engineering, and wound dressing applications. These hydrogels boast biocompatibility, non-toxicity, and stability, with benefits including tunable mechanical strength, enhanced bioadhesion, and customizable swelling behavior. Additionally, PVP's complexation

properties facilitate interactions with drugs and biomolecules, optimizing therapeutic efficacy and expanding its potential in pharmaceutical, biomedical, and cosmetic industries. Its multifaceted role underscores PVP's value in developing advanced biomaterials with tailored properties [43].

1.1 Problem Statement

Microbial infections and antibiotic resistance are major healthcare challenges. Sodium alginate based hydrogels exhibit weak structural integrity and rapid drug diffusion, resulting in burst release rather than sustained antimicrobial action. This uncontrolled release profile compromises their therapeutic effectiveness for localized drug delivery.

1.2 Hypotheses

Incorporation of antibacterial agents into sodium alginate-based hydrogels will improve their physicochemical properties and stability. This enhancement is expected to enable effective and sustained drug delivery with improved antibacterial activity for biomedical applications.

1.3 Gap Analysis

Need for advanced biomaterials with long lasting antibacterial activity and controlled release.

1.4 Aim

The purpose of this work is to synthesize antimicrobial hydrogels based on sodium alginate and to assess their Morphological, physicochemical, controlled release and antibacterial properties for possible biomedical uses.

1.5 Objectives

i. To synthesize hydrogels based on sodium alginate by employing an appropriate cross-linking technique.

ii. To study morphological and physicochemical characteristics of the hydrogels.

iii. To incorporate drug into the developed hydrogels and to investigates its release kinetics.

Chapter 2

Literature Review

2.1 History

For colloidal gels made from inorganic salts, hydrogels were originally mentioned in the 19th century. However, it wasn't until Wichterle and Lim discovered the first hydrogel on cross-linked poly-2-hydroxyethylmethacrylate (pHEMA) in 1954 that the application of gels was brought to light. Since then, the network with three dimensions of hydrophilic polymers has frequently been referred to as "hydrogel." The cross-linked macromolecular system known as pHEMA was used to create soft contact lenses that were widely used throughout Western Europe in the 1960s. Following successful studies, pHEMA-based lenses were approved by the FDA for use in 1971.Hydrogels made from pHEMA were then used in controlled the delivery of drugs applications. Updike and Hicks created sensors in 1967 by trapping the enzyme glucose-oxidize in a hydrogel based on polyacrylamide (PAM).Hydrogels have grown significantly over time. The 1960s saw a major advancement in the chemistry of hydrogels when a variety of uses for them were documented, including the administration of drugs, tissue engineering, skincare goods, food items, and many more biological uses. In order to increase the biocompatibility, novel hydrogel concepts were investigated in the 1970s and materials including vinyl acetate, acrylamides, and N-vinylpyrrolidone were used. Tanaka experimented with

PAM gels during that time and found that the gels tended to collapse when the temperature or mixture of solvents was changed. He anticipated the appearance of critical endpoint in the phase equilibrium and used mean-field theory to explain the phenomena [44].

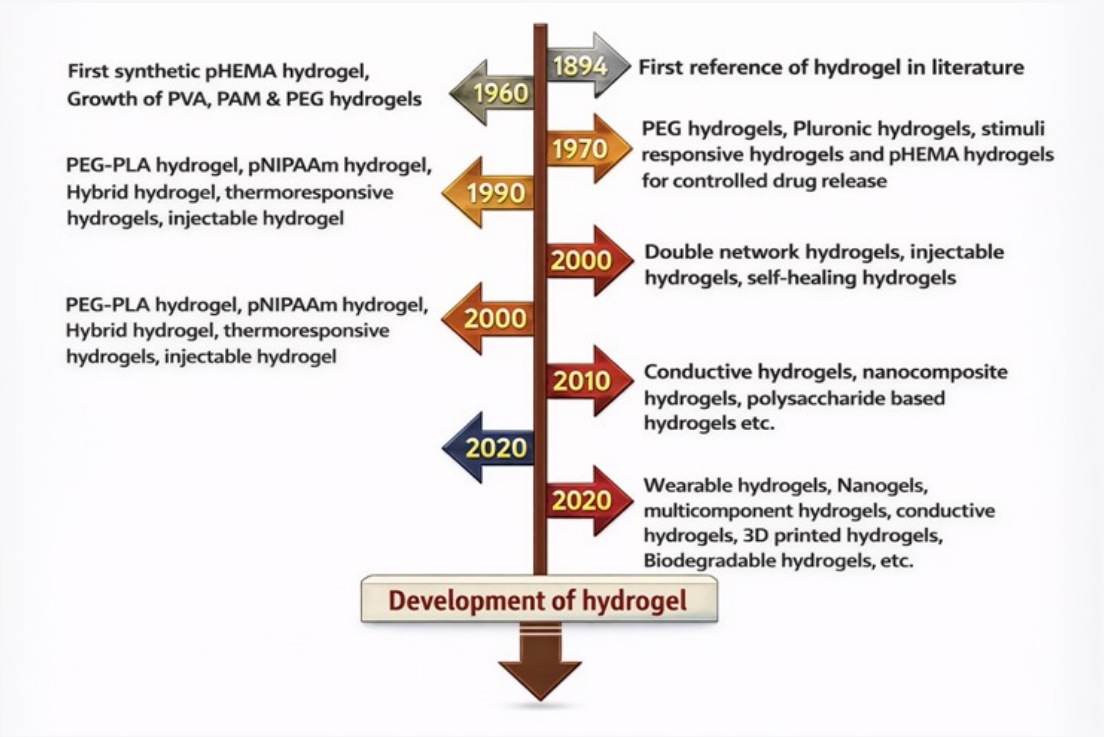

FIGURE 2.1: Hydrogels evolution over time [44].

The development of thermoresponsive hydrogels based on various polymers, including polyvinyl alcohol, (PVA), poly (N-isopropylacrylamide), poly ethylene glycol (PEG), etc., was the focus of increased study in the 1990s. Additionally, these hydrogels were used to create delivery systems that allow molecules to be released on and off below the smaller critical temperature of the solution (LCST).

Injectable hydrogels were extensively studied for biomedical research in the late 1990s Elisseeff *et al.* reported the first use in 1999 for targeted delivery of medicines to tissue utilizing cartilage as an illustrative system. In order to improve the mechanical properties of hydrogels, a new wave of physio-chemical techniques and structural modifications emerged in the 21^{st} century. These techniques included

the addition of various crosslinkers, altering physical architectures of polymer networks, using synthetic and natural polymers, incorporating inorganic materials, creating uniform networks and stereo complex materials, and more [44].

The first novel double-network hydrogels with exceptionally high strength ratings (fraction stress under compression of 17.2 MPa and strain of 92%) were created in 2003 by Gong *et al.* using a free radical polymerization process. Poly (2-acrylamido-2-methylpropanesulfonic acid) was used to create the first network, while PAM was used to create the second. The development of biocompatible hydrogels for vital biomedical applications, such as bone implantable biological sensors, lenses for contacts, tissue engineering, etc, has been made possible by advancements in the manufacture of water-friendly and hydrophobic polymerswith various structural combinations.

Innovative hydrogels such as wearable hydrogel patches, conductive hydrogels, injectable hydrogels that are self-healing hydrogels, multiple- component hydrogels, compostable hydrogels, etc,Is the focus of increased efforts as hydrogel research has recently evolved quickly. 34–36 Research on the development of these incredibly adaptable materials in medical purposes has increased exponentially over the past 20 years, as evidenced by a PubMedsearch for the phrase "hydrogel" in the title or abstract of peer-reviewed publications.

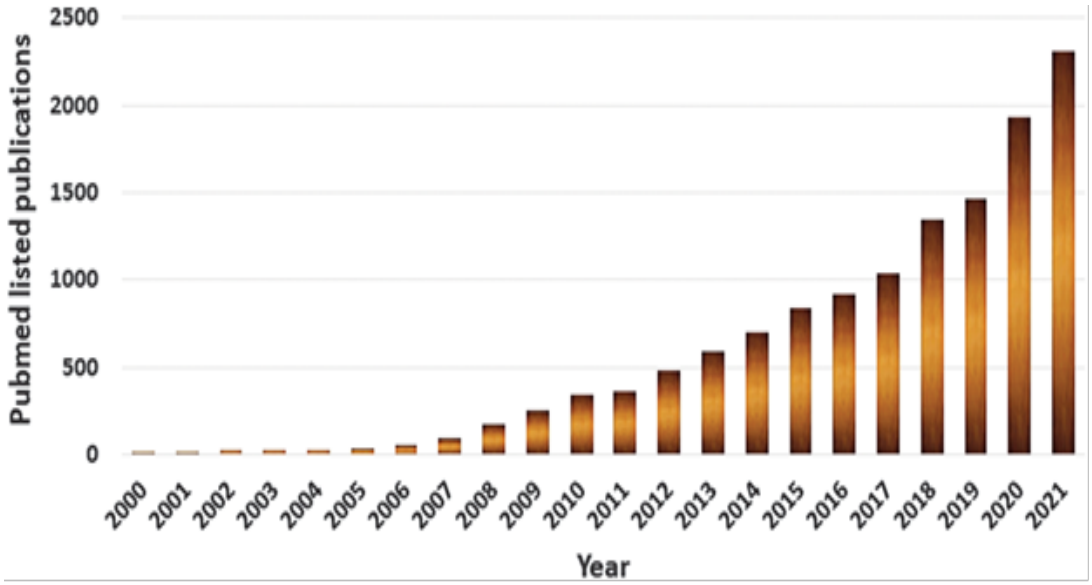

FIGURE 2.2: According to PubMed®, the number of articles on hydrogels has increased dramatically during the last 20 years [44].

2.2 Classification of Hydrogel

The grouping of hydrogels is based on their source, structure, ionic charge, linkage property, configuration, and environmental stimuli. Polymer chains are crosslinked to generate hydrogels. Hydrogels come from three different types of polymers: natural, synthetic, and semi-synthetic. Hydrogels can be classified as organic, synthetic, or partially polymerised hydrogels within the polymer source.

Cellulose, chitosan, collagen, the mineral alginate, agarose hyaluronic acid, gelatin, fibrin, and other materials are examples of naturally generated hydrogels. Although they have comparatively low mechanical strength and stability, they are naturally biocompatible, bioactive, and biodegradable.

While most people can safely use natural hydrogels, in rare instances, certain of its ingredients can cause allergies. Therefore, if sensitive people are treated with natural hydrogels, there may be immunological hazards. Synthetic hydrogels are made of synthetic polymers.

Poly vinyl alcohol (PVA), polyethylene glycol (PEG), the polyethylene oxide (PEO), poly-2-hydroxyethyl methacrylate (PHEMA), poly-N-isopropyl acrylamide (PNIPAM), polyacrylic acid (PAA), and polyacrylamide polymer (PAAM) are examples of human-made polymers that are made by polymerizing a monomer .Even though some of them, like PAAM, are biocompatible, they are strong and stable.

Chemically altered organic polymers or a blend of synthetic and natural polymers are used as semi-synthetic polymers to create semi-hydrogels. Methacryloyl-modifying gelatin (GelMA) and acrylate-treated hyaluronic acid (AcHyA) are two examples of chemically changed natural polymers.

It can also be a blend of synthetic and natural polymers, like albumin and gelatin or PEG-conjugated fibrinogen Thesehydrogels have a variety of chemical parameters that allow for multitunable qualities in addition to the bioactivity characteristics of natural hydrogels charge [45].

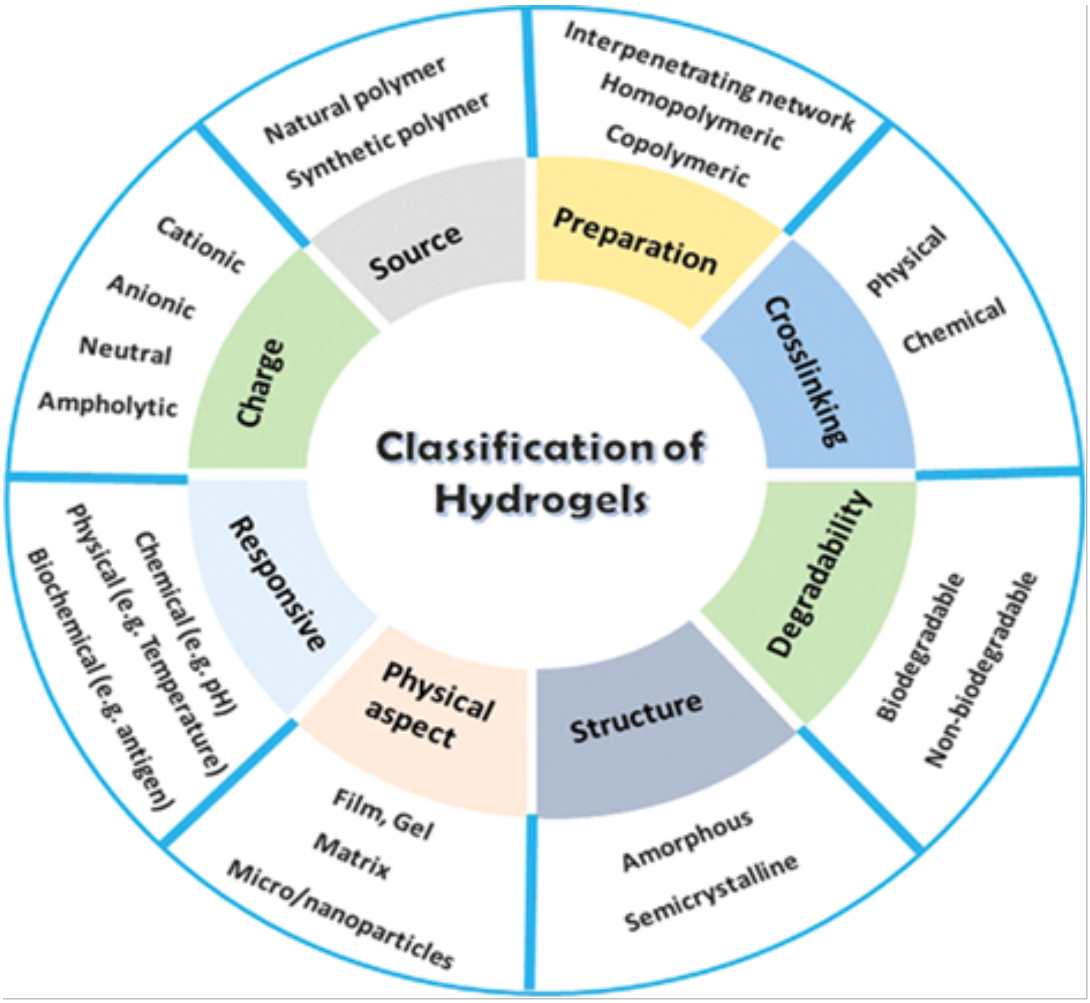

FIGURE 2.3: The image illustrates the "Classification of Hydrogels" that organizes hydrogels into six main categories arranged around a central circle, each with its own sub-classifications: Preparation (interpenetrating network, homopolymeric, copolymeric), Crosslinking (physical, chemical), Degradability (biodegradable, non-biodegradable), Structure (amorphous, semicrystalline),Physical aspect (film, gel matrix, micro/nanoparticles), and Charge (cationic, anionic, neutral, ampholytic), illustrating the various ways hydrogels can be classified in materials science [44].

2.3 Crosslinking Strategies and Synthesis Methods

In order to create a stable three-dimensional network, the production of hydrogels based on sodium alginate (SA) mainly uses chemical or physical crosslinking techniques. The most popular and safe technique is physical crosslinking, particularly ionic gelation with divalent cations like Ca^{2+}. For example, Ling *et al.* (2024) used Ca^{2+} crosslinking to create alginate hydrogel microspheres, demonstrating

the ease of use and efficiency of the technique in creating spherical carriers for controlled release applications [46].

This process creates an "egg-box" structure by exchanging calcium ions with sodium ions from guluronic acid blocks. However, in physiological settings physically crosslinked gels frequently have low mechanical strength and stability.

Chemical crosslinking techniques are used to solve this. Polyvinylpyrrolidone (PVP) / alginate hydrogels were created by Singh and Singh (2012) using gamma radiation. This technique concurrently crosslinks the polymer and decreases embedded silver ions to make antimicrobial nanosilver in situ without the need for further chemical initiators [47].

Similar to this, Mohamadinia *et al.* (2021) used chemical crosslinking to produce sodium alginate/acrylic acid composite hydrogels, which were then coupled to silver nanoparticles (AgNPs) [48].

In order to improve mechanical robustness, dual-crosslinking techniques that combine covalent and ionic connections are becoming more and more common. He *et al.* (2024) demonstrated how chemical crosslinkers can bring multifunctional features including adhesion and antioxidant activity alongside antibacterial effects by creating a composite hydrogel utilizing poly(vinyl alcohol) crosslinked with polydopamine and tannic acid [49].

Advanced and Stimuli-Responsive Synthesis: "smart" hydrogels have been the subject of recent studies. PH-responsive starch/sodium alginate hybrid hydrogels were created by Lei *et al.* in 2025. In the synthesis, SA was mixed with oxidized starch. The hydrogel's pH-sensitive swelling behavior was made possible by the dynamic Schiff base and borate ester linkages, making it appropriate for intelligent drug delivery and monitoring [50].

By adding dynamic covalent bonds, El-Sayed *et al.* (2024) created a dual-adhesive and self-healing alginate-based hydrogel that can heal itself after damage a critical component for long-lasting wound dressings [51].

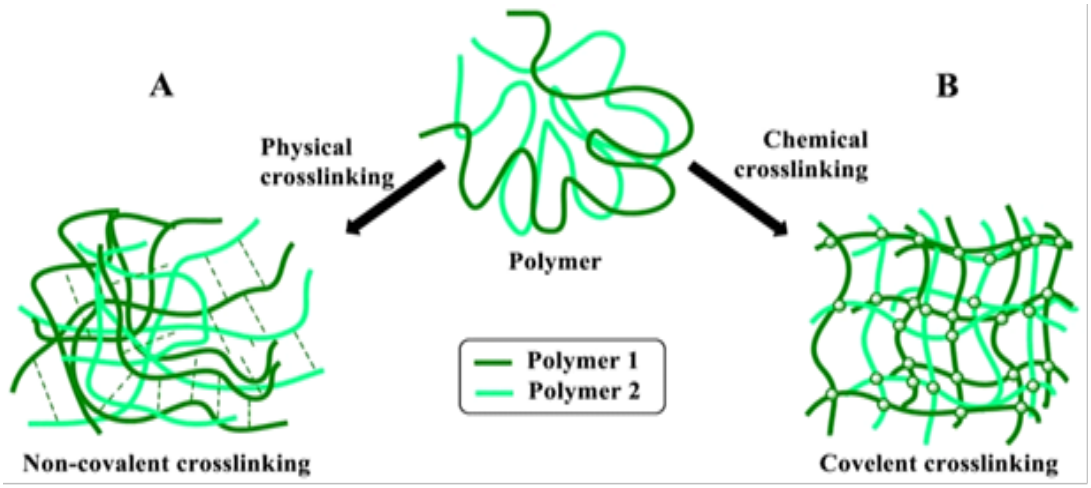

FIGURE 2.4: Physical and chemical cross linking strategies of Hydrogels [76].

2.3.1 Physical Crosslinking Mechanisms

Because of its ease of use, biocompatibility, and ability to preserve bioactive components, ionic crosslinking continues to be the most widely used physical technique for SA hydrogel production. The process creates the distinctive "egg-box" structure by chelating divalent cations (usually Ca^{2+}) with the guluronic acid blocks of alginate chains. This method was proven by Ling *et al.* (2024) in the production of alginate hydrogel microspheres with hollow silica coatings, where the microsphere diameter and crosslinking density directly affected the controlled release features [46]. In addition to calcium, other divalent cations have been investigated, such as Ba^{2+}, Sr^{2+}, and Zn^{2+}, each of which gives the resulting hydrogels unique mechanical and degrading characteristics. Because of their greater affinity for guluronic acid residues and bigger ionic radius, barium ions, for example, form stronger crossslinks not withstanding possible toxicity issues for use in biological applications. Synergistic methods that combine ionic interactions with other non-covalent forces are among the latest developments in physical crosslinking. In order to produce hydrogels with adjustable mechanical properties, Roy and Saha (2012) described how hydrogen bonding between SA and polyvinylpyrrolidone (PVP) might be used in conjunction with ionic crosslinking [52]. By combining

SA with thermo sensitive polymers like pluronics or methylcellulose, temperature-induced gelation has also been accomplished, allowing for in situ gel formation at physiological temperatures.

2.3.2 Chemical Crosslinking Approaches

Covalent connections are created between SA chains by chemical crosslinking, which significantly increases mechanical strength, stability in physiological settings, and resistance to ion exchange. Glutaraldehyde, epichlorohydrin, and carbodiimides (EDC/NHS) are examples of conventional chemical crosslinkers; nevertheless, these frequently cause biocompatibility issues. In order to create antimicrobial hydrogels without any leftover harmful crosslinkers, Singh and Singh (2012) invented a different method that uses gamma radiation to crosslink PVP/alginate mixes while concurrently converting silver ions to nanoparticles [47]. New chemical approaches concentrate on photopolymerization, enzymatic crosslinking, and "click chemistry" processes. Spatial and temporal control over gelation is possible by thiol-ene click reactions between unsaturated molecules and thiolated alginate derivatives. Under mild conditions, biocompatible crosslinks are produced by enzymatic methods employing transglutaminase or horseradish peroxidase.PVA/SA hydrogels with dual adhesive functionality and antioxidant capabilities were produced by He *et al.* (2024) using a complex chemical technique that combined polydopamine chemistry with tannic acid crosslinking [49]. This method of multi-crosslinking demonstrates how chemical modification can simultaneously impart several desired traits.

2.3.3 Advanced and Stimuli-Responsive Synthesis

One area of SA hydrogel research is the creation of "smart" hydrogels that react to environmental cues. Because alginate is a polyelectrolyte and its carboxyl groups are protonated at low pH and deprotonated at physiological pH, pH-responsive systems take advantage of this property. Using dynamic Schiff base and borate

ester linkages that reversibly form and break in response to pH changes, Lei *et al.* (2025) developed pH-responsive starch/SA hybrid hydrogels [50].

These systems have potential for wound dressings that react to pH changes brought on by infections or for targeted drug administration in the gastrointestinal tract. At particular temperatures, temperature-responsive hydrogels containing chitosan derivatives or poly (N-isopropylacrylamide) (PNIPAM) display sol-gel transitions.

In reducing conditions like intracellular compartments or infected wounds, redox-responsive systems with disulfide bonds break down. Site-specific medication release at infection sites is made possible by enzyme-responsive hydrogels that break down in the presence of bacterial enzymes or matrix metalloproteinases (MMPs).

Dual-adhesive, self-healing alginate hydrogels with dynamic covalent linkages (imine bonds) that reversibly break and reconstruct, enabling the hydrogel to mend itself after damage, were developed by El-Sayed *et al.* (2024). This feature is especially useful for wound dressings that need to continue to provide antimicrobial protection while maintaining integrity during patient movement [51].

2.3.4 Radiation-Induced Synthesis

Unique benefits of radiation treatments include homogeneous crosslinking, sterility, and the lack of chemical initiators. Singh and Singh (2012) showed how gamma radiation may be used to both synthesize silver nanoparticles in situ and crosslink PVP/alginate hydrogels [47].

Similarly, El-Din *et al.* (2023) created nanocomposite hydrogels with outstanding antibacterial characteristics by copolymerizing PVP and SA with pre-formed silver nanoparticles using gamma radiation [53].

Gradient hydrogel structures with spatially variable characteristics are made possible by electron beam radiation, which offers even more control over crosslinking density and pattern.

2.4 Composite and Hybrid Hydrogel Systems

The mechanical integrity and functional adaptability of pure SA hydrogels are frequently insufficient. Thus, one important area of research is creating composites using various synthetic or natural polymers. SA is frequently blended with polyvinyl alcohol (PVA) or polyvinylpyrrolidone (PVP). Lu *et al.* (2024) created SA/PVP hydrogels that demonstrated superior adsorption, thermal stability, and swelling capacity, highlighting the contribution of PVP to improving hydrogel performance [54].

Fadeeva *et al.* (2021) showed how multicomponent systems can be customized for certain biomedical purposes by creating composite films from PVP, SA, and hydroxyapatite for bone healing and wound treatment [55].SA combined with chitosan is another important composite system.Although SA is the core topic of the review, the synergistic effect with chitosan is significant. According to Wathoni *et al.* (2024), chitosan-alginate hydrogels take use of the cationic and anionic characteristics of chitosan and alginate, frequently creating polyelectrolyte complexes that improve mechanical strength and adhesion while offering intrinsic antibacterial qualities [56].

In order to distribute polylysine, Liu *et al.* (2018) specifically created chitosan-sodium alginate nanoparticles. The combination action of the carrier and the payload resulted in increased antibacterial activity against food borne pathogens [57]. Nanocomposite Hydrogels, Adding nanoparticles to the SA matrix has been shown to be a very successful way to increase or impart antibacterial activity. Strong antibacterial activities were demonstrated by Ghasemzadeh and Ghanaat's (2014) synthetic alginate/PVA hydrogels embedded with silver nanoparticles (AgNPs) [58].

Rafati and Naderi-Manesh (2025) developed a sodium alginate-graphene oxide bio-nanocomposite to further this idea. In addition to increasing mechanical strength and hemostatic capacity, the use of graphene oxide increased wound healing in a synergistic manner [59]. El-Din *et al.* (2023) produced a nanocomposite hydrogel

with excellent and long-lasting antibacterial properties by copolymerizing PVP and SA in the presence ofAgNPs using gamma radiation [53].

2.5 Characterization Techniques and Key Findings

A thorough characterization is essential to correlate the synthesis parameters with the final hydrogel's properties and performance.

2.5.1 Structural and Morphological Characterization

i. The main method for verifying chemical interactions in SA-based hydrogels is Fourier-transform infrared spectroscopy (FTIR). Asymmetric stretching of carboxylate groups (1600-1610 cm^{-1}), symmetric stretching (1410-1420 cm^{-1}), and the hydroxyl stretching region (3000-3600 cm^{-1}) are examples of characteristic peaks. Successful crosslinking is indicated by shifts in these peaks; Mohamadinia *et al.* (2021) found a shift from 1612 cm^{-1} in pure SA to 1615 cm^{-1} in acrylic acid-composite hydrogels, showing interaction between carboxyl groups [48]. Similarly, the presence of synthetic polymer components such as PVP or PAA is confirmed by additional peaks that arise at 1255 cm^{-1} (amide III) or 1660 cm^{-1} (amide I).

ii. Scanning electron microscopy (SEM) provides critical insights into hydrogel morphology, porosity, and microstructure. Singh and Singh (2012) utilized SEM to demonstrate the highly porous, interconnected network of PVP/alginate-AgNP hydrogels, with pore sizes ranging from 50-200 μm ideal for cell migration and nutrient diffusion in wound healing applications[47]. Freeze-drying preserves this porous structure, allowing visualization of the three-dimensional network. More advanced techniques like cryo-SEM maintain the hydrated state, providing more accurate representation of in vivo conditions.

iii. The crystalline and amorphous portions of hydrogels can be distinguished via X-ray diffraction (XRD) research. When crystalline nanoparticles like AgNPs or ZnO are added, sharp peaks are introduced, but pure SA displays the broad halos typical of amorphous polymers. The face-centered cubic crystalline structure of silver nanoparticles in alginate/PVA hydrogels was verified by Ghasemzadeh and Ghanaat (2014) by XRD [58]. The degree of crystallinity affects degradation rates, swelling behavior, and mechanical characteristics.

2.5.2 Mechanical and Rheological Properties

Both bulk characteristics (compressive/tensile strength) and viscoelastic behavior (rheology) are included in mechanical characterization. The compressive modulus, which for SA-based hydrogels usually ranges from 1 to 100 kPa depending on crosslinking density and composition, is revealed by uniaxial compression testing. Due to several crosslinking methods, He *et al.* (2024) observed compressive strengths for PVA/SA/polydopamine/tannic acid hydrogels surpassing 200 kPa [49].Through storage modulus (G', elastic component) and loss modulus (G", viscous component), rheological study sheds light on viscoelastic behavior. The majority of hydrogels show G' > G" over a range of frequencies, indicating solid-like behavior. The best wound dressings retain constant moduli across physiological frequencies (0.1-10 Hz), and frequency sweeps evaluate structural integrity. Composite hydrogels generally exhibit more frequency-independent behavior than pure SA gels, indicating more stable networks, according to Cao *et al.* (2025) [60]. Time sweeps are essential for injectable formulations that need to gel quickly after delivery because they track the kinetics of gelation.

2.5.3 Swelling Behavior

Water absorption capacity is measured by swelling studies and is commonly represented as equilibrium water content (EWC) or swelling ratio (SR). SA hydrogels

swell in response to pH because of the ionization of carboxyl groups (pKa ∼3.5). For starch/SA hybrid hydrogels, Lei *et al.* (2025) showed significant swelling ratio increases from ∼5 at pH 2.0 to ∼25 at pH 7.4, making them perfect for intestinal-targeted administration [50]. Swelling is also influenced by temperature, ionic strength, and particular ions; settings high in calcium can result in less swelling and more crosslinking.

Degradation studies assess the stability of hydrogels under physiological settings by tracking changes in molecular weight or mass loss over time. Alginate lyase-based enzymatic degradation sheds light on biological breakdown. In vitro breakdown in phosphate-buffered saline (PBS) or simulated bodily fluids (SBF) mimics in vivo activity. Due to more crosslinks or more stable polymer components, composite hydrogels often degrade more slowly than pure SA. While pure SA hydrogels deteriorated in 3-5 days, Lu *et al.* (2024) found that SA/PVP hydrogels retained structural integrity for more than 14 days in PBS [54].

2.5.4 Thermal Analysis

Thermogravimetric analysis (TGA) determines the stages of breakdown by measuring weight loss as a function of temperature. SA usually exhibits total combustion above 400°C, polymer backbone breakdown between 200 and 300°C, and beginning water loss below 100°C. Decomposition temperatures are raised by the addition of thermally stable substances like PVP or nanoparticles. According to Lu *et al.* (2024), SA/PVP hydrogels showed 50% weight loss at 280°C as opposed to 240°C for pure SA, suggesting enhanced thermal stability [54]. Glass transition (Tg), melting (Tm), and crystallization temperatures are among the thermal transitions that can be found using differential scanning calorimetry (DSC). SA-based hydrogels usually have a Tag between 80 and 120°C, which rises with crosslinking density. UV-Vis spectroscopy measures drug loading and release as well as nanoparticle content (e.g., AgNP surface plasmon resonance at ∼420 nm). Fluorescence spectroscopy can be used to detect conformational changes in protein therapeutics or track fluorescently-labeled components.

2.6 Sodium Alginate as a Promising Hydrogel Material

Sodium alginate is a naturally occurring anionic polysaccharide extracted mainly from brown seaweeds. It consists of linear copolymers of β-D-mannuronic acid (M) and α-L-guluronic acid (G) units arranged in varying sequences along the chain. The presence of carboxyl and hydroxyl groups in its structure enables strong water affinity and easy chemical modification. One of the most important properties of sodium alginate is its ability to form hydrogels through ionic crosslinking with divalent cations such as calcium (Ca^{2+}). This "egg-box" model of gel formation provides a stable three-dimensional network with tunable porosity and mechanical strength [61, 62].

Because of its biocompatibility, non-toxicity, and biodegradability, sodium alginate has been widely used in biomedical and pharmaceutical applications. It serves as a carrier matrix for drug encapsulation and controlled release, allowing the protection and sustained delivery of therapeutic molecules. In wound healing, alginate-based hydrogels maintain a moist environment, promote hemostasis, and accelerate tissue regeneration. Moreover, alginate hydrogels are employed in tissue engineering as scaffolds that support cell attachment and growth, and in encapsulation of cells or bioactive agents for targeted therapies [63]. In addition to its biomedical utility, sodium alginate is eco-friendly and sustainable, derived from renewable marine sources. It is safe for biological systems and does not release harmful byproducts upon degradation. These characteristics make it a promising and environmentally responsible material for the development of modern hydrogel-based biomaterials [63].

Alginate-based hydrogels and scaffolds have been extensively researchedcontrolled-release systems are used for a variety of applications, including dermal treatments, cancer therapy and antimicrobial solutions. This research has driven significant progress, enabling the development of personalized systems that respond to external stimuli and promote tissue healing. Notably, the past decade has seen a surge in research on alginate-based materials, with a growing trend expected to continue

in the coming years, driven by advancements in dermal applications, drug delivery, cancer treatment, and antimicrobial material [64].

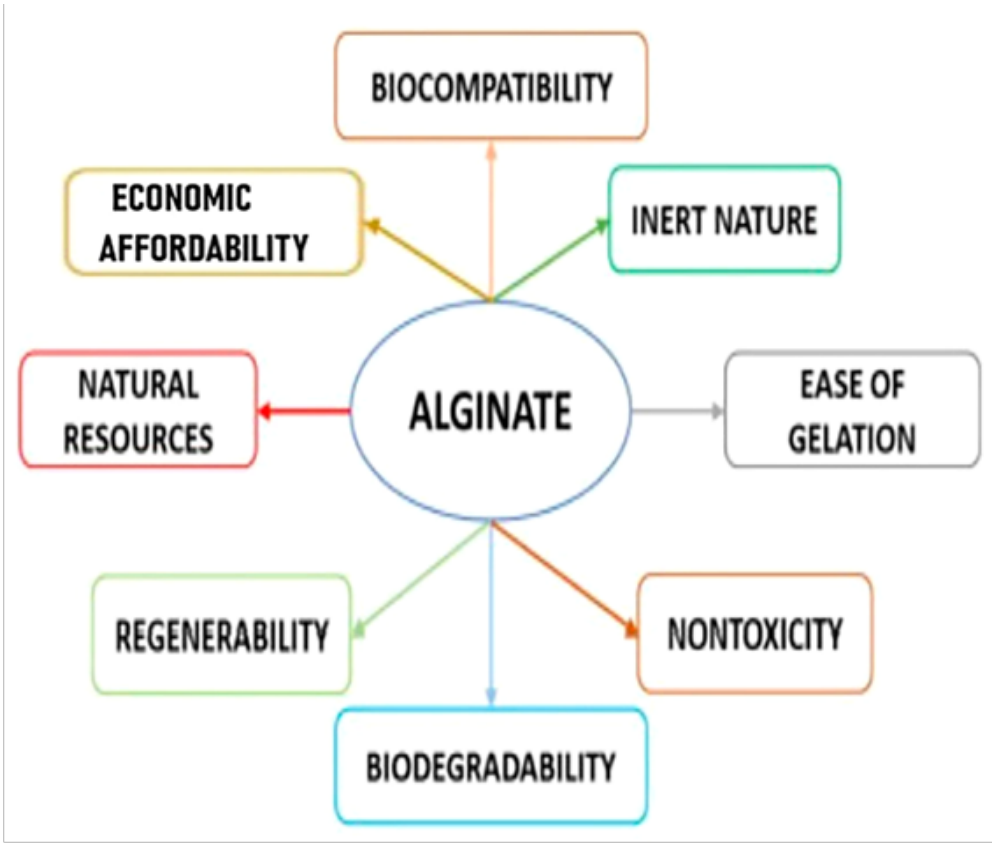

FIGURE 2.5: Illustration of outstanding properties of alginate [64].

2.7 Applications of Hydrogels

Hydrogels have found extensive applications in various biomedical and pharmaceutical fields due to their high-water content, tissue-like consistency, and tunable physicochemical properties. They are widely employed as drug delivery systems that provide controlled and sustained release of therapeutic agents, as wound dressings that maintain a moist healing environment, and as tissue engineering scaffolds that support cell attachment and growth. Additionally, hydrogels are used in biosensors, contact lenses, and regenerative medicine, highlighting their versatility and potential in improving healthcare technologies [65].

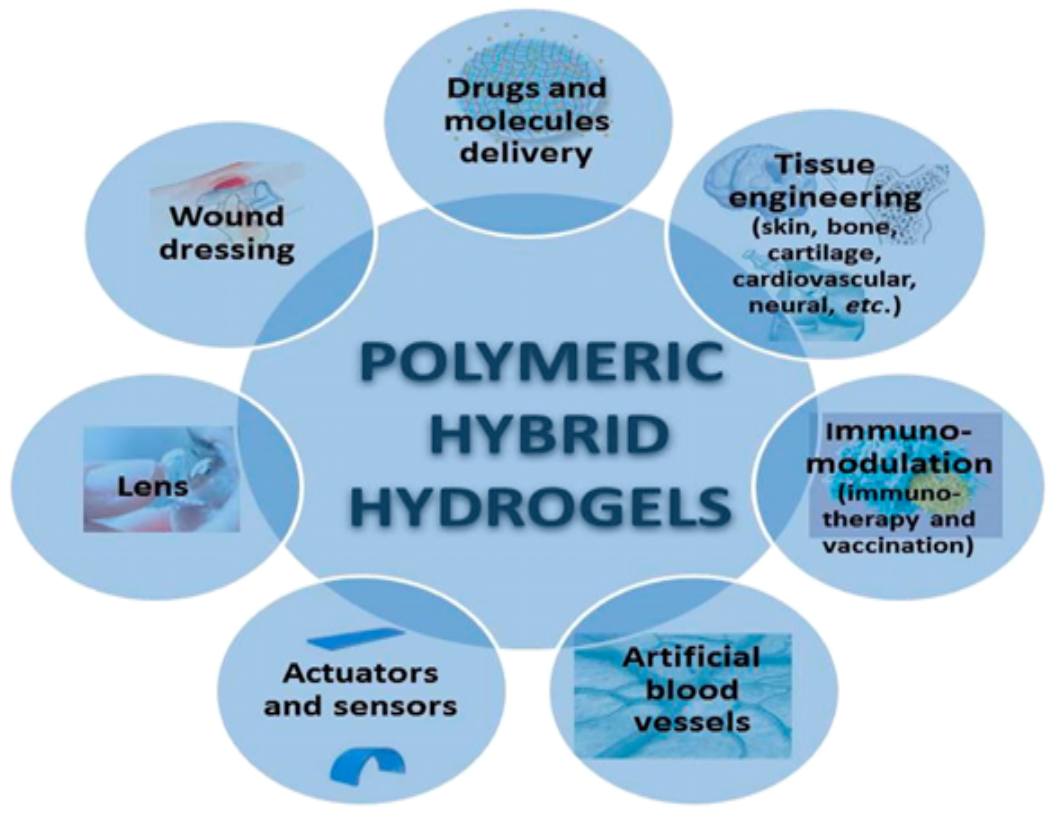

FIGURE 2.6: Hydrogels and its application in various fields [66].

2.8 PVP and Sodium Alginate-Based Hydrogels: Properties and Applications

Colorless and odorless, poly (vinylpyrrolidone) (also referred to as PVP) is a synthetic substance having a wide range of uses in both industry and medicine [72]. Because of its hydrophilic carbonyl groups, it may effectively adsorb aqueous liquids and create hydrogels. Brown seaweed is the source of sodium alginate (NaAlg), a naturally occurring anionic polymer with moderate gel-forming ability, low toxicity, and biocompatibility [68, 69]. A semi-permeable polymer network that improves mechanical stability while retaining high adsorption efficiency can be created by mixing NaAlg with PVP, as many natural polymers have poor mechanical strength on their own [70]. A synthetic polymer that is biocompatible, polyvinylpyrrolidone (PVP) is utilized in medication formulations and biomaterials. PVP crosslinks to create hydrogels, which are highly well-hydrated, swellable polymer networks, in response to stimuli like heat or radiation.

These hydrogels are very biocompatible and transparent. However, PVP hydrogels' low swelling capacity and poor mechanical qualities restrict their application. Hydrogel characteristics are enhanced by combining PVP with polysaccharides (such as alginate and chitosan [52]. The majority of bonded PVP hydrogels are physical hydrogels created by UV crosslinking, electron beam synthesis, γ-irradiation, etc. PVP-based hydrogels offer a wide range of biological uses, including drug delivery, implants, artificial cartilage, and wound healing. They provide advantages like oxygen permeability, bacterial barrier, flexibility, and transparency. Their characteristics can be modified for certain applications, such as grafted structures or semi-IPN.Commercial hydrogels for wounds, burns, and ulcers include BARC (India), Nu-Gel (Johnson & Johnson), Neoheal (Kikgel, Poland), and VIACELL (Czech Republic). They provide sterility through radiation crosslinking, moist healing, pain reduction, and painless removal. PVP-based mix hydrogels are the focus [72].

2.8.1 Mechanisms of Action

i. Metallic Nanoparticles (e.g., Ag, ZnO): Ag^+ ions released from AgNPs disrupt bacterial cell membrane integrity, inhibit respiratory enzymes, and cause DNA damage [47, 53, 58]. Shao *et al.* (2018) highlighted the green synthesis of SA-AgNPs and their potent antibacterial activity [73].

ii. Antibiotics (e.g., Linezolid, Vancomycin): These are released from the hydrogel matrix to exert their specific pharmacological action on bacteria. Sustained release prolongs the effective concentration at the infection site [74, 75].

iii. Natural Polymers (e.g., Chitosan): The cationic amino groups of chitosan interact with negatively charged bacterial cell walls, disrupting membrane permeability [56, 57].

iv. Natural Compounds (e.g., Tannic Acid): Acts as a crosslinker and antimicrobial agent by precipitating microbial proteins and enzymes [49].

2.8.2 Efficacy Assessment

i. Antibacterial activity is typically evaluated in vitro using:

ii. Disk Diffusion/Kirby-Bauer Test: Measures the zone of inhibition (ZOI).

iii. Time-Kill Assays: Evaluates bactericidal kinetics.

iv. Minimum Inhibitory Concentration (MIC) Determination: Finds the lowest concentration that inhibits visible growth.

v. Biofilm Inhibition/Disruption Tests: Crucial for treating chronic wounds.

vi. Studies like Ghasemzadeh and Ghanaat (2014) and El-Din *et al.* (2023) consistently report strong ZOIs and low MICs for SA-based nanocomposite hydrogels against model pathogens like Escherichia coli and Staphylococcus aureus[53, 58].

2.9 Linezolid Loaded Hydrogel Systems

A synthetic oxazolidinone antibiotic, linezolid is effective against a wide range of Gram-positive bacteria, including vancomycin-resistant Enterococci (VRE) and methicillin-resistant Staphylococcus aureus (MRSA). By attaching to the 50S ribosomal subunit and blocking the development of the initiation complex, it inhibits bacterial protein production. Cross-resistance with other antimicrobial drugs is rare because of its unique mode of action [77]. Long-term systemic dosing of linezolid has been linked to side effects include myelosuppression and peripheral neuropathy, despite the drug's superior oral bioavailability and tissue penetration. To enhance safety and therapeutic results, these restrictions require the creation of targeted drug delivery systems [77]. Hydrogels provide a moist environment, encourage tissue regeneration, and improve patient compliance in the treatment of wounds and skin infections. Antibiotics can be sustained at the site of infection by incorporating them into hydrogel matrix, which lowers systemic exposure and dosage frequency [79, 80].

2.10 Linezolid-Loaded Hydrogel Formulations

Hydrogels loaded with linezolid have been created using a variety of synthetic and natural polymers. Because of their advantageous physicochemical and biological characteristics, chitosan, alginate, carbopol, poloxamer, and polyvinyl alcohol are some of the most often researched polymers [78, 80]. Linezolid-containing chitosan-based hydrogels have shown improved antibacterial efficacy and prolonged drug release against resistant bacterial strains. These systems' therapeutic efficacy is further enhanced by chitosan's inherent antibacterial and wound-healing qualities [78].

2.11 Linezolid Drug Release and Antimicrobial Activity

A two-phase release characteristic, comprising an initial burst release and a protracted diffusion-controlled release, is commonly observed in in vitro drug release investigations of linezolid-loaded hydrogels. This strategy is advantageous for quickly lowering the bacterial burden while sustaining long-term therapeutic medication concentrations [78, 81]. After being incorporated into hydrogel systems, linezolid maintains its antibacterial activity, according to antimicrobial evaluation utilizing agar diffusion and time-kill experiments. Significant inhibitory action against Enterococcus species and Staphylococcus aureus has been reported [78, 81].

2.12 Applications in Wound and Skin Infection Treatment

Hydrogels filled with linezolid are very useful for treating burns, post-surgical infections, and infected wounds. High drug concentration at the infection site

is made possible by localized delivery, which also reduces systemic side effects [80, 82]. Hydrogel formulations have been demonstrated to improve wound healing by preserving hydration and promoting tissue regeneration in addition to their antibacterial properties. When compared to traditional topical antibiotic formulations, preclinical research shows better healing results [80, 81]. Despite encouraging outcomes, more investigation is needed to assess the long-term stability, viability of large-scale production, and therapeutic efficacy of hydrogel systems loaded with linezolid. To combat antimicrobial resistance and enhance patient outcomes, future advancements might concentrate on combination medicines and intelligent or stimuli-responsive hydrogels [82].

Chapter 3

Material and Methods

The materials used in this experiment comprises of different chemicals and reagents, apparatus and equipment.

3.1 Chemicals and Reagents

Sodium Alginate (341.36 g/mol) naturally occurring polymer extensively utilized in food, medicine, and biotechnology as a thickening, stabilizer, and gelling agent as well as in wound dressings and drug delivery systems. Polyvinylpyrrolidone (2,500-2,500,000 g/mol)Water-soluble polymer employed as a stabilizer in medicines. $CaCl_2$ (110.98 g/mol) it is employed to cross-link sodium alginate.PBS (239.30 g/mol, PH 7.4), Acetate buffer (0.1 M, PH 3.0), NaOH (0.1 M, PH 13) Linezolid 600mg(110.98 g/mol) bought from a local company (Continental pharmaceuticals Karachi Pakistan) and Distilled water (H_2O) was used for solution preparation.

3.2 Preparation of Hydrogels

Solution casting techniques was used by mixing the components of Na-Alginate, PVP and $CaCl_2$ in specific ratios dissolve in water, and cross-link to form hydrogels.

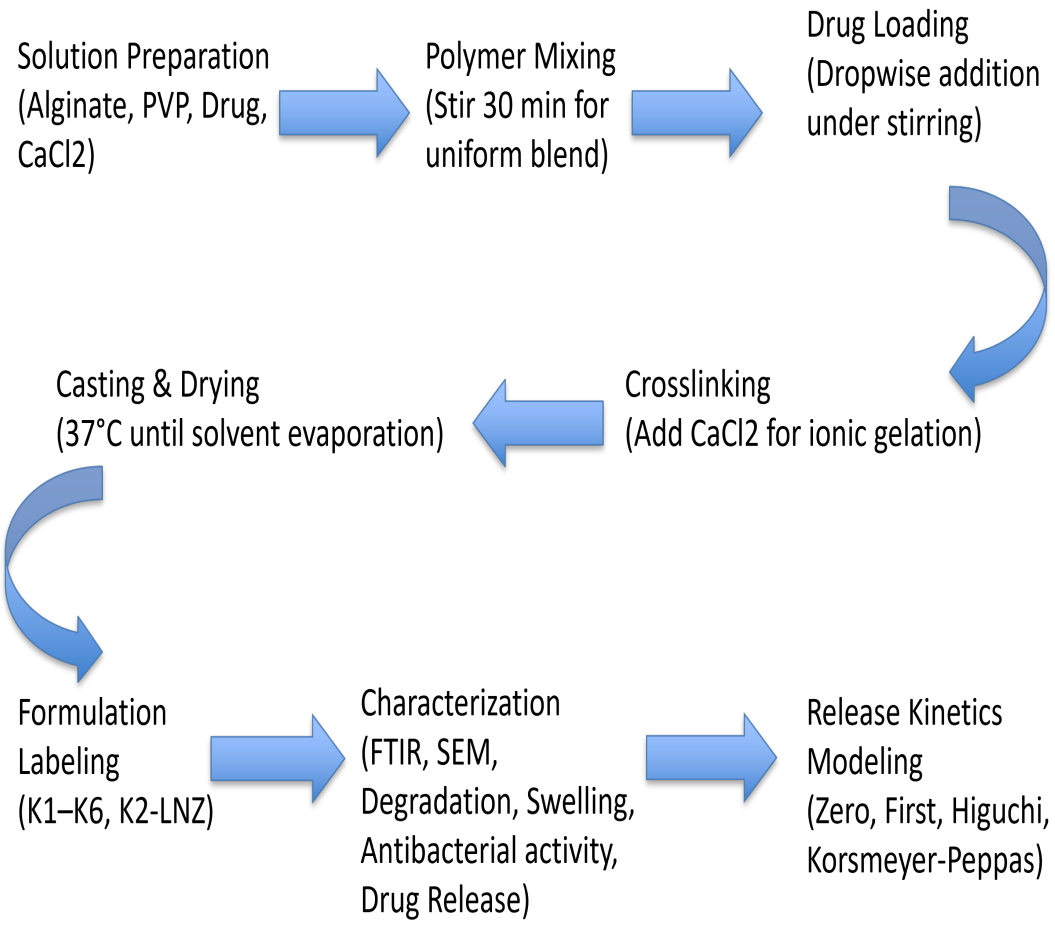

FIGURE 3.1: Modified Schematic representation with synthesis procedure of hydrogels [118].

3.2.1 Preparation of Sodium Alginate Solution

In the first step NA alginate (1.5g & 1g) each dissolved in 100 mL of distilled water under continuous magnetic stirring at room temperature until a clear and homogeneous polymer solution was obtained.

3.2.2 Preparation of PVP Solution

In the second step PVP (1.5g & 1g) each dissolved in 100mL of distilled water under continuous magnetic stirring at room temperature until a clear and homogeneous polymer solution was obtained.

3.2.3 Preparation of Drug Solution

Linezolid 600 mg dissolved in 60 ml of distilled water and stirred gently at 300 rpm until fully dissolved.

3.2.4 Preparation of $CaCl_2$ Solution

Calcium chloride($CaCl_2$) used as a cross linking agent prepared 1% (1g) and 2% (2g) solution by dissolving in 100 ml distilled water.

3.2.5 Mixing Hydrogel Formation

After preparation of NA alginate and PVP solutions both are mixed with different ratios as shown in table below and stirred the mixture for 30 minutes to form a uniform blend.

3.2.6 Drug Loading

Before the addition of cross linker ($CaCl_2$) the selected drug linezolid (1g/1ml) slowly added drop wise into the mixture under constant stirring to ensure uniform dispersion.

3.2.7 Addition of $CaCl_2$

After drug loading the crosslinker calcium chloride solution was added gradually to the polymer mixture to initiate ionic crosslinking.

3.2.8 Casting and Drying

The homogeneous mixture was poured onto clean Petri dishes and dried at 37°C until complete solvent evaporation occurred. After drying stored the dried samples in airtight containers for further characterization and testing.

Hydrogels were labeled K1, K2, K3, K4, K5, K6 and K2-LNZ.

TABLE 3.1: Hydrogels formulation

Hydrogels	**NA alginate (1.5%w/v)**	**NA alginate (1% w/v)**	**PVP (1.5% w/v)**	**PVP (1% w/v)**	**$CaCl_2$ (1% w/v)**	**$CaCl_2$ (2% w/v)**	**Linezolid (mg)**
K1	50ml	-	50ml	-	-	20ml	-
K2	70ml	-	30ml	-	-	20ml	-
K3	-	70ml	-	30ml	-	20ml	-
K4	-	50ml	-	50ml	50ml	-	-
K5	-	60ml	-	40ml	40ml	-	-
K6	-	40ml	-	60ml	50ml	-	-
K2-LNZ	35ml	-	15ml	-	20ml	-	70

3.3 Characterization Techniques

Some of the widely used to analyze and determine the properties of the materials are:

3.3.1 Fourier Transform Infrared Spectroscopy

Thermo Scientific and Nicolet 6700 attenuated total reflection-fourier transform infrared spectroscopy were utilized to ascertain the chemical groups present in K2, K5 and K2-LNZ hydrogels. Infrared radiation is sent through a sample in order for FTIR to function. Certain frequencies that correlate to the vibration modes of bonds of chemical substance are absorbed by the molecules that are in the sample. The consequent interference pattern is captured by an interferometer and then

statistically converted using Fourier analysis to provide an infrared spectrum. The combination of FTIR with microscope (FTIR microscopy) for regionally resolved chemical analysis is one of the recent advancement that is particularly helpful in materials and medicinal research [83].

Certain functional groups, including hydroxyl group, carbonyl amino, and phosphate groups, can be identified by FTIR. It is quick, non-destructive, and requires little sample preparation. The dried hydrogels were subjectedto the instrument under vacuum at a scan range of 400-4000 cm^{-1}.

3.3.2 Scanning Electron Microscopy

3.3.2.1 Working Principle

The K2 and K2-LNZ hydrogels were characterized with a field emission scanning electron microscope (FE - SEM), LEO 435 VP, MIRA TESCAN, and Jena, Germany. The prepared hydrogels' surface morphology and porosity were examined with FE-SEM.

In-situ SEM allows real-time observation of dynamic processes including deformation, decomposition, or drug release, while environmental SEM (ESEM) enablesscanning of hydrated samples [84].

3.3.3 In vitro Degradation

We conducted a 7 days in vitro degradation study and all the six samples K1, K2, K3, K4, K5, and K6 were submerged in four different mediums including PBS, Alkaline, Acidic and Distilled water. All the samples were weighted before submerging in degradation medium and then measured the weight on each day by removing the surface water with the help of a filter paper and weight loss was observed by deduction of initial and final weights using Equation.

The measurements were taken after different time intervals, i.e. days 1, 2, 3, 4, 5, 6 and 7. The weight loss is calculated by utilizing Equation (3.1).

$$Degradation\ Rate\ = \frac{W_{in} - W_{fn}}{W_{in}} \times 100 \tag{3.1}$$

Here, W_{in} and W_{fn} represent the initial weight of the gels before incubation and the final weight of the gels after incubation, respectively.

3.3.4 Swelling Analysis

3.3.4.1 Working Principle

Swelling tests measure weight gain increase change in dimension over time by submerging a hydrated specimen in a fluid. Crosslink the density, hydrophilicity of the material, and network structure all affect the material's ability to absorb fluids, which is reflected in the swelling ratio. Recent Developments & Uses: In order to provide intelligent drug delivery systems, recent research focuses on stimuli-responsive hydrogels that expand or contract in reaction to pH, ambient temperature, or ionic strength [85].

The swelling ability of gels was assessed by keeping in PBS, Alkaline, Acidic and Distilled water. The hydrogels were weighed and kept in 20 ml each medium for 24 h. The analysis of the swelling ability was calculated by using Equation (3.2).

$$SR = \frac{W_d - W_s}{W_d} \times 100 \tag{3.2}$$

Here, W_S represents gels weight after swelling, and Wd shows the initial weight of the gel before swelling.

3.3.5 Antibacterial Activity

The K2 and K2-LNZ hydrogel films were characterized with a field emission scanning electron microscope (FE - SEM), LEO 435 VP, MIRA TESCAN, and Jena,

Germany. The prepared hydrogels' surface morphology and porosity were examined with FE-SEM [86].

An agar disk diffusion method complying with National Committee for Clinical Laboratory Standards guidelines (NCCLS 2000) were per-formed to assess the antibacterial effect of hydrogel. The hydrogel film was tested against *Escherichia coli* (*E. coli*), and *Staphylococcus aureus* (*S. aureus*) in comparison to antibiotics. Initially, nutrient agar (Oxoid - UK) was pre-pared as per manufacturer's instructions and autoclaved at 121oC for 25 min. Later, the agar was transferred to sterile petri dishes and let solidify at room temperature. The overnight cultured inoculum of *Escherichia coli* (*E. coli*) and *Staphylococcus aureus* (*S. aureus*) were uniformly spread over solidified media plates using a sterile glass spreader. The hydrogel film and antibiotic were introduced to the bacteria spread plates and incubated at 37 °C for 24 h. After 24 h, images of inhibition zones on agar culture plates were taken and analyzed by Image J software to measure inhibition zones.

3.3.6 Drug Loading and Release Kinetics

3.3.6.1 Working Principle

Incorporating medicinal chemicals into carriers like hydrogels, microspheres, or nanoparticles is known as drug loading. In order to determine the mechanism of release (diffusion, erosion, or swelling-controlled), release kinetics are examined by submerging the loaded material in a release medium, sampling over time, and fitting data to mathematical models. Current Developments and Uses: For combination treatments, recent studies use nanocarriers with targeted released qualities, responsive to stimuli discharge (pH, temperature), and multiple drugs loading [87].

The release of drug at the targeted site from said hydrogel film was measured by immersion of hydrogel film in 10mL PBS. The fractions were taken at intervals of 1, 2, 3, 4, 5, 6, 7 days and absorbance was measured at OD300 via ultraviolet - visible spectroscope (Thermoscientific, Genesys 10S UV - Vis spectroscope). The calibration curve of drug was drawn by varying the absorbance values from 0 to 1.

The measured absorbance values of drug were compared to the drawn calibration curve and cumulative release was evaluated over time.

Immersion of the hydrogel film (1 mg 0.03 g) in 10 mL PBS was used to measure the drug's release at the intended location. The fractions were taken at intervals of 1, 2, 3, 4, 5, 6, 7 days and absorbance was measured at OD300 via ultraviolet - visible spectroscope (Thermoscientific, Genesys 10S UV - Vis spectroscope).

The drug's calibration curve was created by adjusting the absorbance values from 0 to 1. Drug absorbance values were compared to the calibration curve, and cumulative release over time was evaluated. The mathematical forms of the empirical models of First order, Zero order, Higuchi, and Korsmeyer-Peppas that investigated the time-dependent kinetics of linezolid release can be found in Equations 3.3-3.6, respectively [88]. These models provides mechanistic understanding and process involved in drug (linezolid) release from K2-LNZ hydrogel.

$$\text{First-order model: } Q_t = Q_\infty \left(1 - e^{-k_1 t}\right) \tag{3.3}$$

Where Q_t is the remaining drugs after time (t) and Q_∞ is total amount releasable while k1 First-order release rate constant.

$$\text{Zero-order model: } Q_t = Q_0 + k_0\, t \tag{3.4}$$

In the zero-order release model, the total drug released (Q_t) at any given time (t) is calculated by starting with the initial amount (Q_0) and adding the product of the release rate constant (k_0) and the elapsed time.

$$\text{Higuchi model: } Q_t = k_H \sqrt{t} \tag{3.5}$$

In the Higuchi model, the cumulative drug released (Q_t) at any time point is directly proportional to the square root of time ($\sqrt{t}$), with the Higuchi constant (k_H) representing the rate of this diffusion-controlled release.

$$\text{Korsmeyer-Peppas model: } \frac{M_t}{M_\infty} = k\, t^n \tag{3.6}$$

The Korsmeyer-Peppas model states that the fractional drug released (M_t/M_∞) follows a power-law relationship with time (t^n), where the release exponent (n) reveals the underlying physical mechanism of transport from the delivery system.

3.3.7 Statistical Analysis

MATLAB and Origin software were used to statistically analyze the experimental data. Every experiment was carried out in triplicate, and the mean ± standard deviation (SD) was used to express the results. While MATLAB was utilized for sophisticated numerical analysis and mathematical modeling, Origin software was utilized for data processing, graphical display, and curve fitting. The results' reliability and significance were assessed using the proper statistical methods. To guarantee the accuracy and reliability of the data, correlation and error studies were also carried out. Statistical significance was defined as a significance level of $p < 0.05$. The validity and scientific credibility of the experimental results were guaranteed by this scientific methodology.

Chapter 4

Results

4.1 Scheme

The scheme shows how to create a drug-loaded hydrogel by combining a mixture of calcium chloride ($CaCl_2$), polyvinyl pyrolidone (PVP), and sodium alginate (Na Alg). The resultant matrix is then filled with a drug over controlled release applications after undergoing solution casting to create a cross-linked hydrogel network through Ca^{2+} alginate interaction.

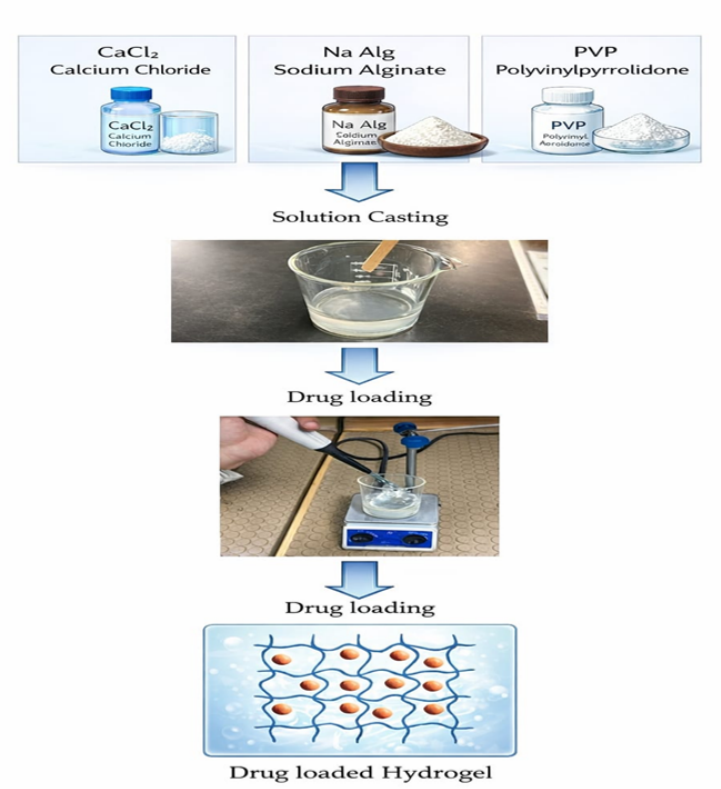

FIGURE 4.1: Graphical representation of gel synthesis and drug loading.

4.2 Hydrogel Synthesis

In figure (4.2) the prepared hydrogels are displayed

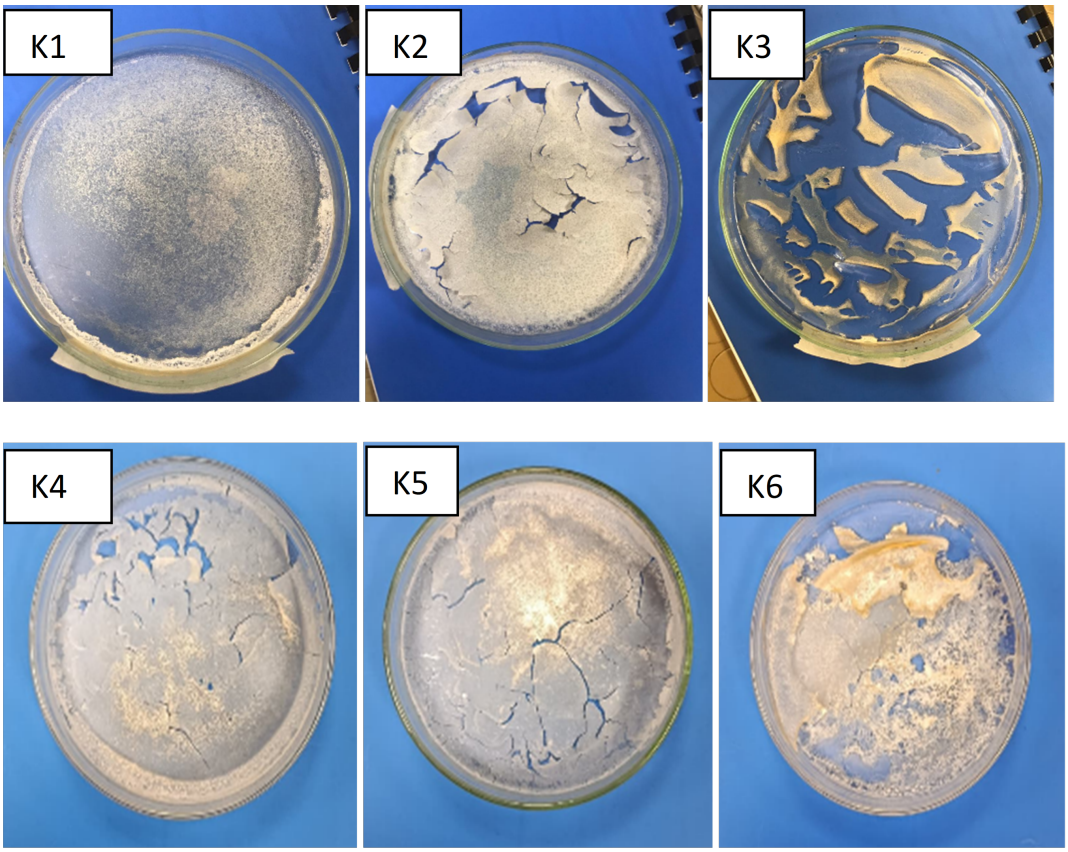

FIGURE 4.2: Pictures of the prepared hydrogels.

4.3 Swelling Studies

To make sure the polymer network has absorbed as much solvent as possible and attained a stable swelled condition, equilibrium swelling is frequently measured in hydrogel swelling investigations following a lengthy immersion period. Since this period of time has been demonstrated to capture near-maximal swelling for a variety of hydrogel formulations and situations, many researchers submerge dry hydrogel samples in aqueous fluid and measure the mass or dimensions after 24 hours to determine the equilibrium swelling ratio.

To assess the absorption behavior of hydrogel, Zhang et al., for instance, provide measurements of the swelling ratio obtained after a 24-hour immersion in water [93].

During 24 hours, we tested the swelling of hydrogel samples using a variety of solutions, such as distilled water plus an acidic solution, PBS, and an alkaline solution. The findings showed that the surrounding environment had a considerable impact on the hydrogel's swelling behavior. Deprotonation of functional groups probably improved electrostatic repulsion within the polymer network in alkaline circumstances, increasing swelling.

On the other hand, the hydrogel may have shrunk or swelled less in acidic conditions due to protonation of these groups. The hydrogel's behaviour was affected differentially by PBS's ionic strength and buffering ability, indicating the hydrogel's potential responsiveness in physiological settings.

This study demonstrates the long-term effects of pH and ionic composition on the hydrogel's characteristics.

4.3.1 Swelling in Alkaline Buffer

All hydrogel samples Figure (4.3) showed an increase in weight after 24 hours in alkaline buffer, confirming that the hydrogels absorb the buffer solution. This indicates that the polymer networks are hydrophilic and capable of retaining fluid under alkaline conditions.

In our K3 absorbed the most buffer in total (highest absolute weight), it started with a much larger initial mass shown in figure (4.3) left graph. K1 and K4, in contrast, started with less material but expanded more dramatically relative to their own size.

In summary the high relative swelling of K1 and K4 highlights their superior swelling efficiency per unit mass, which is a key indicator of a highly responsive and open polymer network structure optimized for expansion under alkaline conditions while K2 and K5 shows moderate but control swelling ratios.

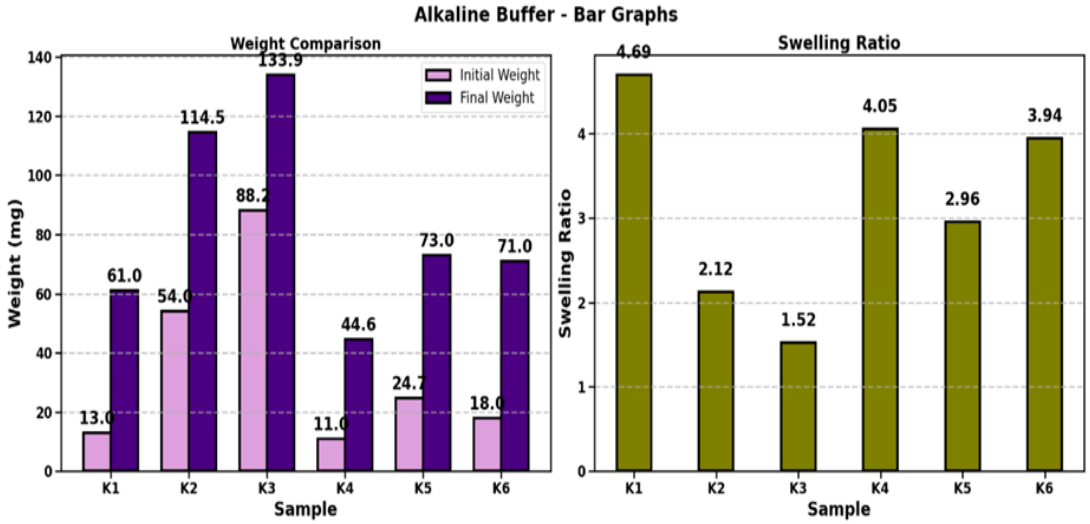

FIGURE 4.3: The left graph shows weight comparison and the right graph shows swelling ratio of Hydrogels in alkaline Buffer.

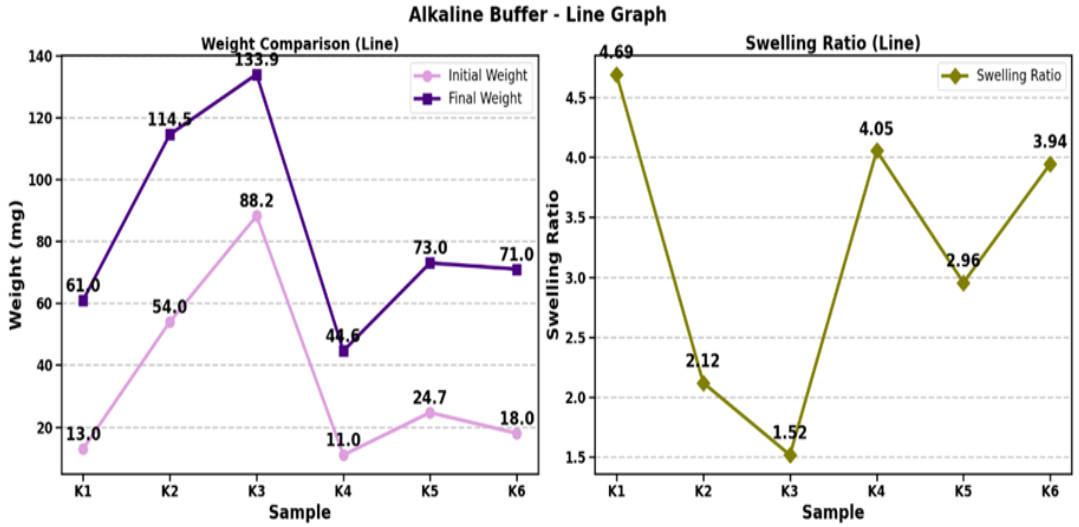

FIGURE 4.4: Swelling and weight progression in Alkaline Buffer.

4.3.2 Swelling in Distilled Water

Distilled water creates an environment for maximum possible swelling in these hydrogels. The graph and data show a clear and significant increase in swelling compared to the alkaline buffer condition. The most striking result is that all hydrogels swelled more in distilled water. This is visually clear from the larger green bars (final weight) in the distilled water graph compared to the purple bars in the alkaline graph. All samples (K1-K6) show substantial weight gain (green bars > gray bars). K6 shows the highest swelling ratio (6.48), indicating it is the most efficient at utilizing osmotic pressure for expansion relative to its own mass.

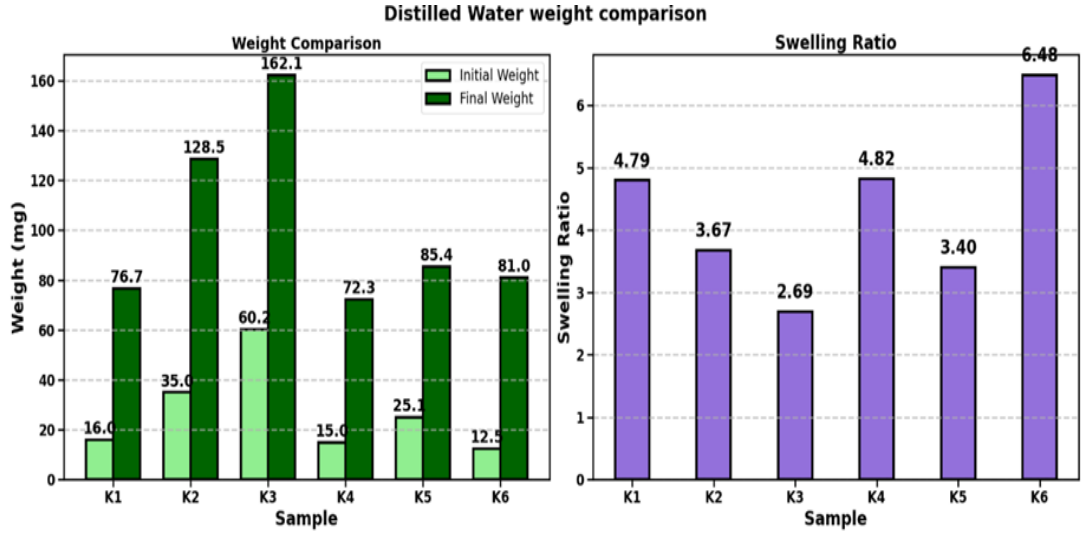

FIGURE 4.5: The left graph shows weight comparison and the right graph shows swelling ratio of Hydrogels in Distilled water.

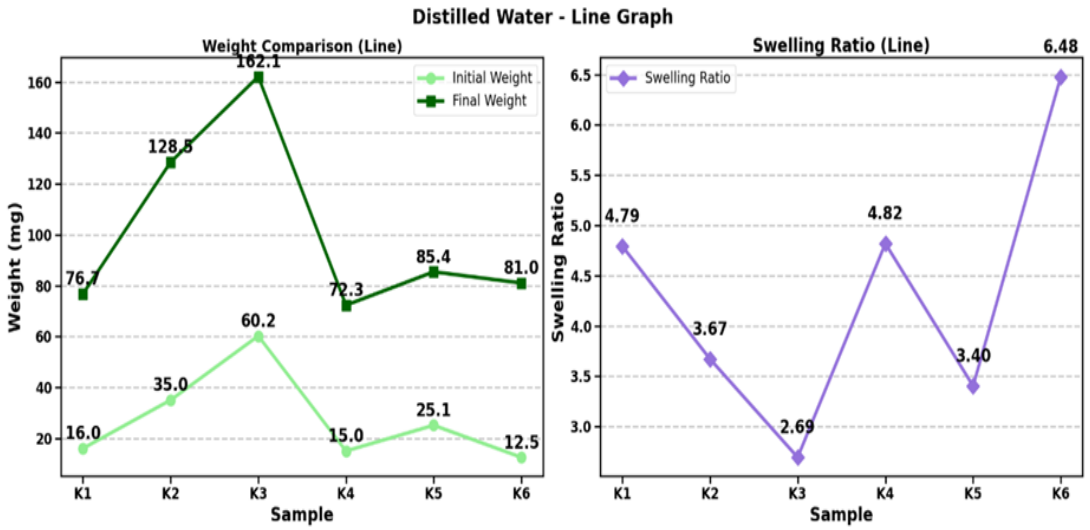

FIGURE 4.6: Swelling and weight progression in distilled water.

4.3.3 Swelling in Acidic Buffer

The swelling performance of six hydrogel samples (K1–K6) in an acidic buffer, expressed as the swelling ratio (final swollen weight divided by initial dry weight). The values clearly show that while all samples absorbed fluid and expanded, the degree of swelling varies significantly between compositions. Sample K6 exhibits the highest swelling ratio (∼4.35), indicating it expanded to over four times its original mass, while K2 shows the lowest ratio (∼2.33). This variation highlights how differences in polymer chemistry, cross-linking density, and the type or density

of ionizable groups influence a hydrogel's responsiveness even under the generally restrictive conditions of a low-pH environment.

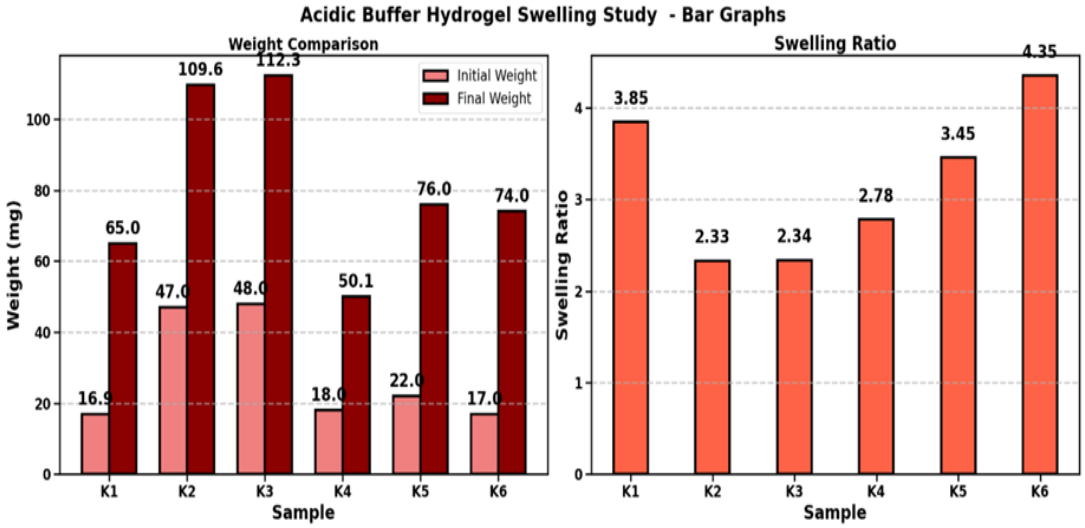

FIGURE 4.7: The left graph shows weight comparison and the right graph shows swelling ratio of Hydrogels in Acidic Buffer.

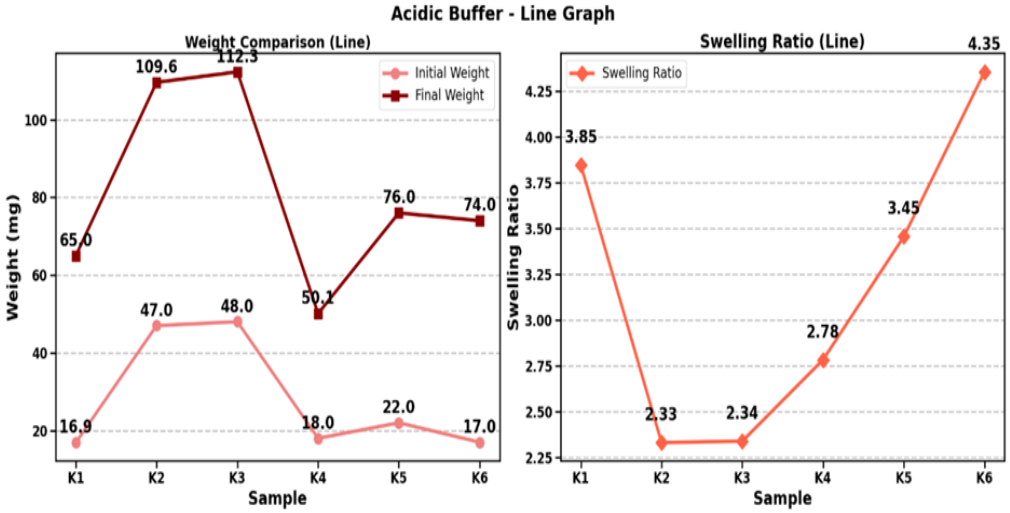

FIGURE 4.8: Swelling and weight progression in acidic Buffer.

4.3.4 Swelling in PBS

The swelling performance of the hydrogels in Phosphate Buffered Saline (PBS) provides essential insight into their behavior under physiologically relevant conditions. PBS, with its neutral pH (∼7.4) and controlled ionic strength, mimics the environment of bodily fluids, making these results directly applicable to potential biomedical uses.

The data reveal that while swelling is substantial across all samples, it is characteristically modulated by the presence of dissolved ions, which induce a partial charge-screening effect.

This screening reduces the electrostatic repulsion between polymers chains compared to distilled water, yet does not suppress it entirely, allowing for considerable hydration and network expansion.

Notably, samples K1 and K4 demonstrated exceptional swelling ratios, indicating highly responsive network architecture capable of massive fluid uptake even in an ionic medium.

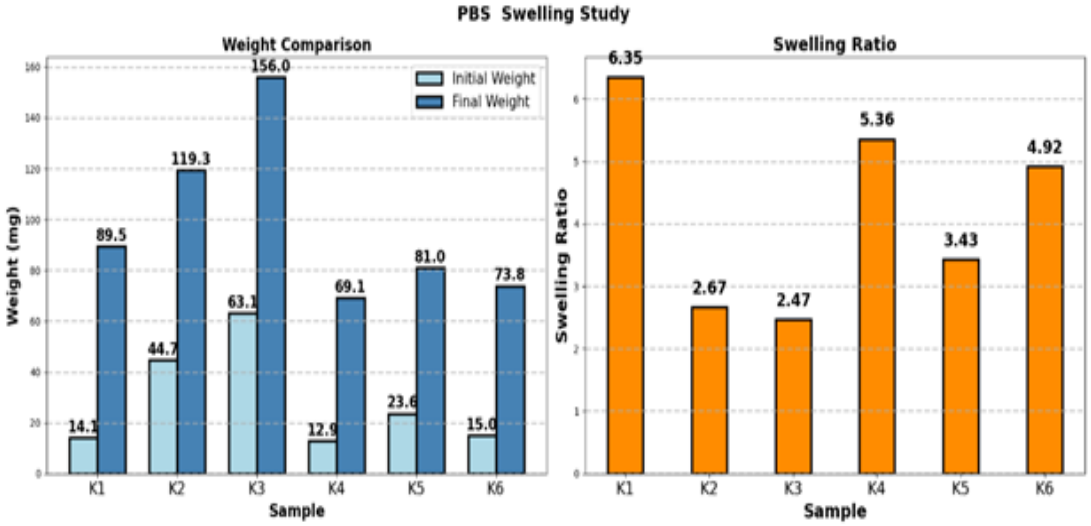

FIGURE 4.9: The left graph shows weight comparison and the right graph shows swelling ratio of Hydrogels in PBS.

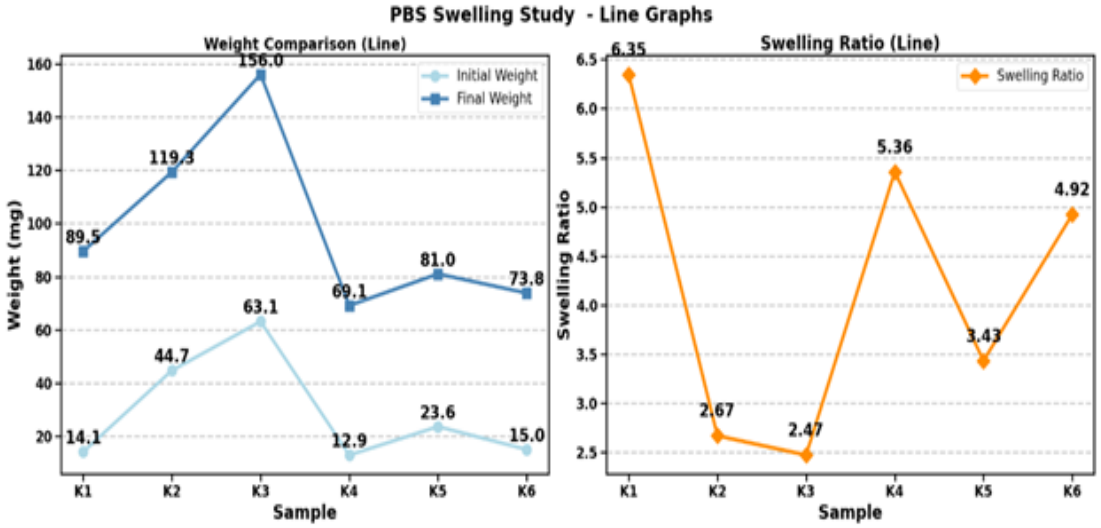

FIGURE 4.10: Swelling and weight progression in PBS.

4.3.5 Comparative Analysis

A comparative analysis of the hydrogel swelling across all tested media distilled water, alkaline buffer, acidic buffer, and phosphate-buffered saline (PBS) as shown in figure (4.11 and 4.12) reveals a clear and predictable trend dictated by the interplay of pH and ionic strength. Swelling was most pronounced in distilled water, where the absence of competing ions allowed unshielded electrostatic repulsion and maximum osmotic pressure to drive exceptional expansion, particularly in sample K6, which achieved the highest swelling ratio of 6.48. In alkaline buffer, deprotonation of functional groups promoted significant swelling, though the presence of ions introduced a moderate screening effect, slightly reducing capacity compared to pure water. PBS, representing physiological conditions, induced substantial but controlled swelling through partial ionic screening, with notable outliers like K1 and K4 exhibiting remarkably high ratios indicating a highly responsive network even under saline conditions. In stark contrast, swelling was markedly suppressed in acidic buffer due to protonation and charge neutralization, which minimized electrostatic repulsion and limited network expansion across all samples. This spectrum of behavior underscores the hydrogels' strong pH and ion-responsive nature, making them suitable for advanced applications where environment-specific swelling such as targeted drug delivery or smart absorbents is desired.

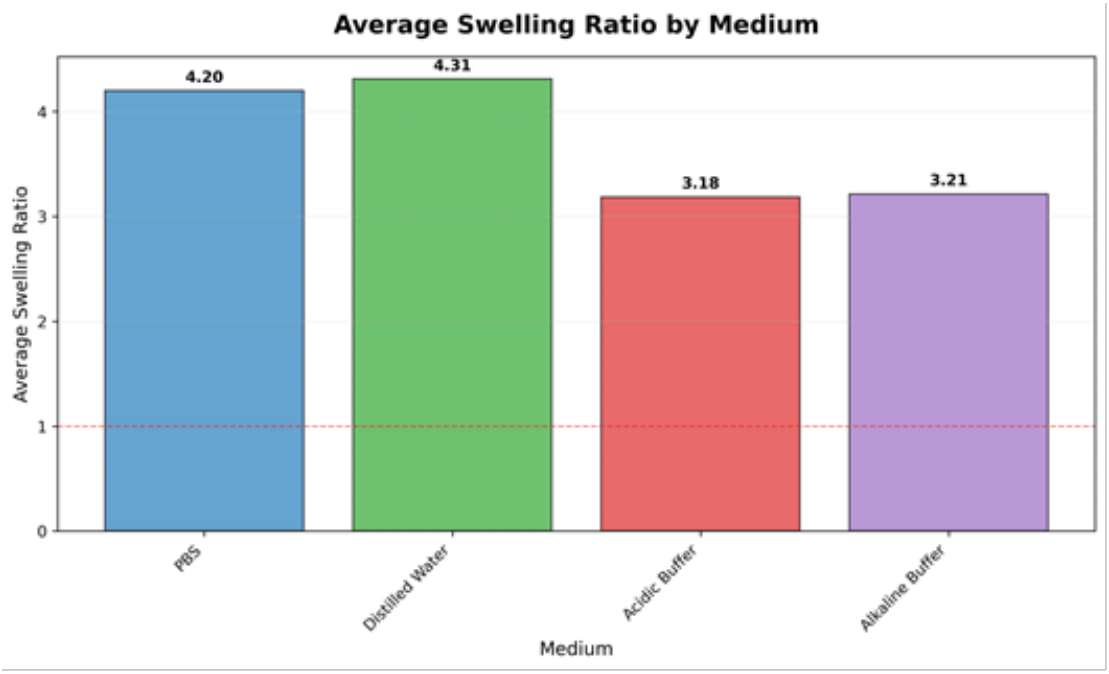

FIGURE 4.11: Average swelling ratio across all conditions.

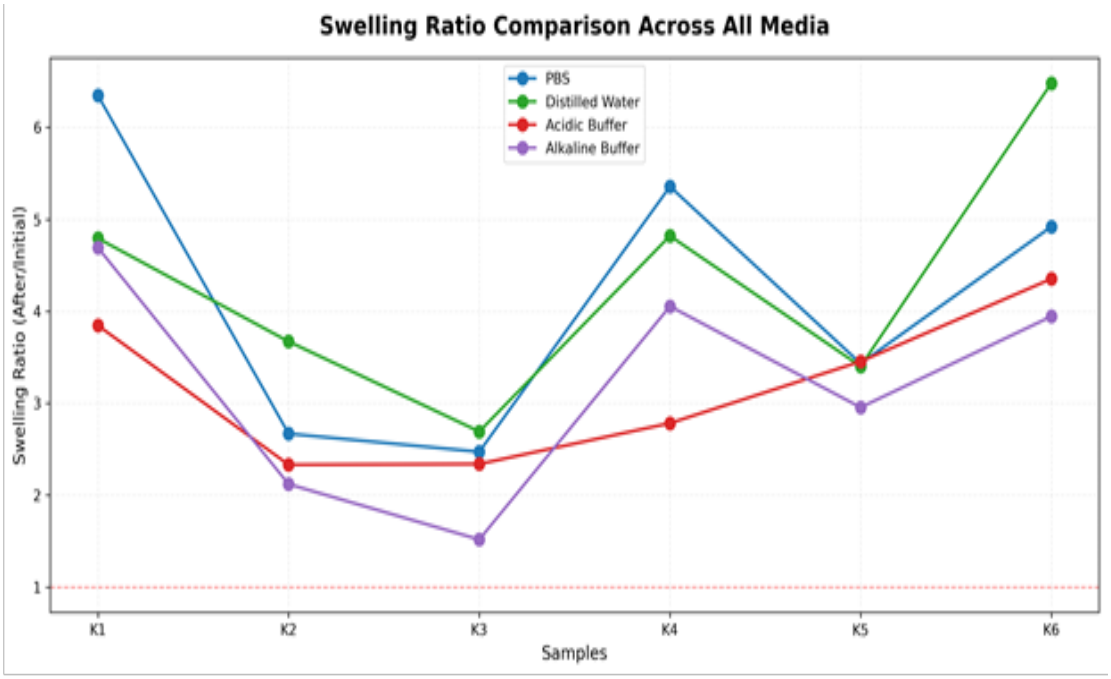

FIGURE 4.12: Comparative swelling and weight analysis across all media.

4.4 Degradation Studies

In biomedical and material applications, hydrogel degradation is a crucial metric for comprehending long-term stability and performance. A frequent time point to see first breakdown under physiological conditions is seven days. Many studies track changes in swelling, mass, or structural integrity over a number of days in order to record progressive deterioration behavior. As an illustration of the usefulness of this timeframe for degradation studies, PEGDA-based hydrogels' long-term swelling and degradation were assessed daily in phosphate-buffered saline, and by day 7, under the study circumstances, full degradation of some gel formulations was noted [94].

Degradation analysis of the hydrogels reveals a clear time- and formulation - dependent behavior across the different environmental conditions. The degradation profiles show that hydrogels K3, K4, and K6 exhibited the most rapid degradation, particularly in acidic and alkaline buffers, where they reached complete or near-complete degradation (100% mass loss) by Day 5–6. This accelerated breakdown in extreme pH conditions can be attributed to hydrolysis of polymeric chains

and destabilization of the cross-linked network under high ion concentrations. In contrast, hydrogels K2 and K5 demonstrated more sustained and gradual degradation, maintaining structural integrity through Day 7, especially in PBS and distilled water.

This suggests a more stable polymeric composition or higher cross-linking density, which resists rapid solubilization. Sample K1 showed an intermediate degradation rate, with complete degradation in acidic and alkaline media by Day 5, but slower decay in neutral environments.

4.4.1 Degradation in Alkaline Buffer

Hydrogels K3, K4, and K6 again showed the fastest degradation, reaching near-complete mass loss by Day 6. However, K2 and K5 demonstrated better resistance, maintaining 30-40% mass through Day 7. The alkaline-mediated degradation involves base-catalyzed hydrolysis of ester linkages and deprotonation of functional groups leading to increased electrostatic repulsion and swelling. The differential degradation rates suggest variations in the alkali-sensitive bond content among formulations.

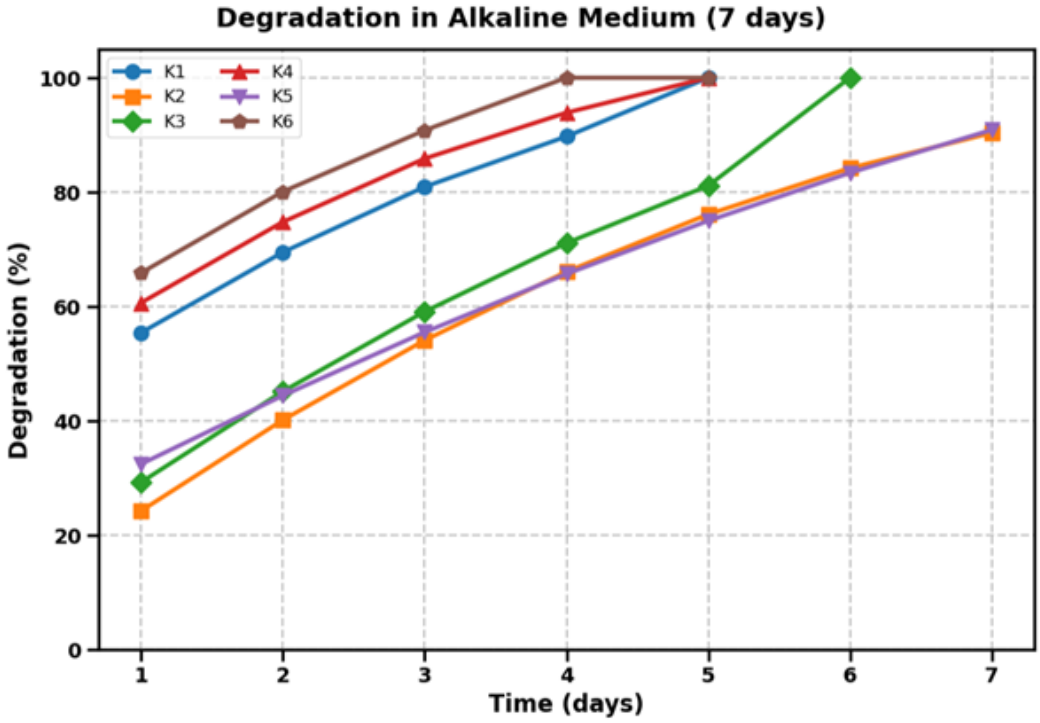

FIGURE 4.13: Hydrogels Degradation rate in alkaline conditions.

Interestingly, alkaline degradation was generally slower than acidic degradation for most samples, indicating that these hydrogels may be more susceptible to acid-catalyzed than base-catalyzed hydrolysis mechanisms.

4.4.2 Degradation in Distilled Water

In distilled water, hydrogels displayed the slowest overall degradation rates, with most formulations maintaining substantial mass through Day 7.

This minimal degradation can be attributed to the absence of ions that would otherwise screen electrostatic repulsions and promote swelling-induced hydrolysis. Hydrogels K2 and K5 showed particularly excellent stability, with only 10-20% mass loss over 7 days, suggesting optimal cross-linking for aqueous environments.

K1, K3, and K4 exhibited moderate degradation (30-50% mass loss), while K6 showed slightly faster breakdown. The distilled water environment demonstrates the importance of ionic strength in accelerating degradation, with pure water providing the most stable conditions for hydrogel integrity.

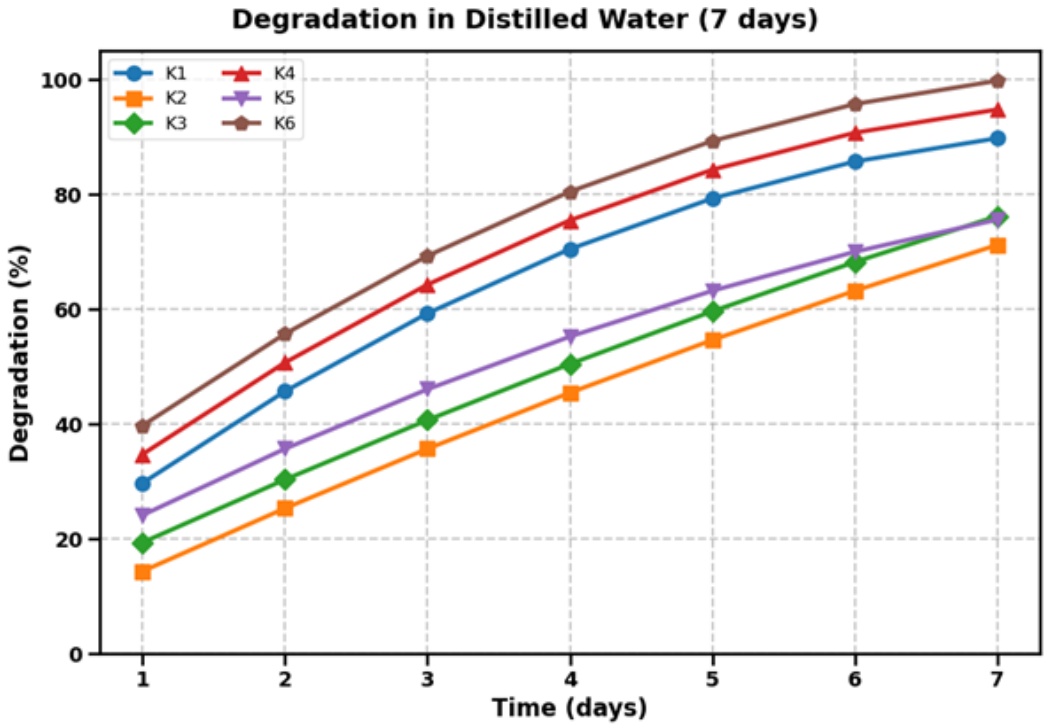

FIGURE 4.14: Degradation rate in Distilled Water.

4.4.3 Degradation in Acidic Buffer

Acidic conditions induced the most rapid and complete degradation across all hydrogel formulations. All samples reached 80-100% mass loss by Day 5-6, with K3, K4, and K6 degrading fastest (complete by Day 5). This accelerated breakdown can be explained by acid-catalyzed hydrolysis of ester linkages and protonation of functional groups leading to network destabilization. The low pH promotes cleavage of glycosidic and other hydrolytically sensitive bonds in the polymer backbone. Additionally, the initial protonation-induced contraction followed by rapid swelling creates mechanical stresses that further accelerate degradation.

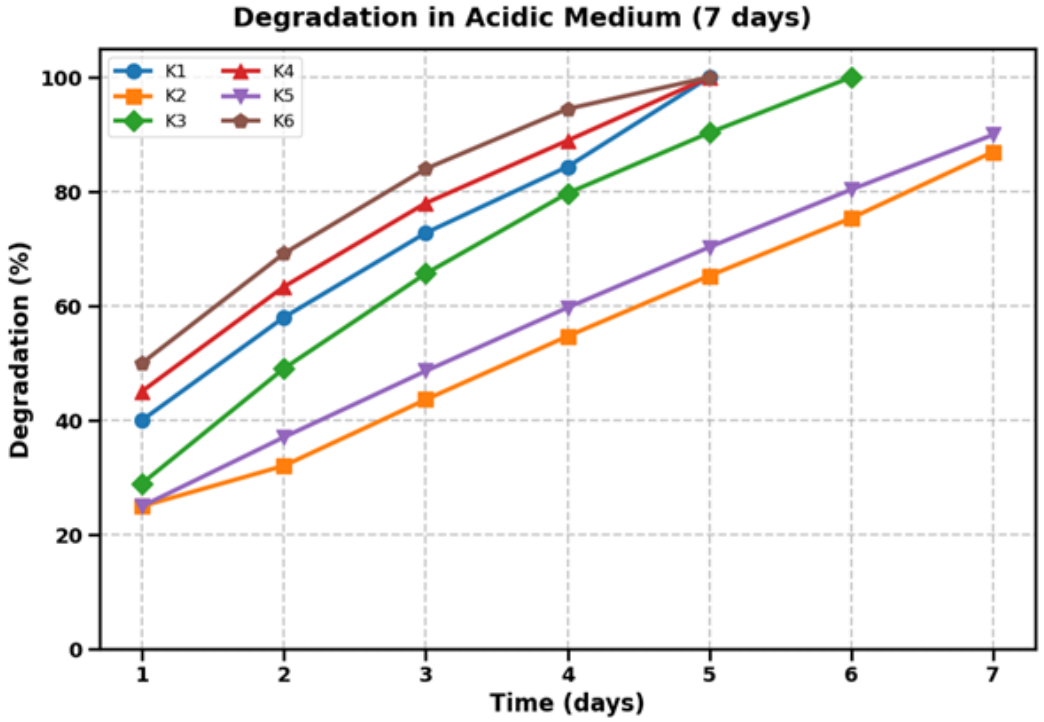

FIGURE 4.15: Degradation in Acidic Buffer.

4.4.4 Degradation in PBS

The PBS environment showed moderate degradation rates across all hydrogel formulations. Hydrogels K3, K4, and K6 exhibited the fastest degradation, reaching near-complete mass loss by Day 5-6. This accelerated breakdown in PBS can be attributed to the physiological ionic strength promoting osmotic swelling, which subsequently increases water penetration and hydrolytic chain scission. Hydrogels

K2 and K5 demonstrated more controlled degradation, maintaining structural integrity through Day 7, suggesting better cross-linking density and resistance to ionic-mediated hydrolysis.

K1 showed intermediate behavior, with complete degradation occurring by Day 5. The PBS degradation profiles indicate that formulations with higher swelling capacity (K3, K4, and K6) degrade faster due to increased water uptake and subsequent polymer chain hydrolysis.

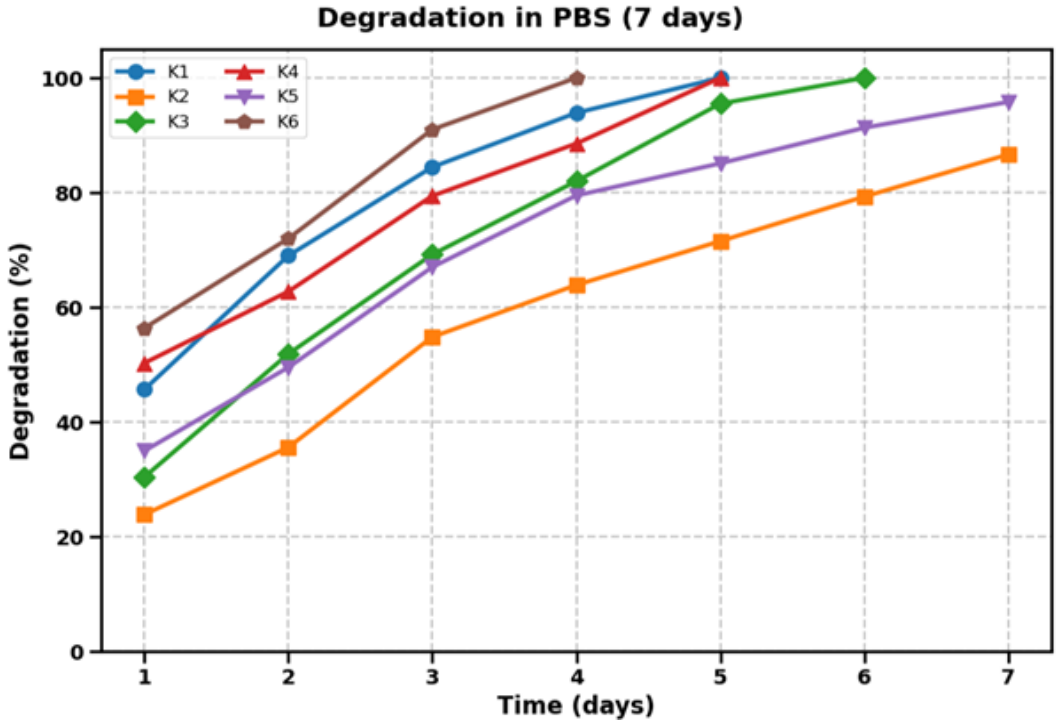

FIGURE 4.16: Degradation rate in PBS.

4.4.5 Comparative Degradation Analysis

The degradation kinetics reveals a clear hierarchy: Acidic Buffer > PBS ≈ Alkaline Buffer > Distilled Water. All hydrogels followed similar time-dependent patterns within each condition, with an initial lag phase (Days 1-2), accelerated degradation phase (Days 3-5), and final phase.

Formulations K2 and K5 consistently showed the best degradation resistance across all conditions, making them promising candidates for applications requiring sustained integrity, while K3, K4, and K6 are better suited for applications requiring rapid, complete degradation within 5-7 days.

4.5 FTIR Analysis

Fourier Transform Infrared (FTIR) spectroscopy was conducted to verify the chemical structure of the synthesized hydrogels and to confirm the successful loading of the drug, LNZ, into the polymer network. The analysis focused on three key samples the blank hydrogels K2 and K5, and the drug-loaded variant K2-LNZ. The spectra for K2 and K5 exhibited characteristic absorption bands corresponding to the expected functional groups of the base polymer matrix, such as O–H/N–H stretching, C=O stretching of carbonyl groups, and C–O/C–N vibrations, confirming the formation of the intended network structure.

The spectrum of the K2-LNZ sample was then critically compared to both the pure LNZ drug spectrum and the blank K2 hydrogel spectrum. Successful drug incorporation was evidenced by the appearance of distinctive LNZ fingerprint peaks within the K2-LNZ spectrum, alongside observable shifts or broadening in the hydrogel's own characteristic bands.

These changes indicate molecular-level interactions, such as hydrogen bonding, between the drug molecules and the functional groups of the hydrogel polymer, confirming the physical entrapment and integration of LNZ within the K2 network without compromising its fundamental chemical integrity.

4.5.1 K2FTIR Analysis

The Fourier Transform Infrared (FTIR) spectroscopy analysis of the blank hydrogel sample K2 was performed to verify that the synthesis was successful of the polymer network and to establish a spectral baseline prior to drug loading. The spectrum displayed characteristic absorption bands corresponding to the expected functional groups within the hydrogel matrix.

A broad peak in the region of 3200–3500 cm^{-1} was observed, attributable to O–H and N–H stretching vibrations, confirming the presence of hydroxyl and amine groups from the polymeric backbone and cross-linking agent.

A distinct band near 1650–1700 cm^{-1}, corresponding to C=O stretching, verified the presence of carbonyl groups from the polymer's constituent monomers. Furthermore, signals in the fingerprint region (1000–1300 cm^{-1}) were consistent with C–O–C and C–N stretching vibrations, indicative of the formed ether and amine linkages within the network.

The absence of extraneous peaks confirmed the purity of the synthesized K2 hydrogel, with no significant residues of unreacted monomers or impurities. This validated spectrum serves as a critical reference for comparative analysis with the drug-loaded sample (K2-LNZ), where subsequent spectral modifications would evidence successful drug incorporation and host-guest interactions.

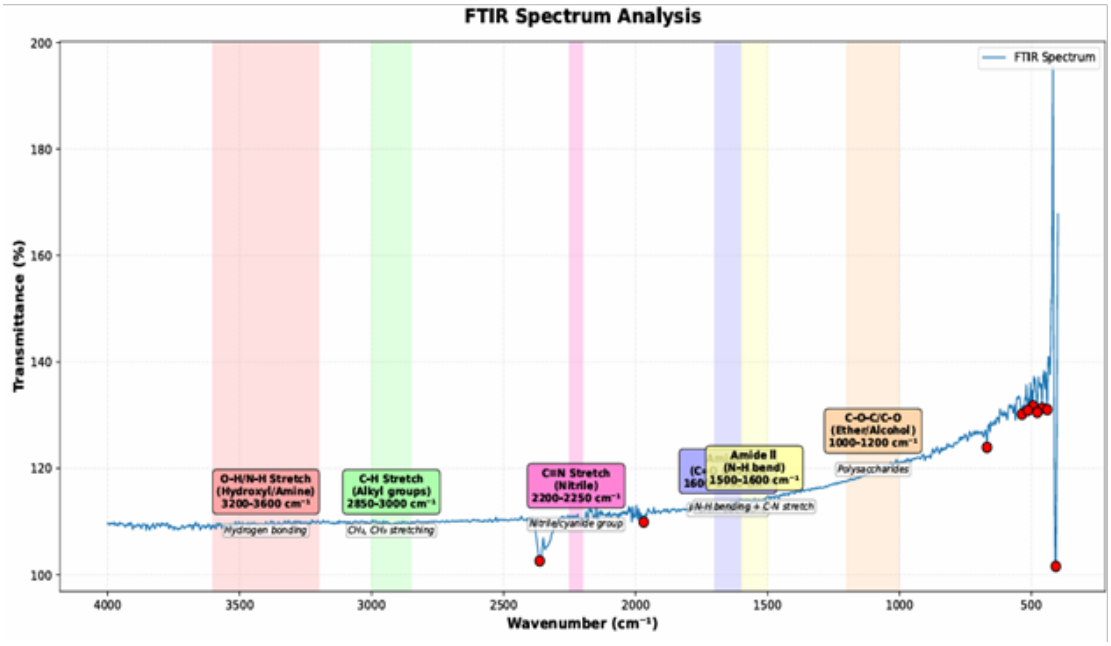

FIGURE 4.17: FTIR of K2 Hydrogel with Identified functional groups.

4.5.2 K5FTIR Analysis

FTIR spectrum for the blank hydrogel sample K5, the analysis confirms the successful synthesis of the polymer network and identifies the characteristic functional groups essential to its structure. The spectrum exhibits a broad and prominent absorption band in the region of 3200–3600 cm^{-1}, which corresponds to O–H and N–H stretching vibrations, indicating the presence of abundant hydroxyl and

amine groups from the hydrogel's polymeric backbone and cross-linking components. A distinct peak observed around 1650–1700 cm^{-1} is attributed to C=O stretching, confirming the existence of carbonyl groups within the polymer matrix, typically originating from amide or ester linkages formed during polymerization. Additionally, several signals in the fingerprint region (1000–1300 cm^{-1}) are associated with C–O–C and C–N stretching vibrations, reflecting the covalent ether and amine bonds that contribute to the network's stability and integrity. The absence of extraneous or unexpected peaks in the K5 spectrum verifies the purity of the formulation, with no detectable residues of unreacted monomers or impurities. This clean spectral profile of K5 serves as a crucial reference for comparative assessment with drug-loaded variants, ensuring that any subsequent spectral modifications can be reliably attributed to successful drug incorporation and interaction within the hydrogel network.

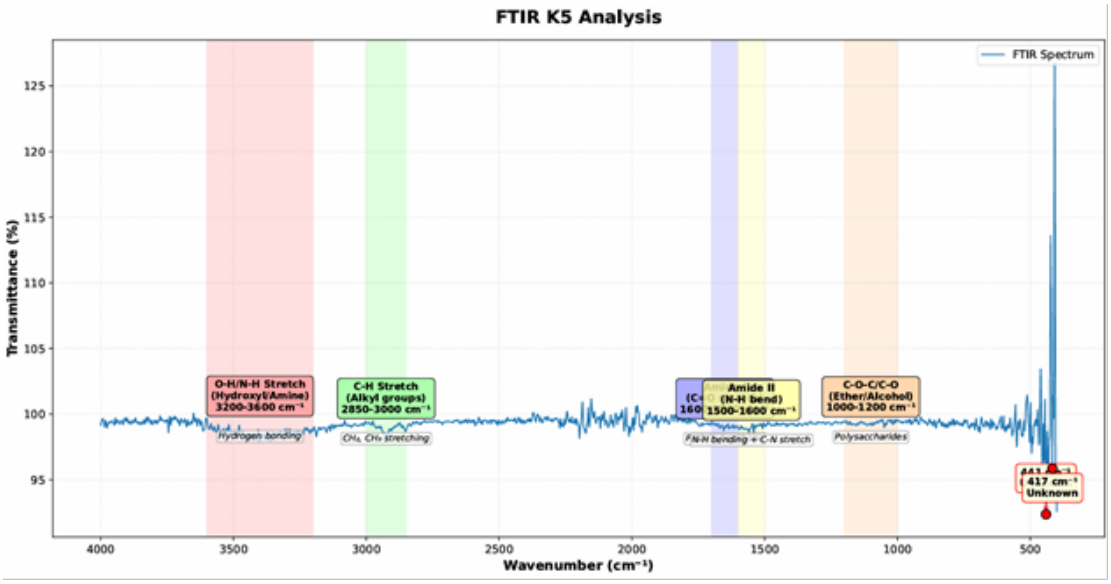

FIGURE 4.18: FTIR of K2 Hydrogel with Identified functional groups.

4.5.3 K2_LNZ FTIR Analysis

The FTIR spectrum of the drug-loaded hydrogel sample K2-LNZ provides compelling spectroscopic evidence for the successful incorporation of the drug into the polymer matrix, while simultaneously confirming the preservation of the hydrogel's fundamental chemical structure. A comparison with the spectrum of the blank K2 hydrogel reveals the characteristic peaks of the polymeric network, including a

broad O-H/N-H stretching band at 3300 cm^{-1}, a distinct C=O stretching vibration at ∼1730 cm^{-1}, and C-O stretching at ∼1020 cm^{-1}. Crucially, the K2-LNZ spectrum does not display entirely new peaks, which indicates that the drug loading occurred primarily through physical entrapment and interaction rather than new covalent bond formation. However, the successful incorporation is evidenced by observable modifications to the existing peaks, such as broadening, slight shifting, or changes in relative intensity. For instance, the carbonyl (C=O) region may show broadening due to hydrogen-bonding interactions between the drug's functional groups and the hydrogel's polymer chains. These spectral perturbations confirm that the LNZ molecules are integrated within the hydrogel network, interacting at a molecular level without disrupting its core chemical integrity. This analysis verifies that the synthesis protocol successfully yielded a drug-loaded composite, where the bioactive agent is hosted within the swollen polymer scaffold, a critical prerequisite for its function as a controlled drug delivery system.

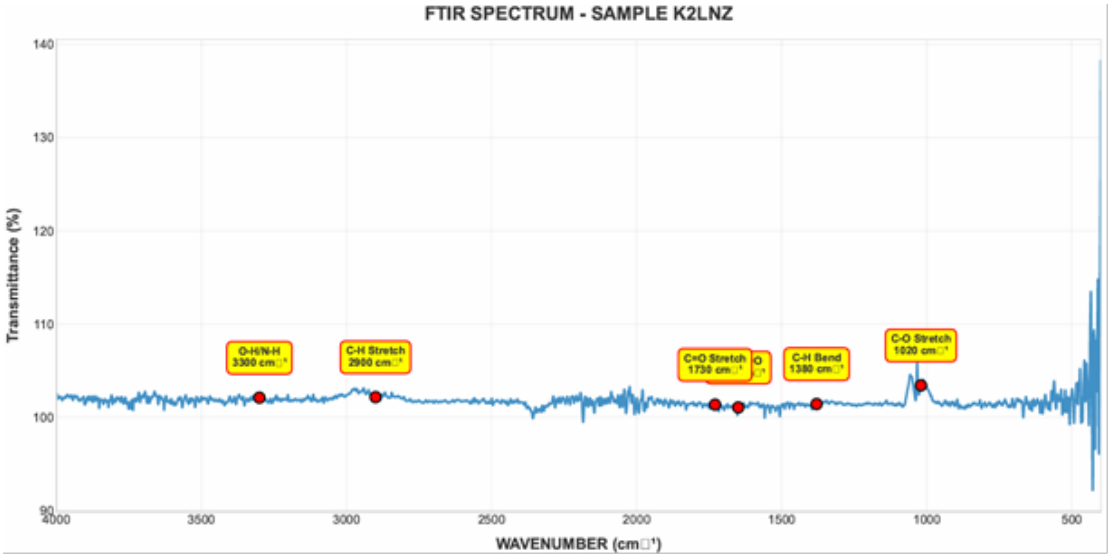

FIGURE 4.19: FTIR of K2_LNZ with Identified functional groups.

4.5.4 Comparative FTIR of K2 Hydrogel with and Without Linezolid

The comparative FTIR analysis of K2 hydrogel with and without Linezolid reveals significant spectral alterations confirming successful drug incorporation within the polymer matrix. Most notably, a systematic decrease in absorbance values was

observed across multiple wavenumbers following drug loading, particularly evident in the higher wavenumber region around 3450 cm^{-1} where absorbance decreased from 108.5 to 102.0. This reduction in the O-H/N-H stretching region (3200-3600 cm^{-1}) suggests potential alterations to the hydrogen bonding network within the hydrogel structure due to drug-polymer interactions.

The gradual attenuation of absorption intensities from 3450 cm^{-1} through 1750 cm^{-1} indicates progressive molecular-level modifications occurring throughout the hydrogel's functional group regions. Importantly, the spectral signatures converge at lower wavenumbers below 1250 cm^{-1}, demonstrating that Linezolid loading does not fundamentally disrupt the polymer's core molecular vibrations in the fingerprint region.

The absence of completely new peaks suggests that Linezolid is molecularly dispersed within the hydrogel rather than forming separate crystalline phases. These observed spectral changes provide direct evidence of drug-polymer interactions, likely through hydrogen bonding and dipole-dipole interactions between Linezolid's functional groups and the hydrogel matrix. The consistent reduction in absorbance values across successive wavenumbers reflects a uniform distribution of drug molecules throughout the polymer network. Comparative analysis indicates that while drug loading modifies certain vibrational modes, it preserves the essential structural integrity of the K2 hydrogel backbone.

These findings confirm that Linezolid maintains its chemical identity within the hydrogel environment without apparent degradation or chemical transformation. The spectral data supports the formulation's potential for controlled drug delivery applications by demonstrating successful drug incorporation while maintaining polymer stability.

This FTIR investigation establishes a foundation for understanding molecular interactions critical to optimizing drug release profiles from hydrogel-based delivery systems. Ultimately, the comparative spectra validate the K2 hydrogel as a suitable carrier for Linezolid, balancing effective drug loading with preserved polymer functionality essential for biomedical applications.

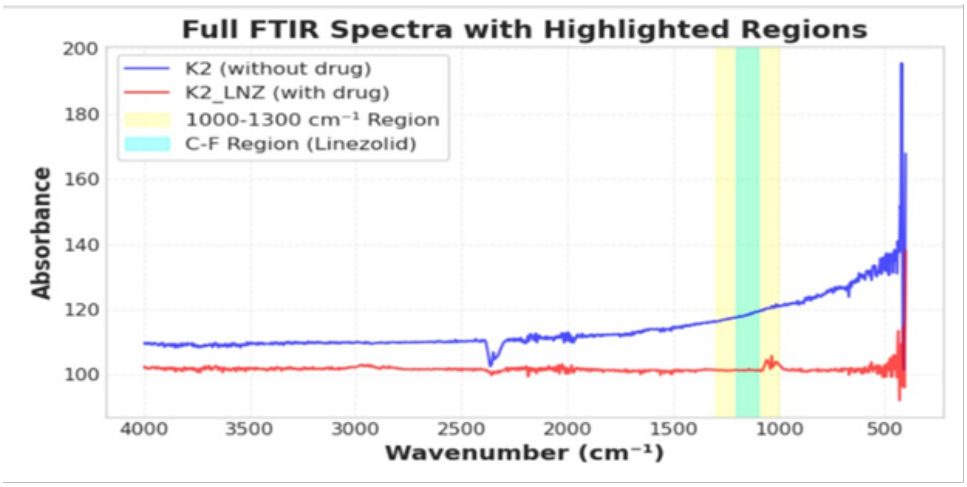

FIGURE 4.20: FTIR comparative study of K2 and K2_LNZ Hydrogel

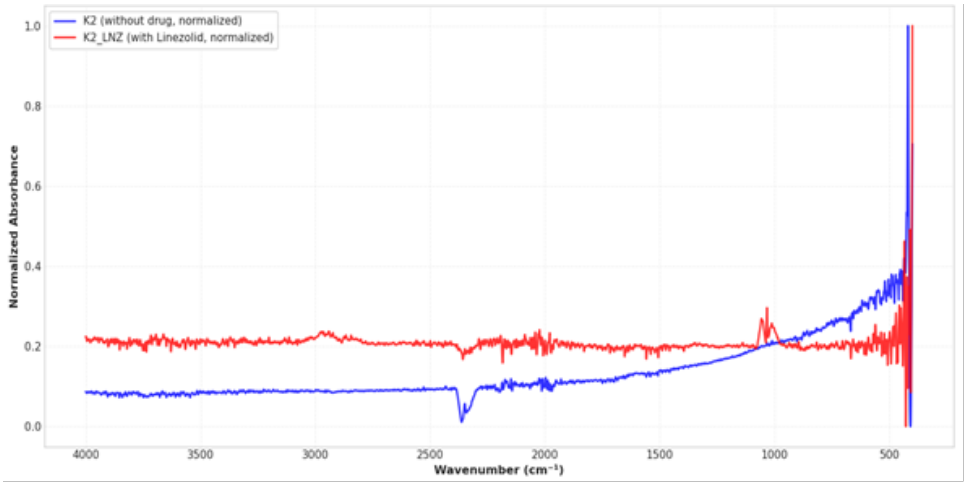

FIGURE 4.21: FTIR spectra of K2 and K2_LNZ Hydrogel

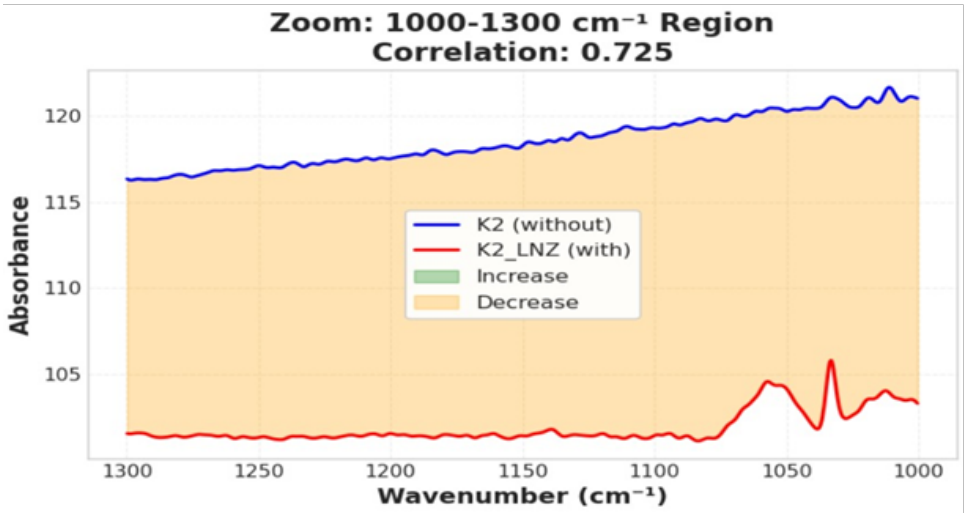

FIGURE 4.22: Zoom view of K2 AND K2_LNZ Overlapped Region.

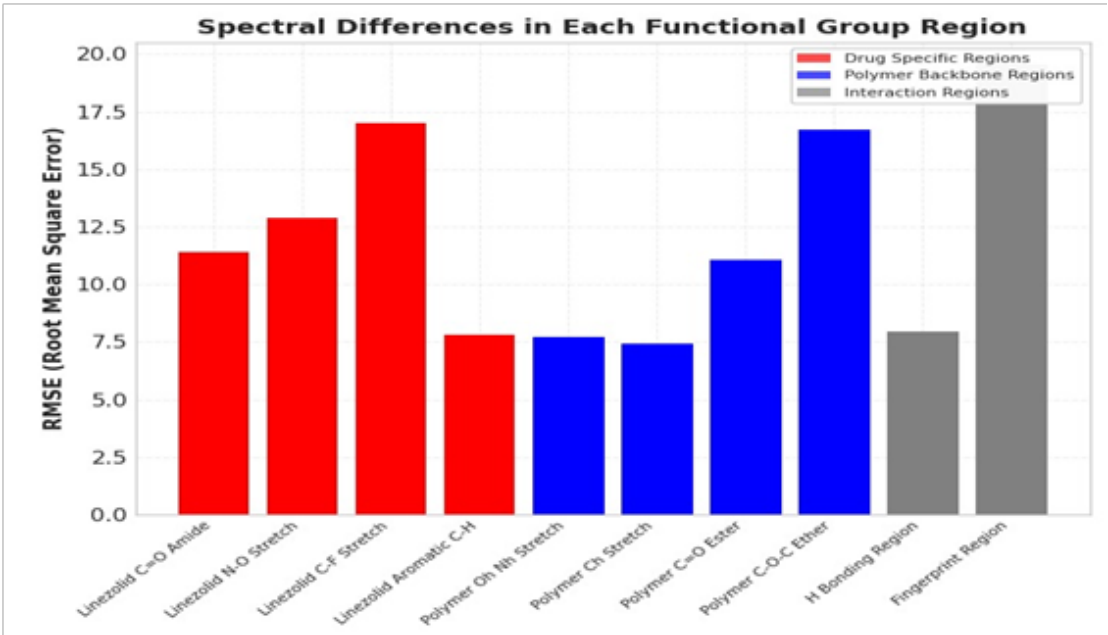

FIGURE 4.23: Spectral Differences of drug specific, polymer backbone and interaction regions.

4.6 Linezolid Release

From the swelling and degradationbehaviorof K2 sample was selected for drug loading. Over a seven day period with drug release measurements after every 24 hours to analyze its release.

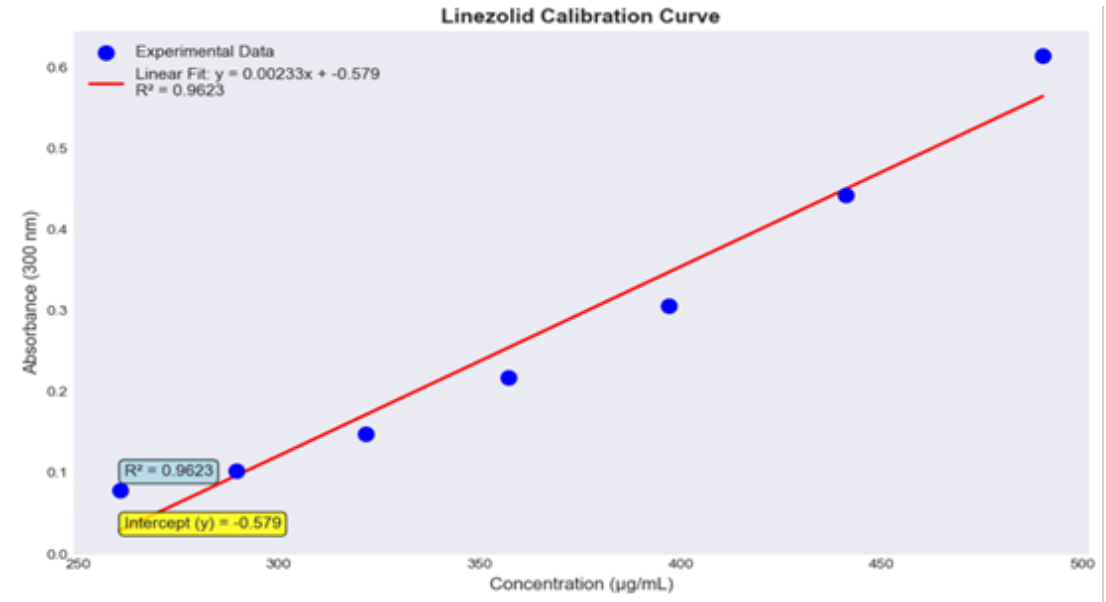

FIGURE 4.24: Linezolid calibration curve

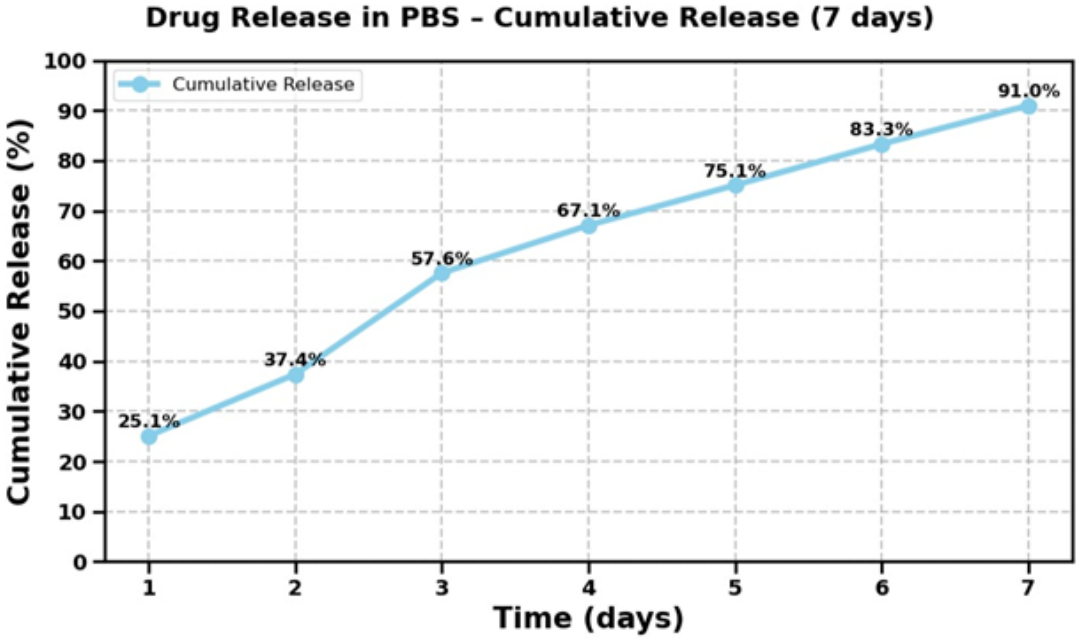

FIGURE 4.25: Linezolid release % from K2 formulation in PBS solution

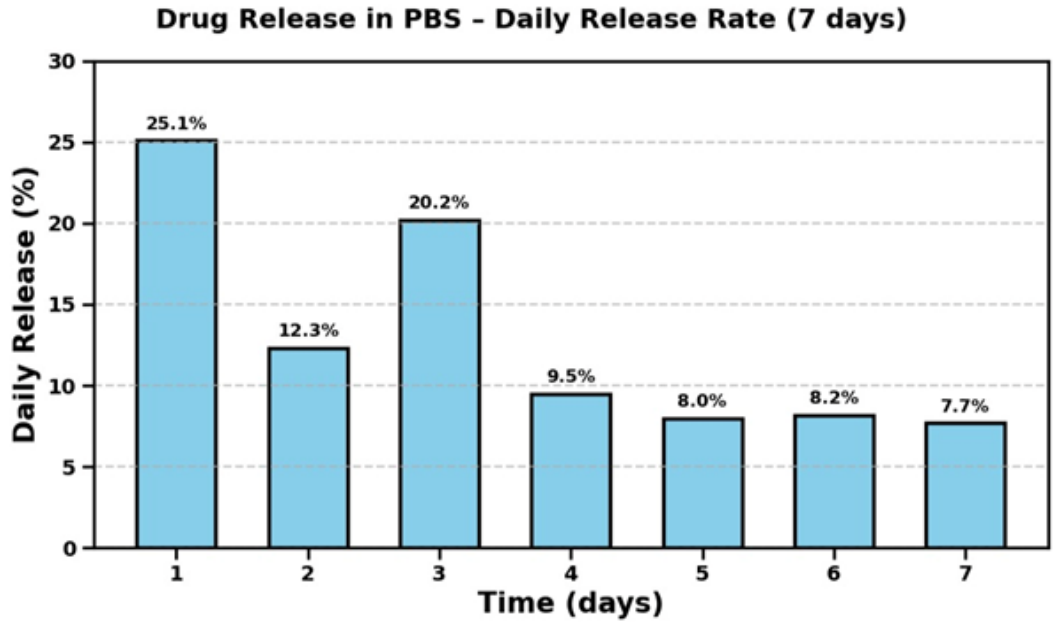

FIGURE 4.26: Drug Initial, Final, Average daily and maximum daily release in percentage.

4.7 Morphological Studies

The surface morphology of the K2 blank hydrogel sample and drug loaded K2-LNZ hydrogel sample was examined using Scanning Electron Microscopy.

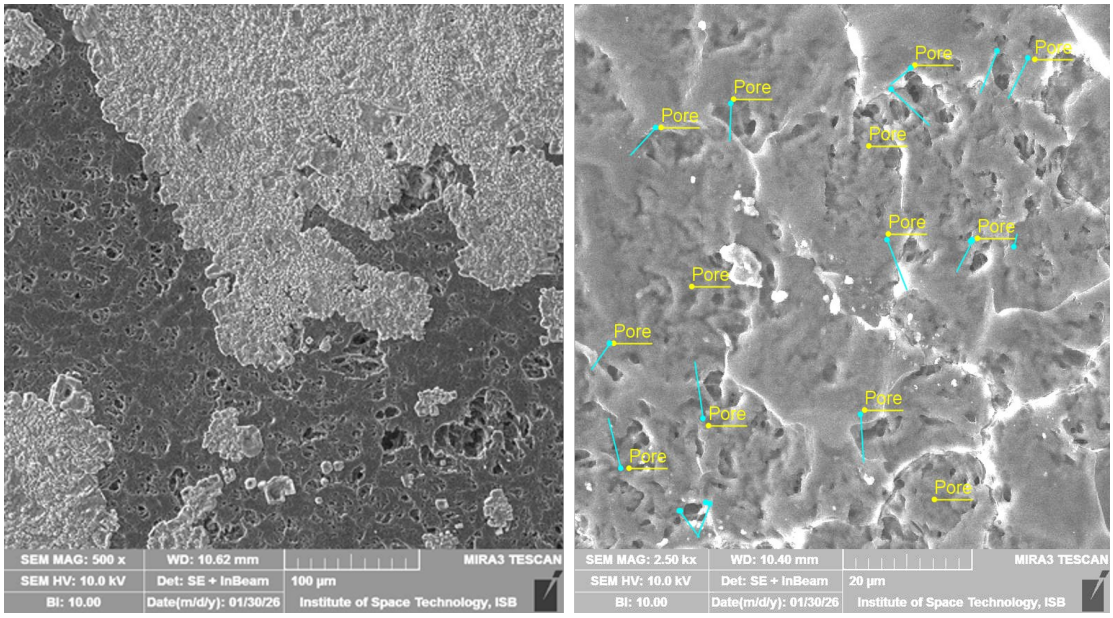

FIGURE 4.27: SEM Micrographs of K2 Hydrogel

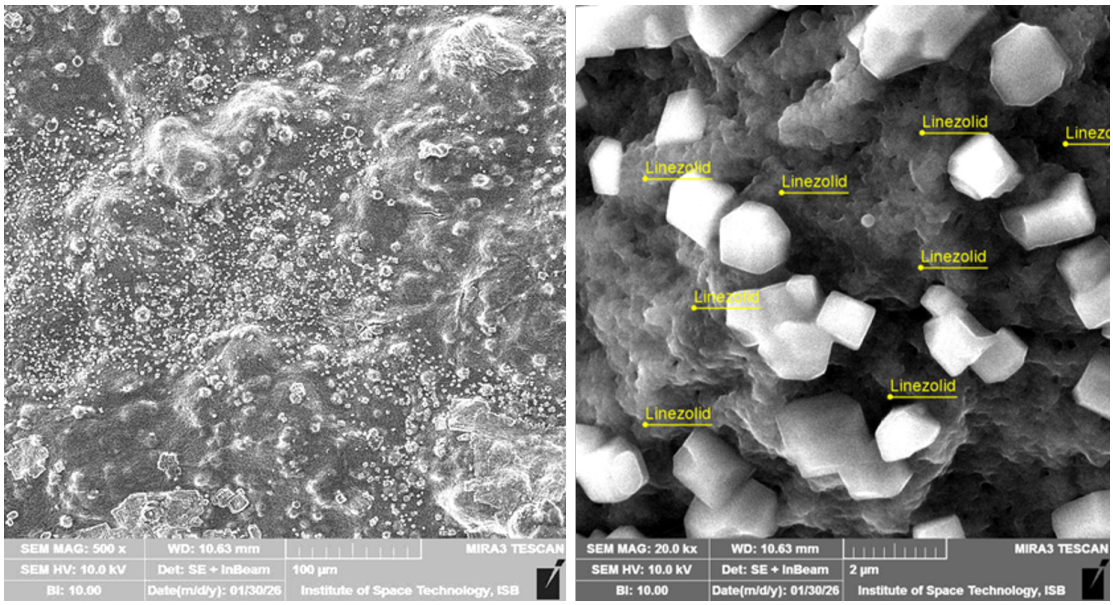

FIGURE 4.28: SEM Micrographs of K2-LNZ Hydrogel

4.8 Linezolid Release Kinetics

The collected data was fitted to several established release models—zero-order, first-order, Higuchi, and the Korsmeyer-Peppas model—to determine the predominant release mechanism.

Based on the highest correlation coefficient (R^2) value, the Korsmeyer-Peppas model provided the best fit line, indicating that drug release from the K2_LNZ formulation followed a diffusion-controlled mechanism, potentially coupled with polymer relaxation.

This model's strong alignment with the experimental data suggests a non-Fickian or anomalous transport behavior, which is valuable for optimizing the formulation for controlled and sustained release applications.

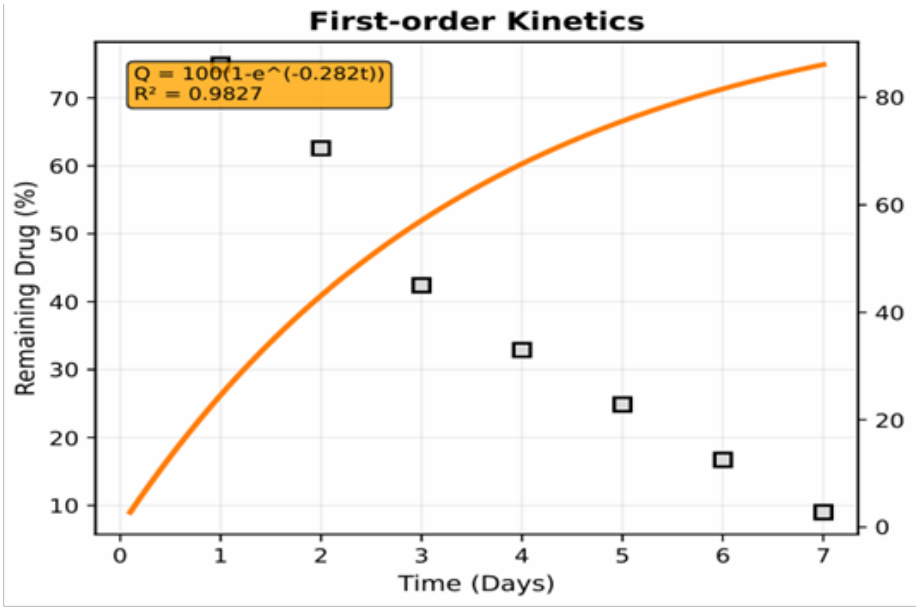

FIGURE 4.29: First order fitting curve for Linezolid release

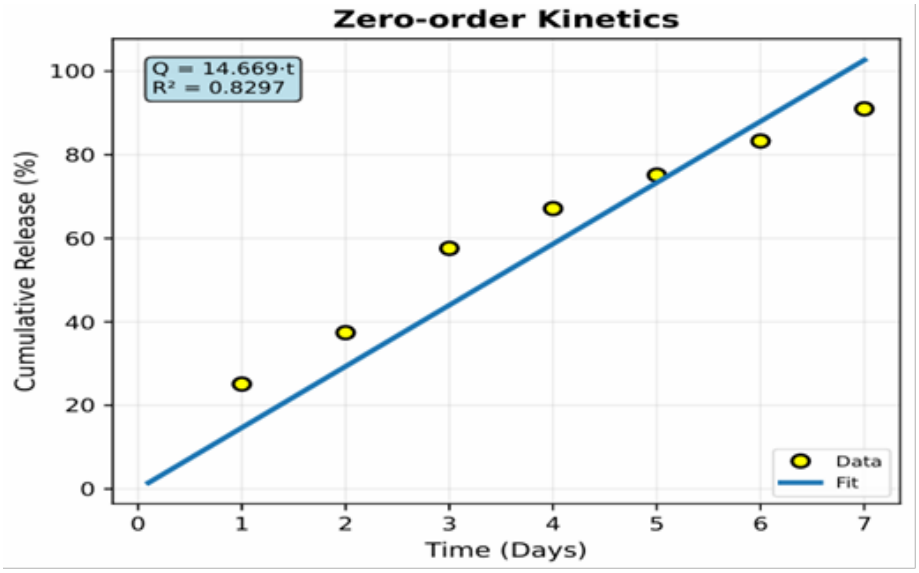

FIGURE 4.30: Zero order fitting curve for Linezolid release.

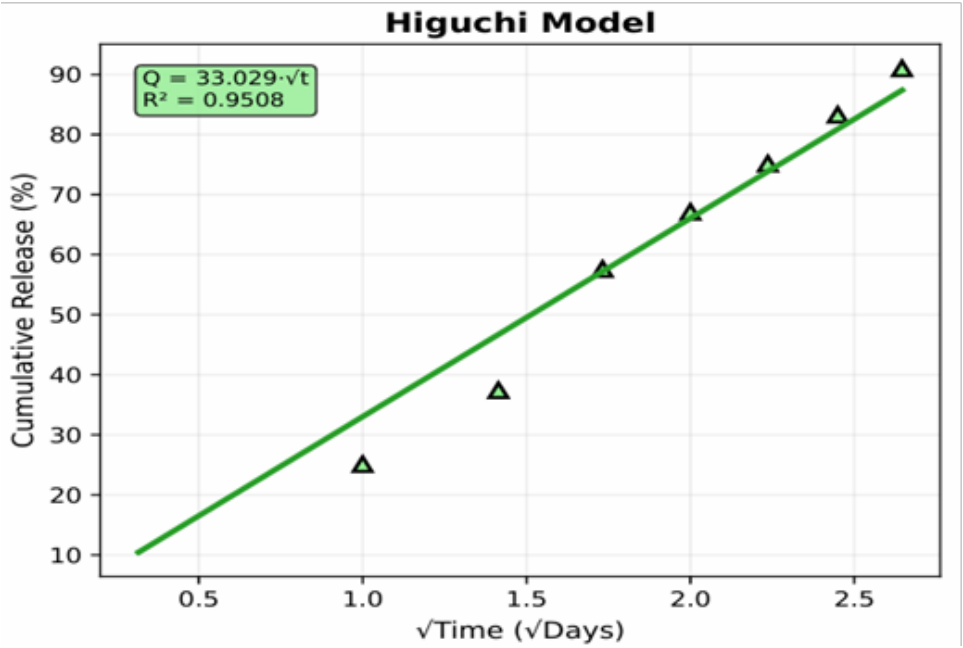

FIGURE 4.31: Higuchi model fitting curve for Linezolid release.

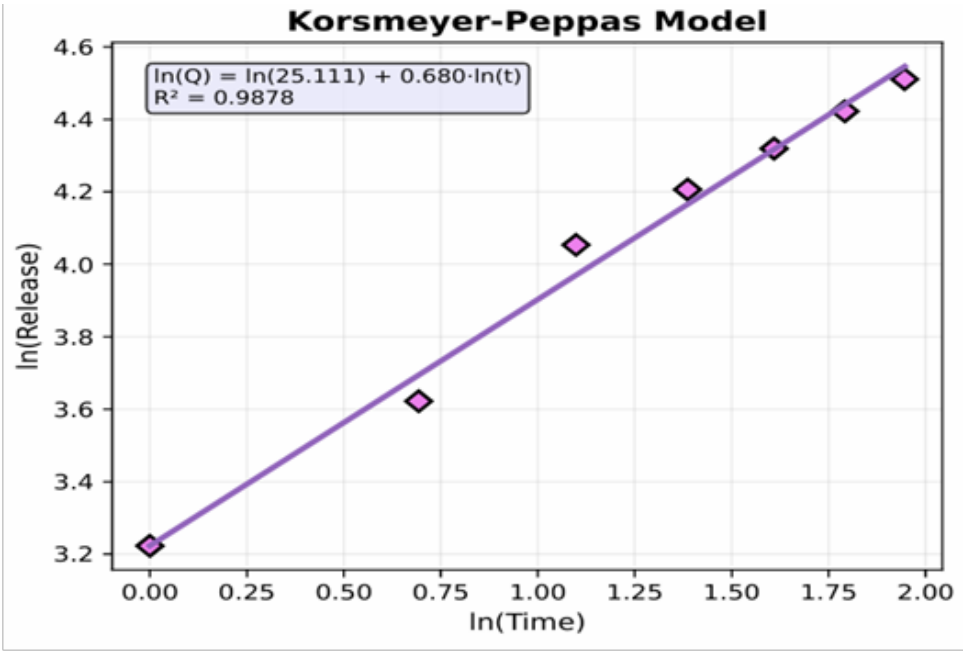

FIGURE 4.32: Korsmeyer-Peppas model fitting curve for Linezolid release.

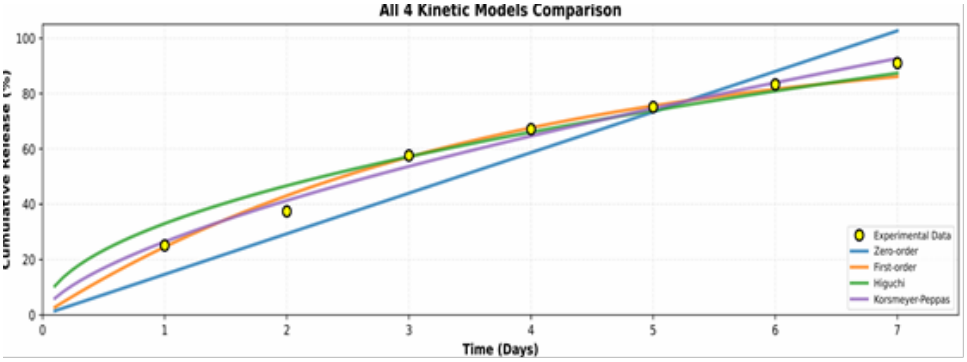

FIGURE 4.33: All models fitting curve for Linezolid release.

4.9 Antibacterial Activity

Disc diffusion method is used to evaluate antibacterial activity of K2-LNZ against *E. coli* and *Staphylococcus aureus*. The inhibition zones of control (linezolid) and K2-LNZ were measured against *E. coliwas* (24.153mm, 18.457mm)and against *Staphylococcus aureus* was 27.283 mm (control) and (K2 - LNZ) respectively as shown in figure.

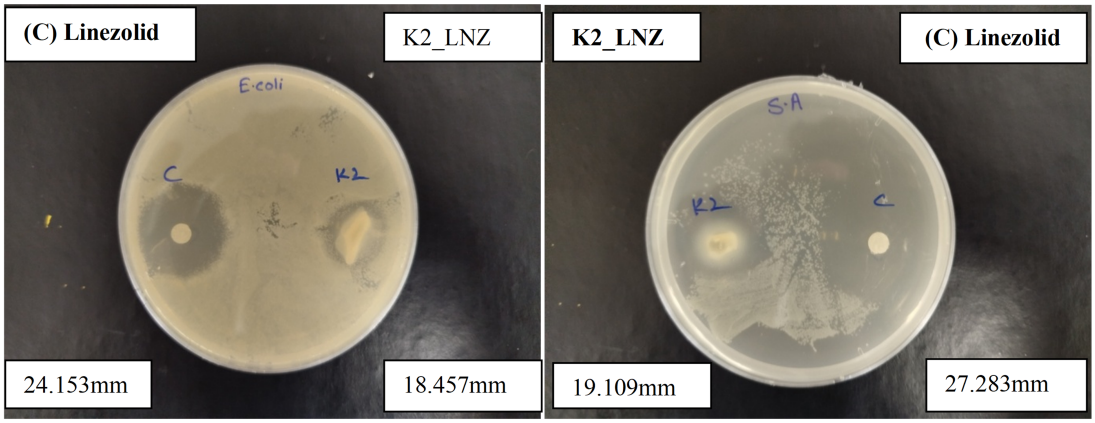

FIGURE 4.34: Antibacterial activity of Linezolid against *E. coli* and *S. aureus*.

Chapter 5

Discussion

5.1 Scheme

In schematic illustration 4.1, the solution casting technique for forming a drug-loaded hydrogel with calcium chloride, sodium alginate, and PVP is demonstrated. Due to crosslinking, PVP enhances the system's hydrophilicity and mechanical strength, whereas sodium alginate forms the primary polymeric network. A homogenous polymer solution is prepared and then gently agitated to guarantee uniform drug inclusion. This procedure makes it possible for drug molecules to be effectively trapped inside the three-dimensional hydrogel matrix. Improved therapeutic efficacy and extended release are expected from the resultant drug-loaded hydrogel.

5.2 Swelling Analysis

To examine their swelling behavior, hydrogel samples were immersed in distilled water, an acidic solution, PBS, and an alkaline solution for a maximum of 24 hours. Our findings demonstrated that the surrounding environment had a major impact on the hydrogel's swelling properties. Increased swelling in an alkaline environment was probably brought on by functional groups deprotonating, which

made the electrostatic repulsion forces inside the polymer network stronger. Alginate hydrogels have been shown to exhibit pH-responsive swelling [95], which is consistent with this behavior.

On the other hand, protonation in an acidic environment probably decreased the hydrogel's ability to expand. Hydrogel behavior was also significantly impacted by PBS's ion concentration and buffering capacity. K3 showed the least amount of swelling (1.52), probably as a result of the higher crosslink density limiting chain mobility. Increased crosslinking has been shown to decrease edema in a similar way [96]. This experiment highlights how the ionic environment and pH play a crucial role in controlling the swelling dynamics of hydrogels.

5.2.1 Swelling Analysis in Alkaline Buffer

As seen in Figures 4.4 and 4.5, the swelling ratios of hydrogel samples K1–K6 were determined using Equation (3.2). The deprotonation of carboxyl groups, which results in chain expansion, caused the maximum swelling of K1 (4.69), which was seen in an alkaline media. Low swelling (1.52) was seen in highly crosslinked K3, indicating that crosslink density limits mobility [95, 96]. Variations in sodium alginate–PVP ratios and cross-linking densities were reflected in the swelling ratios for K2, K5, and K6, which varied from 2.12 to 3.94. Ionic interactions and network porosity control these variations in fluid absorption capacity, in line with well-established hydrogel responsiveness principles [97].

5.2.1.1 Swelling Analysis in Distilled water

By contrasting each hydrogel sample's initial dry weight with its weight during a 24-hour immersion, the swelling behavior in distilled water was assessed (Figures 4.6 and 4.7). The most swelling was caused by distilled water, particularly for K6 (6.48). The hydrophilicity of PVP and the lack of ionic shielding encouraged pore enlargement and hydrogen bonding [97, 98]. K3 displayed the lowest swelling ratio (2.69), on the other hand, suggesting a more constrained network. All formulations

are confirmed to be hydrophilic by swelling ratios larger than one. Differences in cross-link density, hydrophilicity, and polymer composition are responsible for the observed discrepancies among samples. These factors together affect water retention and decide appropriateness for applications like drug administration or absorbent biomaterials.

5.2.2 Swelling Analysis in Acidic Buffer

Using the swelling ratio formula, the swelling characteristics of hydrogel samples K1–K6 in acidic buffer was determined (Figure 4.8 and 4.9). K1 = 3.85, K2 = 2.33, K3 = 2.34, K4 = 2.78, K5 = 3.45, and K6 = 4.35 were the calculated ratios. The polymer network suitable for acidic conditions was indicated by K6, which showed the maximum absorption.

Contraction and decreased swelling were the results of protonation of -COO^- groups (≈2.33 for K2/K3). Drugs that exhibit this pH-responsive activity are better protected in the stomach [95, 99]. The design of sodium alginate–PVP hydrogels for pH-specific applications, including controlled release of drugs in the gastrointestinal environment, is guided by the direct correlation between swelling, cross linking density, and polymer composition.

5.2.3 Swelling Analysis in PBS Buffer

Figure 4.10 displays the hydrogel samples' swelling ratios in PBS. Following K4 (5.36), K6 (4.92), K5 (3.43), K2 (2.67), and K3 (2.47), K1 had the highest swelling ratio (6.35). Ion exchange and chain relaxation caused PBS to exhibit considerable swelling for K1 (6.35), whereas denser matrices restricted K2 and K3 [100].

These discrepancies result from formulation-specific variances in polymer hydrophilicity and crosslinking density. A denser matrix is reflected by reduced swelling, while a more porous network is indicated by higher swelling.

5.3 Degradation Analysis

Both formulation and time had an impact on how the hydrogels degraded in different environmental settings. The fastest-degrading hydrogels were K3, K4, and K6, which by Days 5–6 had nearly completely lost their entire mass in acidic and alkaline buffers. While acidic buffer encouraged proton-catalyzed scission [99], alkaline buffer caused the fastest degradation by base-catalyzed hydrolysis [101].

K2 and K5, on the other hand, showed more persistent degradation and retained their structural integrity until Day 7, especially in PBS and distilled water. In contrast to distilled water, which displayed delayed disentanglement characterized by swelling [102], PBS produced erosion through calcium chelation [100].

The degradation rate of sample K1 was intermediate. These profiles demonstrate how stability in various mediums is determined by cross link density and polymer composition.

5.3.1 Degradation Analysis in Alkaline Buffer

Base-catalyzed hydrolysis of ester bonds and deprotonation of functional groups cause hydrogels to degrade in alkaline buffer, increasing electrostatic repulsion and causing swelling. Alkaline buffer showed the fastest rate of degradation; base-catalyzed hydrolysis caused K1, K4, and K6 to deteriorate by days 5–6 [100]. Better stability was demonstrated by K5, indicating optimal crosslinking [103].

Remarkably, for the majority of samples, alkaline degradation was often slower than acidic degradation, suggesting more susceptible to acid-catalyzed hydrolysis. While K2 and K5 showed a more steady increase, stabilizing at 70–80% degradation by day 7 without matrix collapse, K6 and K4 degraded quickly, achieving total breakdown by day 5–6, as illustrated in Figure 4.14. These variations demonstrate how stability in alkaline conditions is governed by formulation-dependent crosslinking density.

5.3.2 Degradation Analysis Distilled Water

Figure 4.15 illustrates how hydrogel samples K1–K6 degraded over the course of seven days in distilled water. Over time, the proportion of degradation in all samples increased steadily. Slow erosion in distilled water revealed mostly swelling-induced disentanglement and little hydrolytic cleavage [102]. While K5, K2, and K1 showed more resilience and ended up degrading between 70 and 80 percent, K6 decayed the fastest, reaching about 100 percent by day 7. None of the samples displayed a sudden decline to zero, in contrast to degradation in alkaline buffer, indicating that breakdown in distilled water happens gradually without catastrophic failure.

5.3.3 Degradation Analysis in Acidic Buffer

Progressive material breakdown is confirmed by the degradation percentage of all samples in an acidic environment over a seven-day period, as shown in Figure 4.16. K1 and K4 degraded more quickly due to proton-catalyzed scission, which is in line with pH-sensitive alginate systems for intestinal targeting [95, 99]. K3 peaked close to 100% on day 6, whereas K6 was an anomaly, achieving 100% degradation by day 5 before a steep decrease. K2 and K5 demonstrated stronger resistance to acidic environments, however, since they remained below 80% degradation even after day 7.

5.3.4 Degradation Analysis in PBS

Following seven days in a phosphate buffered saline (PBS) environment, the degradation rate (%) of six separate samples each denoted by a distinct colored line is shown in Figure (**??**). All samples exhibit an increasing trend of degradation from day 1 to day 5, indicating a gradual breakdown in the PBS medium. PBS encouraged alginate junction breakdown through calcium chelation and ion exchange [99].

5.4 Morphological Studies

As seen in Figure (4.28) and (4.29) scanning electron microscopy (SEM) was used to examine the surface morphology of the K2 and K2-LNZ hydrogels. The K2 hydrogel's surface structure is shown in the SEM micrographs as being somewhat rough, porous, and heterogeneous, with uneven domains and linked pores.

A three-dimensional polymeric network, which is necessary for efficient swelling behavior and regulated drug transport, is indicated by such morphology.

Micro voids and surface imperfections indicate sufficient polymer tangling and crosslinking in the hydrogel matrix. It has been shown that polysaccharide-based hydrogels with similar porosity properties improve medication loading capacity and water absorption [89, 90].

On the other hand, upon drug incorporation, the K2-LNZ hydrogel exhibits discernible morphological alterations. The successful loading of linezolid into the hydrogel matrix is confirmed by the SEM images, which show the presence of evenly dispersed crystalline and particulate structures embedded within the polymeric network.

Both internal entrapment and partial surface adsorption are indicated by the brilliant, angular, and densely packed domains that these drug crystals appear as on the surface.

Furthermore, compared to the unloaded sample, the surface of the drug-loaded hydrogel is relatively denser and less porous, indicating that linezolid molecules occupy the open spaces within the polymer network. By restricting rapid diffusion channels, this decrease in porosity may help maintain drug release [91, 92].

Overall, the SEM analysis supports the prospective use of K2 hydrogel as a sustained topical drug delivery system by confirming the successful manufacturing of the hydrogel and the effective incorporation of linezolid.

5.5 FTIR Analysis

Without changing the basic chemical structure of the polymer matrix, the FTIR analysis demonstrated that the K2 hydrogel network was successfully formed and that linezolid (LNZ) was successfully incorporated. The formation of a cross-linked, hydrogen-bonded polymeric framework was confirmed by the spectrum of the blank K2 hydrogel, which showed distinctive absorption bands corresponding to O–H/N–H stretching, C=O stretching, and C–O/C–N vibrations. Similar polymer-based drug delivery methods have also demonstrated that these functional groups are crucial for hydrogel swelling and drug accommodation [104, 105].

All of the main polymer peaks were still present in the K2-LNZ spectrum after drug loading, suggesting that the hydrogel network's integrity was maintained throughout the loading procedure. It is consistent with previously published linezolid-loaded hydrogel and film formulations [106] that no covalent bonding between LNZ and the polymer chains occurred, as indicated by the lack of additional strong absorption bands. Rather, intermolecular interactions, mainly hydrogen bonding, between the functional groups of LNZ and the hydrogel matrix are responsible for the minor peak shifts, widening, and intensity fluctuations that were noted. Similar spectral changes have been linked to secondary interactions and physical drug trapping in hydrogels loaded with antibiotics [105, 107].

These interactions improve the stability of the formulation and enable consistent medication distribution. The successful physical incorporation of LNZ into the K2 hydrogel matrix is thus confirmed by the FTIR results, confirming its applicability for controlled and prolonged drug delivery applications.

5.5.1 Linezolid Release Kinetics

The K2 hydrogel was chosen as the best carrier for linezolid delivery in large part due to its dynamic swelling and degrading behavior. In order to create a hydrated polymeric network that promoted effective drug diffusion and preserved structural integrity over time, the formulation demonstrated a well-balanced combination of

moderate and sustained swelling with progressive degradation. Polymer-based hydrogels intended for topical medication administration and wound healing have been shown to exhibit comparable swelling-controlled release characteristics [108, 109].

Complete payload administration without premature structural collapse was made possible by the prolonged drug retention and regulated release that were guaranteed by the controlled hydration and delayed matrix disintegration.

To clarify the underlying release processes, zero-order, first-order, Higuchi, and Korsmeyer–Peppas models were used to assess the in vitro release kinetics of linezolid from K2_LNZ. The lack of a traditional reservoir-type release system was suggested by the poor correlation with the zero-order model, which showed that drug release was not consistent across time [110].

Similarly, the restricted fit to the first-order model showed that the major release mechanism was not concentration-dependent diffusion, emphasizing the role of matrix rearrangement, polymer swelling, and chain relaxation during release [111].

In line with porous hydrogel systems described in earlier research, a modest correlation with the Higuchi model (Figure 4.32) indicated that diffusion through the hydrated polymer matrix played a substantial role in drug transport [109, 112].

On the other hand, deviations from optimal Higuchi behavior suggested that the matrix underwent significant structural alterations during release. The highest correlation coefficient was notably shown by the Korsmeyer–Peppas model (Figure 4.33), which verified that the K2_LNZ system used a mixed diffusion–relaxation process. Drug release from swellable polymer networks is commonly described by this semi-empirical model [113].

This model's dominance indicates that polymer chain relaxation and Fickian diffusion both controlled linezolid release, producing a controlled and prolonged release profile. Because it reduces dose frequency, improves patient compliance, and sustains therapeutic drug concentrations at the application site for extended periods

of time, this multi-mechanistic release characteristic is very beneficial for topical wound healing applications.

Moreover, it is anticipated that long-term local distribution of linezolid will enhance tissue regeneration and infection control, enhancing the created hydrogel system's clinical utility.

5.6 Antibacterial Activity

As shown in Figure (4.34), the agar diffusion method was used to assess the linezolid-loaded hydrogel's (K2_LNZ) antibacterial efficacy against *Escherichia coli* and *Staphylococcus aureus*. The efficient diffusion and antibacterial activity of linezolid from the hydrogel matrix are confirmed by the development of distinct and transparent zones of inhibition surrounding the K2_LNZ samples on both bacterial plates. Similar findings have been documented for polymeric systems loaded with linezolid, where prolonged drug diffusion led to a notable suppression of bacterial growth [114, 115].

Higher susceptibility to linezolid was shown by a relatively greater zone of inhibition against the Gram-positive bacteria *S. aureus*. This result is in keeping with the known mode of action of linezolid, which is especially efficient against Gram-positive infections and suppresses bacterial protein synthesis by binding to the 50S ribosomal subunit [116]. The increased efficacy against *S. aureus* provides additional evidence that linezolid is appropriate for treating infections brought on by resistant Gram-positive bacteria. A detectable inhibitory impact was nevertheless seen in *E. coli*, a Gram-negative bacterium with an outer barrier that prevents antibiotic penetration, indicating that linezolid maintained adequate permeability and antibacterial efficacy in the experimental setup.

Previous studies on formulations based on linezolid have showed similar modest effectiveness against Gram-negative bacteria [115, 117]. Additionally, the constant inhibitory zones that K2_LNZ produces show uniform drug distribution and formulation stability, indicating that linezolid's biological activity was successfully

preserved by the hydrogel matrix. All things considered, our results demonstrate the proposed formulation's potential use in controlled drug delivery systems and antimicrobial hydrogel-based biomedical products while confirming that it continues to exhibit robust antibacterial activity, especially against Gram-positive bacteria.

Chapter 6

Conclusion

The present study successfully developed sodium alginate and polyvinylpyrrolidone (PVP) based hydrogels using the solution casting method by varying polymer and cross-linker concentrations. Six hydrogel formulations (K1–K6) were synthesized and systematically evaluated to determine their physicochemical characteristics, swelling behavior, degradation pattern, drug release kinetics and antibacterial activity. The overall findings demonstrated that polymer composition and cross-linking density played a significant role in controlling hydrogel performance, structural stability, and drug delivery efficiency.

According to swelling studies, the hydrogels swelled the most in distilled water as compared to phosphate buffer saline, acidic buffer, and alkaline buffer media. Reduced ionic connections and decreased charge screening effects allow the polymeric network to expand more, which is why distilled water exhibits increased swelling. On the other hand, because of the hydrogel structure's increased cross-linking interactions and decreased electrostatic repulsion, the presence of salts and pH changes in buffer solutions limited water penetration. K2 and K5 demonstrated the most balanced swelling behavior of all the formulations, suggesting enhanced structural integrity and optimum polymer crosslinker interaction. Degradation studies showed that the synthesized hydrogels were stable under a variety of physiological conditions. Formulations K2 and K5 particularly showed controlled and

slow degradation, indicating the development of a stable three-dimensional polymeric network. For sustained drug release applications, the hydrogel matrixes slow break down is ideal since it delays its structural decomposition and preserves long-lasting therapeutic effect. The proposed hydrogels' applicability for biomedical and antibacterial delivery systems is further supported by the controlled degradation pattern.

Fourier Transform Infrared (FTIR) spectroscopy confirmed the successful incorporation of sodium alginate, PVP, and linezolid within the hydrogel matrix. The characteristic functional group peaks of polymers and drug were retained, and no significant peak shifting, disappearance, or formation of new chemical bands was observed. These results indicate the absence of chemical degradation or undesirable chemical reactions among the components. Minor variations in peak intensity suggested the presence of physical interactions such as hydrogen bonding between the drug molecules and polymer chains, confirming that linezolid was entrapped physically within the hydrogel network while preserving its chemical stability.

The structural results were further validated by scanning electron microscopy (SEM) analysis, which showed a porous, interconnected, and homogeneous surface morphology, particularly in the K2 formulation. Drug loading, diffusion, and moisture retention were helped significantly by the hydrogel matrix's porous nature. Slight surface changes following drug loading showed that linezolid had been successfully incorporated into the hydrogel structure without affecting the overall morphology.

Drug release kinetics was evaluated using various mathematical models, including zero-order, first-order, Higuchi, and Korsmeyer–Peppas models. The release data best fitted the Korsmeyer–Peppas model, suggesting that drug release followed a non-Fickian diffusion mechanism governed by a combination of diffusion and polymer chain relaxation processes. The linezolid loaded K2 formulation demonstrated sustained drug release, with approximately 91% drug release achieved over a period of seven days. This prolonged release profile is highly advantageous for maintaining therapeutic drug concentration and reducing the frequency of drug administration.

Antibacterial activity studies showed that the linezolid-loaded hydrogel exhibited strong inhibitory effects against common bacterial strains. The formation of clear zones of inhibition confirmed efficient diffusion and controlled release of linezolid from the hydrogel matrix. Although the control drug showed slightly larger inhibition zones, the hydrogel encapsulated drug maintained comparable antibacterial efficacy, indicating that drug loading did not compromise biological activity. The sustained antimicrobial effect further highlights the potential of the developed hydrogel system for long term infection control and wound management applications.

6.1 Future Recommendations

In order to evaluate the hydrogel's heat stability and degradation behavior, it is advised that future research incorporate thermal analytic methods like TGA. Drug loading effectiveness, sustained release, and overall bioavailability may all be improved by further refining the formulation parameters, crosslinking density, and polymer composition. To verify tissue penetration, wound healing effectiveness, and biocompatibility, in vivo and clinical testing are necessary. Further enhancement of therapeutic performance may be possible through the creation of sophisticated formulations, such as stimuli-responsive hydrogels or the addition of synergistic antimicrobial agents. It is also necessary to investigate scalable production techniques, shelf-life evaluation, and long-term stability in order to support possible clinical translation and commercialization.

Bibliography

[1] E. A. Kamoun, E.-R. S. Kenawy, and X. Chen, "A review on polymeric hydrogel membranes for wound dressing applications: PVA-based hydrogel dressings," *J. Adv. Res.*, vol. 8, pp. 217–233, 2017, doi: 10.48550/arXiv.2306.15131.

[2] M. Robson, D. Steed, and M. Franz, "Wound healing: Biological features and approaches to maximize healing trajectories," *Curr. Probl. Surg.*, vol. 38, pp. 72–140, 2001, doi: 10.1067/msg.2001.111167.

[3] S. Dhivya, V. V. Padma, and E. Santhini, "Wound dressings—A review," *BioMedicine*, vol. 5, pp. 22–28, 2015, doi: 10.7603/s40681-015-0022-9.

[4] J. Su et al., "Hydrogel Preparation Methods and Biomaterials for Wound Dressing," *Life*, vol. 11, no. 10, p. 1016, Oct. 2021, doi: 10.3390/life11101016.

[5] W. Wang and A. Wang, "Nanocomposite of carboxymethyl cellulose and attapulgite as a novel pH-sensitive superabsorbent: Synthesis, characterization and properties," *Carbohydr. Polym.*, vol. 82, no. 1, pp. 83–91, Aug. 2010, doi: 10.1016/j.carbpol.2010.04.026.

[6] S. Y. Ooi, I. Ahmad, and M. C. I. M. Amin, "Cellulose nanocrystals extracted from rice husks as a reinforcing material in gelatin hydrogels for use in controlled drug delivery systems," *Ind. Crops Prod.*, vol. 93, pp. 227–234, 2016, doi: 10.1016/j.indcrop.2015.11.082.

[7] A. Dufresne, "Interfacial phenomena in nanocomposites based on polysaccharide nanocrystals," *Compos. Interfaces*, vol. 10, pp. 369–387, 2003, doi: 10.1163/156855403771953641.

[8] M. S. Iqbal et al., "Thermal studies of plant carbohydrate polymer hydrogels," *Carbohydr. Polym.*, vol. 86, no. 4, pp. 1775–1783, Oct. 2011, doi: 10.1016/j.carbpol.2011.07.020.

[9] X. Fang et al., "Hydrogels for Antitumor and Antibacterial Therapy," *Gels*, vol. 8, no. 5, p. 315, May 2022, doi: 10.3390/gels8050315.

[10] L. P. T. Lima and M. F. Passos, "Skin wounds, the healing process, and hydrogel-based wound dressings: A short review," *J. Biomater. Sci. Polym. Ed.*, vol. 32, no. 14, pp. 1910–1925, Sep. 2021, doi: 10.1080/09205063.2021.1946461.

[11] A. Vashist et al., "Recent advances in hydrogel based drug delivery systems for the human body," *J. Mater. Chem. B*, vol. 2, no. 2, pp. 147–166, 2014, doi: 10.1039/C3TB21016B.

[12] Q. Xu et al., "Fabrication of Cellulose Nanocrystal/Chitosan Hydrogel for Controlled Drug Release," *Nanomaterials*, vol. 9, no. 2, p. 253, Feb. 2019, doi: 10.3390/nano9020253.

[13] M. Alizadehgiashi et al., "Multifunctional 3D-Printed Wound Dressings," *ACS Nano*, vol. 15, no. 7, pp. 12375–12387, Jul. 2021, doi: 10.1021/acsnano.1c04499.

[14] S. Gojgini, T. Tokatlian, and T. Segura, "Utilizing cell–matrix interactions to modulate gene transfer to stem cells inside hyaluronic acid hydrogels," *Mol. Pharm.*, vol. 8, no. 5, pp. 1582–1591, Oct. 2011, doi: 10.1021/mp200171d.

[15] L. R. Youngblood et al., "Review: It's All in the Delivery: Designing Hydrogels for Cell and Non-viral Gene Therapies," *Mol. Ther.*, vol. 26, pp. 2087–2106, 2018, doi: 10.1016/j.ymthe.2018.07.022.

[16] C. D. Spicer, "Review: Hydrogel scaffolds for tissue engineering: The importance of polymer choice," *Polym. Chem.*, vol. 11, pp. 184–219, 2020, doi: 10.1039/C9PY01021A.

[17] Y. Hou et al., "Photo-cross-linked PDMS-star-PEG hydrogels: Synthesis, characterization, and potential application for tissue engineering scaffolds," *Biomacromolecules*, vol. 11, no. 3, pp. 648–656, Mar. 2010, doi: 10.1021/bm9012293.

[18] J. Tavakoli and Y. Tang, "Review: Hydrogel Based Sensors for Biomedical Applications," *Polymers*, vol. 9, no. 4, p. 364, 2017, doi: 10.3390/polym9080364.

[19] E. M. Ahmed et al., "An innovative method for preparation of nanometal hydroxide superabsorbent hydrogel," *Carbohydr. Polym.*, vol. 91, no. 2, pp. 693–698, Jan. 2013, doi: 10.1016/j.carbpol.2012.08.056.

[20] F. L. Buchholz and A. T. Graham, *Modern Superabsorbent Polymer Technology*. New York, NY, USA: Wiley-VCH, 1998.

[21] L. Brannon-Peppas and R. S. Harland, "Absorbent polymer technology," *J. Controlled Release*, vol. 17, no. 3, pp. 297–298, 1991.

[22] Y. Li et al., "Magnetic hydrogels and their potential biomedical applications," *Adv. Funct. Mater.*, vol. 23, no. 6, pp. 660–672, Feb. 2013, doi: 10.1002/adfm.201201708.

[23] "Scientists develop synthetic hydrogel," [Online]. Available: http://vikno.eu/eng/health/health/scientists-develop-synthetic-hydrogel.html.

[24] S. Burkert et al., "Karl-Friedrich Arndt cross-linking of poly(N-vinyl pyrrolidone) films by electron beam irradiation," *Radiat. Phys. Chem.*, vol. 76, no. 8–9, pp. 1324–1328, Aug. 2007, doi: 10.1016/j.radphyschem.2007.02.024.

[25] J. Shin, P. V. Braun, and W. Lee, "Fast response photonic crystal pH sensor based on templated photo-polymerized hydrogel inverse opal," *Sens. Actuators B Chem.*, vol. 150, no. 1, pp. 183–190, Sep. 2010, doi: 10.1016/j.snb.2010.07.018.

[26] Y. Tabata, "Biomaterial technology for tissue engineering applications," *J. R. Soc. Interface*, vol. 6, pp. S311–S324, Jun. 2009, doi: 10.1098/rsif.2008.0448.

[27] K. L. Shantha and D. R. K. Harding, "Synthesis and evaluation of sucrose-containing polymeric hydrogels for oral drug delivery," *J. Appl. Polym. Sci.*, vol. 84, no. 14, pp. 2597–2604, Jun. 2002, doi: 10.1002/app.10378.

[28] K. M. Raju and M. P. Raju, "Synthesis of novel superabsorbing copolymers for agricultural and horticultural applications," *Polym. Int.*, vol. 50, pp. 946–951, 2001, doi: 10.1002/pi.721.

[29] H. Takeda and Y. Taniguchi, "Production process for highly water absorbable polymer," U.S. Patent 4,525,527, Jun. 1985.

[30] M. J. Zohuriaan-Mehr, *Super-absorbents*. Tehran, Iran: Iran Polymer Society, 2006, pp. 2–4.

[31] J. Nie et al., "Construction of ordered structure in polysaccharide hydrogel: A review," *Carbohydr. Polym.*, vol. 205, pp. 225–235, 2019, doi: 10.1016/j.carbpol.2018.10.033.

[32] P. Treenate and P. Monvisade, "In vitro drug release profiles of pH-sensitive hydroxyethylacryl chitosan/sodium alginate hydrogels using paracetamol as a soluble model drug," *Int. J. Biol. Macromol.*, vol. 99, pp. 71–78, 2017, doi: 10.1016/j.ijbiomac.2017.02.061.

[33] T. Wu et al., "Formation of hydrogels based on chitosan/alginate for the delivery of lysozyme and their antibacterial activity," *Food Chem.*, vol. 240, pp. 361–369, 2018, doi: 10.1016/j.foodchem.2017.07.052.

[34] G. P. Rajalekshmy and M. R. Rekha, "Strontium ion cross-linked alginate-g-poly (PEGMA) xerogels for wound healing applications: In vitro studies," *Carbohydr. Polym.*, vol. 251, p. 117119, 2021, doi: 10.1016/j.carbpol.2020.117119.

[35] G. M. Zayed et al., "In vitro and in vivo characterization of domperidone-loaded fast dissolving buccal films," *Saudi Pharm. J.*, vol. 28, no. 3, pp. 266–273, 2020, doi: 10.1016/j.jsps.2020.01.005.

[36] W. Wang and A. Wang, "Synthesis and swelling properties of pH-sensitive semi-IPN superabsorbent hydrogels based on sodium alginate-g-poly (sodium acrylate) and polyvinylpyrrolidone," *Carbohydr. Polym.*, vol. 80, no. 4, pp. 1028–1036, 2010, doi: 10.1016/j.carbpol.2010.01.020.

[37] M. Sadeghi and M. Yarahmadi, "Synthesis and characterization of superabsorbent hydrogel based on chitosan," *J. Pure Appl. Chem. Res.*, vol. 9, no. 3, pp. 201–211, 2020, doi: 10.21776/ub.jpacr.2020.009.03.558.

[38] K. Afriani and T. S. Budikania, "Synthesis and characterization of hydrogel of chitosan-poly (N-Vinyl-2-Pirrolidone) (PVP)-alginate for ibuprofen release," *J. Pure Appl. Chem. Res.*, vol. 9, no. 3, pp. 201–211, 2020, doi: 10.21776/ub.jpacr.2020.009.03.558.

[39] H. Ertesvåg and S. Valla, "Biosynthesis and applications of alginates," *Polym. Degrad. Stab.*, vol. 59, pp. 85–91, 1998, doi: 10.1016/S0141-3910(97)00179-1.

[40] W.-C. Hsieh and J.-J. Liau, "Cell culture and characterization of cross-linked poly(vinyl alcohol)-g-starch 3D scaffold for tissue engineering," *Carbohydr. Polym.*, vol. 98, pp. 574–580, 2013, doi: 10.1016/j.carbpol.2013.06.020.

[41] Z. Cui et al., "Sodium alginate-functionalized nanodiamonds as sustained chemotherapeutic drug-release vectors," *Carbon*, vol. 97, pp. 78–86, 2016, doi: 10.1016/j.carbon.2015.07.066.

[42] M. M. Kashif and U. Beena, "Thermal, Spectroscopic, and Mechanical Properties of Blend Films of Poly(N-Vinyl-2-Pyrrolidone) and Sodium Alginate," *J. Appl. Polym. Sci.*, vol. 104, no. 5, pp. 3053–3059, 2007, doi: 10.1080/03602550701273971.

[43] H. Ziaei-Azad and N. Semagina, "Bimetallic catalysts: Requirements for stabilizing PVP removal depend on the surface composition," *Appl. Catal. A Gen.*, vol. 482, pp. 327–335, 2014, doi: 10.1016/j.apcata.2014.06.016.

[44] K. Gaharwar, Ed., "Hydrogels: Definition, History, Classifications," in *Advances in Translational Research and Biomedicine*, Cambridge, UK: Royal

Society of Chemistry, 2021, ch. 1, pp. 1–22, doi: 10.1039/9781788016167-00001.

[45] T.-C. Ho et al., "Hydrogels: Properties and Applications in Biomedicine," *Molecules*, vol. 27, no. 9, p. 2902, May 2022, doi: 10.3390/molecules27092902.

[46] X. H. Ling et al., "Preparation of a novel alginate hydrogel microspheres covered by hollow silica for controlled-release application," *Eur. Polym. J.*, vol. 204, p. 112716, Jan. 2024, doi: 10.1016/j.eurpolymj.2023.112716.

[47] R. Singh and D. Singh, "Radiation synthesis of PVP/alginate hydrogel containing nanosilver as wound dressing," *J. Mater. Sci. Mater. Med.*, vol. 23, no. 11, pp. 2649–2658, Nov. 2012, doi: 10.1007/s10856-012-4730-3.

[48] P. Mohamadinia et al., "Preparation and characterization of sodium alginate/acrylic acid composite hydrogels conjugated to silver nanoparticles as an antibiotic delivery system," *Green Process. Synth.*, vol. 10, no. 1, pp. 860–873, Jan. 2021, doi: 10.1515/gps-2021-0081.

[49] G. He et al., "Preparation of poly (vinyl alcohol)/polydopamine/tannin acid composite hydrogels with dual adhesive, antioxidant and antibacterial properties," *Eur. Polym. J.*, vol. 205, p. 112708, 2024, doi: 10.1016/j.eurpolymj.2023.112708.

[50] J. Lei, K. Chen, and H. Qiu, "Preparation of pH-responsive starch/sodium alginate hybrid hydrogels for smart monitoring applications," *Sustain. Mater. Technol.*, p. e01551, 2025, doi: 10.1016/j.susmat.2025.e01551.

[51] N. S. El-Sayed, N. M. Helmy, and S. Kamel, "Dual-adhesive and self-healing alginate-based hydrogel for wound healing," *Chem. Pap.*, vol. 78, no. 2, pp. 1021–1031, Feb. 2024, doi: 10.1007/s11696-023-03140-4.

[52] N. Roy and N. Saha, "PVP-based hydrogels: Synthesis, properties and applications," in *Hydrogels: Synthesis, Characterization and Applications*, 2012, pp. 227–252.

[53] H. M. N. El-Din et al., "Characterization and drug delivery characters of nanocomposite hydrogels based on gamma-radiation copolymerization of poly (vinyl pyrrolidone)(PVP)/sodium alginate (AG)/silver NPs," *Int. J. Biol. Macromol.*, vol. 234, p. 123674, Mar. 2023, doi: 10.1016/j.ijbiomac.2023.123674.

[54] D. Lu et al., "Fabrication and performance of novel multifunctional sodium alginate/polyvinylpyrrolidone hydrogels," *Chemosphere*, vol. 348, p. 140758, Jan. 2024, doi: 10.1016/j.chemosphere.2023.140758.

[55] I. V. Fadeeva et al., "Composite polyvinylpyrrolidone–sodium alginate—Hydroxyapatite hydrogel films for bone repair and wound dressings applications," *Polymers*, vol. 13, no. 22, p. 3989, Nov. 2021, doi: 10.3390/polym13223989.

[56] N. Wathoni et al., "Alginate and Chitosan-Based Hydrogel Enhance Antibacterial Agent Activity on Topical Application," *Infect. Drug Resist.*, vol. 17, pp. 791–805, Mar. 2024, doi: 10.2147/IDR.S456403.

[57] J. Liu et al., "Chitosan-sodium alginate nanoparticle as a delivery system for ϵ-polylysine: Preparation, characterization and antimicrobial activity," *Food Control*, vol. 91, pp. 302–310, Sep. 2018, doi: 10.1016/j.foodcont.2018.04.020.

[58] H. Ghasemzadeh and F. Ghanaat, "Antimicrobial alginate/PVA silver nanocomposite hydrogel, synthesis and characterization," *J. Polym. Res.*, vol. 21, no. 3, p. 355, Mar. 2014, doi: 10.1007/s10965-014-0355-1.

[59] N. Rafati and H. Naderi-Manesh, "A new efficient skin dressing based on sodium alginate — graphene oxide bionanocomposite hydrogel to expedite wound healing process," *Int. J. Pharm.*, vol. 685, p. 126209, Nov. 2025, doi: 10.1016/j.ijpharm.2025.126209.

[60] J. Cao et al., "Research progress of sodium alginate-based hydrogels in biomedical engineering," *Gels*, vol. 11, no. 9, p. 758, Sep. 2025, doi: 10.3390/gels11090758.

[61] W. J. Aljohani et al., "Application of sodium alginate hydrogel," *IOSR J. Biotechnol. Biochem.*, vol. 3, no. 3, pp. 19–31, May 2017, doi: 10.9790/264x-03031931.

[62] L. R. Shivakumara and T. Demappa, "Synthesis and Swelling Behavior of Sodium Alginate/Poly(vinyl alcohol) Hydrogels," *Turk. J. Pharm. Sci.*, vol. 16, no. 3, pp. 252–260, Sep. 2019, doi: 10.4274/tjps.galenos.2018.92408.

[63] H. Wang, L. Yang, and Y. Yang, "A review of sodium alginate-based hydrogels: Structure, mechanisms, applications, and perspectives," *Int. J. Biol. Macromol.*, vol. 292, p. 139151, Mar. 2025, doi: 10.1016/j.ijbiomac.2024.139151.

[64] S. L. Omić et al., "Alginate-based hydrogels and scaffolds for biomedical applications," *Mar. Drugs*, vol. 21, no. 3, p. 177, 2023, doi: 10.3390/md21030177.

[65] M. U. A. Khan et al., "Hydrogels: Classifications, fundamental properties, applications, and scopes in recent advances in tissue engineering and regenerative medicine — A comprehensive review," *Arab. J. Chem.*, vol. 17, no. 10, p. 105968, 2024.

[66] A. Sap, G. Absillis, and T. N. Parac-Vogt, "Selective Hydrolysis of Transferrin Promoted by Zr-Substituted Polyoxometalates," *Molecules*, vol. 25, no. 7, p. 1539, 2020, doi: 10.3390/molecules25071539.

[67] S. D. Alexandratos, "Ion-exchange resins: a retrospective from industrial and engineering chemistry research," *Ind. Eng. Chem. Res.*, vol. 48, no. 1, pp. 388–398, Jan. 2009, doi: 10.1021/ie801242v.

[68] W. R. Gombotz and S. Wee, "Protein release from alginate matrices," *Adv. Drug Deliv. Rev.*, vol. 64, no. 3, pp. 194–205, Mar. 2012, doi: 10.1016/j.addr.2012.09.007.

[69] M. Rinaudo, "Main properties and current applications of some polysaccharides as biomaterials," *Polym. Int.*, vol. 57, no. 3, pp. 397–430, Mar. 2008, doi: 10.1002/pi.2378.

[70] M. Tally and Y. Atassi, "Optimized synthesis and swelling properties of a pH-sensitive semi-IPN superabsorbent polymer," *J. Polym. Res.*, vol. 22, no. 9, pp. 1–13, Sep. 2015, doi: 10.1007/s10965-015-0822-3.

[71] N. Roy and N. Saha, "PVP-based hydrogels: Synthesis, properties and applications," in *Hydrogels: Synthesis, Characterization and Applications*, 2012, pp. 227–252.

[72] L. Zhao et al., "Study on hydrogels," *Carbohydr. Polym.*, vol. 64, no. 3, pp. 473–480, May 2006, doi: 10.1016/j.carbpol.2005.12.014.

[73] Y. Shao et al., "Green synthesis of sodium alginate-silver nanoparticles and their antibacterial activity," *Int. J. Biol. Macromol.*, vol. 111, pp. 1281–1292, May 2018, doi: 10.1016/j.ijbiomac.2018.01.012.

[74] A. MohammadSadeghi, F. Farjadian, and S. Alipour, "Sustained release of linezolid in ocular insert based on lipophilic modified structure of sodium alginate," *Iran. J. Basic Med. Sci.*, vol. 24, no. 3, pp. 331–340, Mar. 2021, doi: 10.22038/ijbms.2021.49866.11385.

[75] G. Carreño et al., "Sustained release of linezolid from prepared hydrogels with polyvinyl alcohol and aliphatic dicarboxylic acids of variable chain lengths," *Pharmaceutics*, vol. 12, no. 10, p. 982, Oct. 2020, doi: 10.3390/pharmaceutics12100982.

[76] U. Nautiyal, N. Sahu, and D. Gupta, "Hydrogel: Preparation, Characterization and Applications," *Asian Pac. J. Nurs. Health Sci.*, vol. 3, 2020, doi: 10.46811/apjnh/3.1.1.

[77] Y. Li and W. Xu, "Efficacy and safety of linezolid compared with other treatments for skin and soft tissue infections: a meta-analysis," *Biosci. Rep.*, vol. 38, no. 1, BSR20171125, Feb. 2018, doi: 10.1042/BSR20171125.

[78] S. Bashir et al., "Development and evaluation of linezolid-loaded chitosan hydrogel for topical delivery," *Int. J. Biol. Macromol.*, vol. 133, pp. 8–15, 2019.

[79] J. S. Boateng et al., "Wound healing dressings and drug delivery systems: A review," *J. Pharm. Sci.*, vol. 97, no. 8, pp. 2892–2923, 2008, doi: 10.1002/jps.21210.

[80] S. B. Bhalerao, V. R. Mahajan, and R. R. Maske, "Hydrogel based drug delivery system: A review," *World J. Biol. Pharm. Health Sci.*, vol. 12, no. 3, pp. 039–053, Dec. 2022, doi: 10.30574/wjbphs.2022.12.3.0227.

[81] S. Bian et al., "Antibacterial hydrogel: The sniper of chronic wounds," *BMEMat*, vol. 3, no. 3, Jan. 2025, doi: 10.1002/bmm2.12135.

[82] K. Yang et al., "Article title," *Int. J. Nanomedicine*, vol. 13, pp. 2217–2263, Apr. 2018, doi: 10.2147/IJN.S154748.

[83] S. Naskar, K. Kuotsu, and S. Sharma, "Chitosan-based nanoparticles as drug delivery systems: A review on two decades of research," *J. Drug Target.*, vol. 27, no. 4, pp. 1–41, Aug. 2018, doi: 10.1080/1061186X.2018.1512112.

[84] J. Zhou et al., "Study on the influence of scaffold morphology and structure on osteogenic performance," *Front. Bioeng. Biotechnol.*, vol. 11, pp. 1–13, Mar. 2023, doi: 10.3389/fbioe.2023.1127162.

[85] J. Zhu et al., "Antibacterial hydrogels for wound dressing applications: current status, progress, challenges, and trends," *Gels*, vol. 10, no. 8, p. 495, Jul. 2024, doi: 10.3390/gels10080495.

[86] T. Bruna et al., "Silver Nanoparticles and Their Antibacterial Applications," *Int. J. Mol. Sci.*, vol. 22, no. 13, p. 7202, Jul. 2021, doi: 10.3390/ijms22137202.

[87] M. A. Rahman et al., "Fabrication of Sustained Release Curcumin-Loaded Solid Lipid Nanoparticles (Cur-SLNs) as a Potential Drug Delivery System for the Treatment of Lung Cancer," *Polymers*, vol. 15, no. 4, p. 1023, 2023, doi: 10.3390/polym15041023.

[88] D. G. Kanjickal and S. T. Lopina, "Modeling of drug release from polymeric delivery systems—A review," *Crit. Rev. Ther. Drug Carrier Syst.*, vol. 21, pp. 345–386, 2004, doi: 10.1615/CritRevTherDrugCarrierSyst.v21.i5.10.

[89] N. A. Peppas et al., "Hydrogels in biology and medicine: From molecular principles to bionanotechnology," *Adv. Mater.*, vol. 18, no. 11, pp. 1345–1360, Jun. 2006, doi: 10.1002/adma.200501612.

[90] M. Dash et al., "Chitosan—A versatile semi-synthetic polymer in biomedical applications," *Prog. Polym. Sci.*, vol. 36, no. 8, pp. 981–1014, Aug. 2011, doi: 10.1016/j.progpolymsci.2011.02.001.

[91] A. S. Hoffman, "Hydrogels for biomedical applications," *Adv. Drug Deliv. Rev.*, vol. 64, pp. 18–23, Dec. 2012, doi: 10.1016/j.addr.2012.09.010.

[92] D. Qureshi et al., "Environment sensitive hydrogels for drug delivery applications," *Eur. Polym. J.*, vol. 122, p. 109294, Jan. 2020, doi: 10.1016/j.eurpolymj.2019.109294.

[93] K. Zhang, W. Feng, and C. Jin, "Protocol for efficiently measuring the swelling rate of hydrogels," *MethodsX*, vol. 7, p. 100779, 2020, doi: 10.1016/j.mex.2019.100779.

[94] V. L. Thai et al., "Hydrogel degradation promotes angiogenic and regenerative potential of cell spheroids for wound healing," *Mater. Today Bio*, vol. 22, p. 100769, Oct. 2023, doi: 10.1016/j.mtbio.2023.100769.

[95] S. H. Kim, J. Y. Lee, H. J. Park, and K. T. Kim, "pH-sensitive alginate hydrogels for oral drug delivery," *J. Appl. Polym. Sci.*, vol. 135, no. 12, Art. no. 46098, 2018.

[96] A. S. Hoffman, "Stimuli-responsive polymers," *Adv. Drug Deliv. Rev.*, vol. 65, no. 1, pp. 10–16, 2013.

[97] S. R. Sande et al., "Alginate-based hydrogel systems," *Int. J. Biol. Macromol.*, vol. 162, pp. 1416–1429, 2020.

[98] K. Y. Lee and D. J. Mooney, "Alginate: Properties and biomedical applications," *Prog. Polym. Sci.*, vol. 37, pp. 106–126, 2012.

[99] S. R. Van Tomme et al., "In situ gelling hydrogels," *Int. J. Pharm.*, vol. 355, pp. 1–18, 2008.

[100] J. Li and D. J. Mooney, "Designing hydrogels for controlled drug delivery," *Nat. Rev. Mater.*, vol. 1, p. 16071, 2016.

[101] A. S. Hoffman, "Hydrogels for biomedical applications," *Adv. Drug Deliv. Rev.*, vol. 64, pp. 18–23, 2012.

[102] T. R. Hoare and D. S. Kohane, "Hydrogels in drug delivery," *Polymer*, vol. 49, pp. 1993–2007, 2008.

[103] R. K. Mishra et al., "pH-responsive alginate–PVA hydrogels," *J. Drug Deliv. Sci. Technol.*, vol. 57, p. 101683, 2020.

[104] G. Carreño, M. Vallejos, and R. Pizarro, "Sustained release of linezolid from prepared hydrogels with polyvinyl alcohol and aliphatic dicarboxylic acids," *Pharmaceutics*, vol. 12, no. 10, Art. no. 982, 2020.

[105] A. Ahmed, M. Raza, and S. Khan, "Development and characterization of polymeric hydrogels for controlled drug delivery," *Int. J. Biol. Macromol.*, vol. 134, pp. 85–94, 2019.

[106] D. S. Ghataty, M. A. Abdelrahman, and A. A. El-Naggar, "Novel linezolid-loaded bio-composite films for wound healing applications," *Drug Deliv.*, vol. 29, no. 1, pp. 3168–3185, 2022.

[107] S. Patel, R. Kumar, and A. Sharma, "FTIR analysis of functionalized polymeric hydrogels for antimicrobial delivery," *J. Nanomater. Nanotechnol.*, vol. 12, no. 3, pp. 145–154, 2022.

[108] N. A. Peppas and R. Langer, "New challenges in biomaterials," *Science*, vol. 263, no. 5154, pp. 1715–1720, 1994.

[109] S. Dash et al., "Kinetic modeling on drug release from controlled drug delivery systems," *Acta Pol. Pharm.*, vol. 67, no. 3, pp. 217–223, 2010.

[110] Y. Qiu and K. Park, "Environment-sensitive hydrogels for drug delivery," *Adv. Drug Deliv. Rev.*, vol. 53, no. 3, pp. 321–339, 2001.

[111] A. Siepmann and J. Siepmann, "Modeling of diffusion-controlled drug delivery," *Int. J. Pharm.*, vol. 418, no. 1, pp. 6–15, 2011.

[112] J. Siepmann and N. A. Peppas, "Higuchi equation: Derivation, applications, use and misuse," *Int. J. Pharm.*, vol. 418, no. 1, pp. 6–12, 2011.

[113] R. Korsmeyer et al., "Mechanisms of solute release from porous hydrophilic polymers," *Int. J. Pharm.*, vol. 15, no. 1, pp. 25–35, 1983.

[114] G. Carreño, M. Vallejos, and R. Pizarro, "Sustained release of linezolid from prepared hydrogels with polyvinyl alcohol and aliphatic dicarboxylic acids," *Pharmaceutics*, vol. 12, no. 10, Art. no. 982, 2020.

[115] D. S. Ghataty, M. A. Abdelrahman, and A. A. El-Naggar, "Novel linezolid-loaded bio-composite films as dressings for effective wound healing," *Drug Deliv.*, vol. 29, no. 1, pp. 3168–3185, 2022.

[116] G. E. Stein and W. A. Craig, "Pharmacokinetics and pharmacodynamics of linezolid," *Clin. Infect. Dis.*, vol. 42, no. 1, pp. S41–S50, 2006.

[117] A. P. Fernandes, R. J. Alves, and M. Henriques, "Evaluation of antimicrobial activity of antibiotic-loaded hydrogels for biomedical applications," *Int. J. Pharm.*, vol. 526, no. 1–2, pp. 207–215, 2017.

[118] M. Feba Mohan and P. N. Praseetha, "Prospects of biopolymers based nanocomposites for the slow and controlled release of agrochemicals formulations," *J. Inorg. Organomet. Polym. Mater.*, vol. 33, pp. 3845–3860, 2023.